

# Lawrence Berkeley National Laboratory

## Recent Work

**Title**

PERSPECTIVE ON TeV SCALE PHYSICS

**Permalink**

<https://escholarship.org/uc/item/93r2k4d2>

**Author**

Chanowitz, Michael S.

**Publication Date**

1989-02-01



# Lawrence Berkeley Laboratory

UNIVERSITY OF CALIFORNIA

## Physics Division

Five lectures presented at the Heavy Flavor  
Physics Symposium, Beijing, PRC, August 11-20, 1988,  
and to be published in the Proceedings

### Perspective on TeV-Scale Physics

M.S. Chanowitz

February 1989

RECEIVED  
LAWRENCE  
BERKELEY LABORATORY

MAY 24 1989

LIBRARY AND  
DOCUMENTS SECTION



LBL-26547  
c. 2

## **DISCLAIMER**

This document was prepared as an account of work sponsored by the United States Government. While this document is believed to contain correct information, neither the United States Government nor any agency thereof, nor the Regents of the University of California, nor any of their employees, makes any warranty, express or implied, or assumes any legal responsibility for the accuracy, completeness, or usefulness of any information, apparatus, product, or process disclosed, or represents that its use would not infringe privately owned rights. Reference herein to any specific commercial product, process, or service by its trade name, trademark, manufacturer, or otherwise, does not necessarily constitute or imply its endorsement, recommendation, or favoring by the United States Government or any agency thereof, or the Regents of the University of California. The views and opinions of authors expressed herein do not necessarily state or reflect those of the United States Government or any agency thereof or the Regents of the University of California.

## **Perspective on TeV-Scale Physics**

**Five lectures presented at the Heavy Flavor  
Physics Symposium, Beijing, PRC, August 11–20, 1988,  
and to be published in the Proceedings**

**Michael S. Chanowitz**

**February 1989**

---

**\*This work was supported by the Director, Office of Energy Research,  
Office of High Energy and Nuclear Physics, Division of High Energy Physics  
of the U.S. Department of Energy under Contract DE-AC03-76SF00098.**

### Abstract

These lectures review theoretical motivations and experimental prospects for the study of TeV-scale physics. Three clues to the importance of TeV physics are discussed:

1. implications of quantum corrections for the masses of a fourth generation quark-lepton family,
2. the gauge hierarchy problem and known solutions,
3. implications of symmetry and unitarity for the symmetry-breaking sector of the electroweak gauge theory.

The experimental prospects are reviewed with emphasis on the multi-TeV pp colliders that may be built in the 1990's. The topics include new phenomena that *might* occur — e.g., a fourth generation, heavy gauge bosons, composite structure, and supersymmetry — as well as the signals of the unknown  $SU(2)_L \times U(1)_Y$  breaking mechanism that *must* occur within the TeV domain.

## 1. INTRODUCTION

Physics in the domain between 100 MeV and 100 GeV has been very rich. In the last twenty years it yielded a beautiful synthesis, summarized by the gauge structure  $SU(3)_{Color} \times SU(2)_L \times U(1)_Y$ . Though beautiful the synthesis is clearly incomplete. Some of the missing elements will be far more difficult to find than others. In the landscape of this search the TeV scale is the only indisputable landmark below the gravitational scale of  $10^{19}$  GeV. The success of the standard model clearly identifies the  $\text{TeV} = 10^3$  GeV scale as the domain of one of the key missing elements: the unknown “fifth” force that breaks the  $SU(2)_L \times U(1)_Y$  symmetry, giving mass to the  $W$  and  $Z$  while leaving the photon massless. Unitarity and  $SU(2)_L \times U(1)_Y$  gauge invariance alone identify a scale<sup>(1,2)</sup>

$$\frac{16\pi}{\sqrt{2}G_F} = (1.7 \text{ TeV})^2 \quad (1.1)$$

at or below which the symmetry breaking mechanism must emerge.

In such a vast landscape we are fortunate that there is a landmark so close at hand. It is especially exciting that multi-TeV proton-proton colliders will allow us to begin to explore directly TeV scale physics in this century. The U.S. government will probably decide in 1989 whether to construct the Superconducting Super Collider, an 83 km ring with 6.6 Tesla magnets that will create pp collisions at  $\sqrt{s} = 40$  TeV center of mass energy. With a luminosity  $\mathcal{L} = 10^{33} \text{cm}^{-2} \text{sec}^{-1}$  the SSC is an optimal exploratory probe for the upper reaches of the domain defined by equation 1.1, as will be discussed in detail in these lectures. At CERN a proposal is in preparation to place a Large Hadron Collider in the LEP tunnel, with a 27 km circumference. For magnetic fields from 7 to 10 Tesla, the LHC would have proton-proton center of mass energies from 10 to 16 TeV. In these lectures I will assume  $\sqrt{s} = 16$  TeV for the LHC, although the required 10 Tesla magnets would require considerable development beyond the existing state of the art, which may or may not be feasible on the desired time scale.

Most experiments at both the SSC and LHC are visualized with luminosities of about  $\mathcal{L} = 10^{33} \text{cm}^{-2} \text{sec}^{-1}$ . It may be possible to operate the machines at higher luminosities, but it is not clear that detectors could withstand the increased radiation damage or could successfully extract useful data (except for certain special purposes such as muon detection). In fact these problems are

already very serious for  $\mathcal{L} = 10^{33} \text{cm}^{-2} \text{sec}^{-1}$ !

As in the past, experiments would be much easier at  $e^+e^-$  colliders since the ratio of interesting physics to “junk” is many orders of magnitude higher than at proton colliders. A  $\sqrt{s} \cong 2 - 3 \text{ TeV}$   $e^+e^-$  collider with  $\mathcal{L} = 10^{33} \text{cm}^{-2} \text{sec}^{-1}$  would in many respects be roughly equivalent to the SSC. But we do not know how to (or even if we ever can) build such a collider. To avoid unacceptable energy loss it must be a linear collider. To obtain the necessary luminosity from single pass collisions, the beams must then be very small — much less than 1 micron. The Stanford Linear Collider is the first step toward this technology but much more research and development will be needed before we will know with confidence whether and how to proceed. It is clearly very important for the future of high energy physics to support a strong R and D program on linear colliders.

In contrast, today the design of pp colliders is comparatively straightforward. The SSC design is conservatively based on proven technology, as is only prudent for so large and costly a project. But many of the experiments will be extremely difficult because of large background rates. To realize the goal of exploring TeV physics in this century, experimenters and theorists must work hard now to ensure the effective use of pp colliders.

These lectures are in two parts. The first, consisting of three lectures, addresses the question “What is special about 1 TeV?”. The focus is on three topics:

- 1) A general, model independent analysis, based on unitarity and symmetry, that identifies the TeV scale as the upper limit for the unknown physics that breaks the electroweak symmetry.
- 2) “Naturalness” and the gauge hierarchy problem which also point to the TeV scale as the upper limit for the physics of  $SU(2)_L \times U(1)_Y$  breaking. These considerations lead many theorists to be skeptical of ordinary Higgs boson models, preferring instead either supersymmetric Higgs models below 1 TeV, a new strong force just above 1 TeV, or (maybe best of all) something else not yet imagined.
- 3) Implications of electroweak quantum corrections for the mass scale of a

possible fourth generation.

The second part, consisting of two lectures, describes the experimental signals for the new physics discussed in the first part. Because I am concerned with what can be accomplished in this century, the focus is on proton-proton colliders. The topics include

- 1) QCD as the ocean in which the physics signals swim.
- 2) Reconnaissance for new forces and new matter.
- 3) Supersymmetry — definitive searches should be possible if supersymmetry is the solution to the gauge hierarchy problem.
- 4) Electroweak symmetry breaking — a collider with the energy and luminosity of the SSC is sure to point to the symmetry breaking mechanism.

In science it is a truism that the most important discovery is the completely unexpected. The best we can do to prepare for this possibility is to be ready to look for the broadest range of new physics that we are able to imagine. At the same time it is important to keep in mind the uniqueness of the impending exploration of the TeV scale: while any new experiment has a chance to make a basic unexpected discovery, we can be confident that the TeV domain holds the key to understanding at least one fundamental gap in the standard model. When this key is found it will also help us along the trail leading to the other missing elements.

## 2. WHAT'S SPECIAL ABOUT 1 TeV?

A marvelous series of discoveries were made from the 1950's to 1973, culminating in the synthesis that we now call the standard model. This period should be understood and appreciated to have a perspective on where we are today. There is not time to review this story properly so I will just mention a few highlights:

- Systematic experimental study of the hadron spectrum led to recognition of the patterns of  $SU(3)_{Flavor}$  symmetry.
- The quark model was put forward as a mnemonic for the flavor symmetry, but almost no one dared take quarks seriously as real dynamical degrees of freedom.
- The  $SU(2)_L \times U(1)_Y$  model of electroweak interactions was formulated but initially received little attention — even from the physicists who proposed it.
- Scaling in deep inelastic electron scattering led to the formulation of the parton model. Deep inelastic neutrino scattering then showed that the partons carry quark quantum numbers. This introduced a contradiction as blatant as the instability of the classical atom, since the weak binding approximation of the parton model implied that quarks should appear among the collision products.
- The asymptotic freedom of unbroken nonabelian gauge theories was discovered and understood to resolve the contradictions of the parton model.
- The discovery of weak neutral currents and proofs of its renormalizability taught us to take the electroweak theory seriously.

The culmination of these and other important developments, omitted in this too brief sketch, is the standard model: forces described by an  $SU(3)_{Color} \times SU(2)_L \times U(1)_Y$  gauge structure and matter described by at least three quark-lepton generations. This is a tremendous advance beyond the state of our knowledge 25 years ago. Our success allows and requires us to ask questions at a deeper level. Among the questions we ask are these:

- What breaks the  $SU(2)_L \times U(1)_Y$  symmetry and gives the  $W$  and  $Z$  mass? How is  $M_W$  related to other scales such as  $M_{Planck} = 10^{19}$  GeV?
- How many fermion generations are there and why? What determines their masses?
- Is there a larger architecture of gauge interactions, as in grand unified theories or in models with horizontal (intergenerational) symmetries. Are some or even all standard model quanta actually composite?
- Does nature have a broken supersymmetry relating bosons and fermions? Is it a local symmetry as in supergravity or superstring models? If not, how is gravity related to the other forces?
- Can our understanding of these microphysical laws be used to construct a verifiable theory of the origin of the universe?

Many of these questions may involve energy scales as high as  $M_{Planck} = 10^{19}$  GeV; certainly the last does. Why should we expect any answers at  $\lesssim O(1)$  TeV? Usually when a new accelerator enters a new energy domain we say “you pays your money and you takes your chances”. As in most explorations since the days of Columbus there is no guarantee that important discoveries will be made. This is not the case for the first accelerators that step into the TeV domain. In addition to the possibility of revolutionary unanticipated results, they are certain to illuminate at least some of these fundamental questions. In particular,

- We will learn the energy scale of the mechanism of  $SU(2)_L \times U(1)_Y$  breaking and will probably discover the mechanism.
- We will discover supersymmetry if it is relevant to electroweak symmetry breaking.
- We will learn whether there is a fourth generation of quarks and leptons even if the fourth neutrino is too heavy to be produced in  $Z$  decay, as long as it is not too nearly degenerate with the corresponding charged lepton.

In each case however the experimental problems are challenging and will require considerable attention by both experimenters and theorists.

Other questions can be explored to multi-TeV scales at the SSC and LHC, though with no similar guarantee of definitive results. For instance, quarks can be probed for compositeness to distance scales of  $(18 \text{ TeV})^{-1}$  and  $(12 \text{ TeV})^{-1}$  at the SSC and LHC respectively. The neutral  $Z'$  gauge boson of  $SO(10)$  models can be discovered for masses below 6 and 3 TeV at the two colliders respectively, and a heavy replica of the standard  $W$  boson could be discovered with mass as large as 9 or 5 TeV respectively. It is well worth considering the physics “reach” for these and other signals, not only because they may exist but because such exercises are the best guide to our “reach” for the unexpected.

A few years ago, when simple  $SU(5)$  grand unification seemed a possibility, there was talk of a “desert” stretching from  $M_W$  to  $M_{GUT} \cong 10^{14}$  GeV, with nothing in between except one Higgs boson at  $\lesssim 1$  TeV. Today more accurate measurements of the parameters of the electroweak theory indicate just the opposite: grand unification now seems to require new physics below  $M_{GUT}$ . Analysis of one loop corrections<sup>(3)</sup> show that the running coupling constants of  $SU(3)_{Color}$ ,  $SU(2)_L$ , and  $U(1)_Y$  do not meet at a point (at the 90% confidence level) unless new physics below  $M_{GUT}$  intervenes to bend the trajectories (shown in figure 1) from the courses they follow in the minimal standard model. Of course this new physics need not be at the TeV scale.

Discoveries made at the TeV scale could also be very important for the efforts to understand physics at  $M_{GUT}$  or  $M_{Planck}$ . If a heavy  $Z'$  boson were discovered, measurement of its couplings to quarks and leptons would pin down the symmetry of a grand unified theory. Discovery of supersymmetry would give a tremendous boost (psychologically and maybe also scientifically) to Planck-scale modelers and super-stringers. Measurement of superpartner masses would illuminate physics at and just below  $M_{Planck}$  in models of Planck scale physics.

In this section I will focus on the answers that are sure to be found within the TeV domain:

1. Unless it is nearly degenerate with the associated neutrino, we know from one loop radiative corrections that a fourth generation charged lepton could not be heavier than  $\sim 350 - 500$  GeV.

2. The technical unnaturalness of ordinary Higgs models is remedied in two known ways. One requires a strong confining force above (but not too far above) 1 TeV. The other requires supersymmetry below 1 TeV.
3. Unitarity and the known symmetry of the electroweak gauge theory imply that whatever its nature, the mechanism of electroweak symmetry breaking must emerge at or below the 1.7 TeV scale. By measuring the scattering of longitudinally polarized  $W$ 's and  $Z$ 's between 1 and 2 TeV we will determine whether the mass scale of the symmetry breaking quanta is above or below 1 TeV, and in most cases we will be able to observe them directly.

The global symmetry of the symmetry breaking sector plays an important part in each of these topics. Therefore I will preface the discussion with a review of the standard Higgs boson model, paying particular attention to the global symmetry of the Higgs sector, which experimental measurements of the rho parameter tell us must in general be a low energy symmetry of any strongly interacting symmetry breaking sector.<sup>(2)</sup> As discussed below, the standard Higgs model will play a role like that of the sigma model<sup>(4)</sup> in QCD if  $SU(2)_L \times U(1)_Y$  is broken by a new strong force above 1 TeV.

## 2.1 The Minimal Higgs Sector of the Standard Model

I will briefly review the structure of the minimal model.<sup>(5,6)</sup> The lagrangian for the complete theory is the sum of three terms,

$$\mathcal{L} = \mathcal{L}_{\text{gauge}} + \mathcal{L}_{SB} + \mathcal{L}_f. \quad (2.1)$$

The first term,  $\mathcal{L}_{\text{gauge}}$ , describes an *unbroken*  $SU(2)_L \times U(1)_Y$  gauge theory, consisting of massless gauge bosons interacting with massless fermions. The symmetry breaking component,  $\mathcal{L}_{SB}$ , contains the dynamics that induces an  $SU(2)_L \times U(1)_Y$  asymmetric ground state. The third term  $\mathcal{L}_f$  contains the couplings of the fermions to the fields of  $\mathcal{L}_{SB}$  that acquire condensates in the asymmetric ground state, thereby generating the fermion masses.

Consider first the gauge interactions,  $\mathcal{L}_{\text{gauge}}$ . There are four gauge bosons,  $\vec{W} = W^1, W^2, W^3$  and  $X$  corresponding to the four generators of  $SU(2)_L$  and  $U(1)_Y$ . For simplicity we consider just the first generation of fermions, consisting of the quark and lepton  $SU(2)_L$  doublets  $(u, d)_L$  and  $(e, \nu_e)_L$  and the right



chirality components  $u_R, d_R$ , and  $e_R$  which are  $SU(2)_L$  singlets (i.e., do not carry left-isospin). The hypercharge  $Y$  of the various fermions are fixed by  $T_{3L} = Q + Y$  using these  $SU(2)_L$  assignments and the known electric charges. Then following the usual prescription for constructing a gauge invariant theory (e.g., reference (7)) we have in a compact notation

$$\mathcal{L}_{\text{gauge}} = -\frac{1}{4}\vec{F}_{\mu\nu}(W) \cdot \vec{F}^{\mu\nu}(W) - \frac{1}{4}F_{\mu\nu}(X)F^{\mu\nu}(X) + i\bar{\psi}\mathcal{D}\psi. \quad (2.2)$$

The gauge invariant kinetic energies for the gauge bosons are

$$\begin{aligned} F^{\mu\nu}(X) &= \partial^\mu X^\nu - \partial^\nu X^\mu \\ \vec{F}^{\mu\nu}(W) &= \partial^\mu \vec{W}^\nu - \partial^\nu \vec{W}^\mu + g\vec{W}^\mu \times \vec{W}^\nu. \end{aligned} \quad (2.3)$$

The field  $\psi$  is a multicomponent spinor, consisting of the  $(u, d)_L$  and  $(e, \nu_e)_L$   $SU(2)_L$  doublets and the three  $SU(2)_L$  singlets  $u_R, d_R$ , and  $e_R$ , coupled gauge invariantly to the gauge bosons by the covariant derivative

$$\mathcal{D}^\mu = \partial^\mu - ig\vec{W}_L \cdot \vec{T}_L - ig'XY \quad (2.4)$$

with  $g$  and  $g'$  the  $SU(2)_L$  and  $U(1)_Y$  coupling respectively. In equation 2.4,  $\vec{T}_L$  and  $Y$  are matrices that act on  $\psi$  in accordance with the isospin and hypercharge assignments of its components.

In the minimal model<sup>(6)</sup> the quanta of  $\mathcal{L}_{SB}$  consist of four spin zero bosons arranged to form a complex doublet under the  $SU(2)_L$  group,

$$\Phi = \frac{1}{\sqrt{2}} \begin{pmatrix} w_1 + iw_2 \\ H + iw_3 \end{pmatrix}. \quad (2.5)$$

Here  $w^+ = \frac{1}{\sqrt{2}}(w_1 + iw_2)$  carries positive electric charge while  $H$  and  $w_3$  are electrically neutral. Then for this case

$$\mathcal{L}_{SB} = (\mathcal{D}_\mu \Phi)^\dagger (\mathcal{D}^\mu \Phi) - V(\Phi^\dagger \Phi) \quad (2.6)$$

where to insure gauge invariance  $\mathcal{D}_\mu$  is again of the form of equation 2.4 with  $\vec{T}_L$  given by the familiar Pauli matrices appropriate to isospin 1/2 and  $Y$  is a diagonal matrix constructed in accordance with  $Q = T_{3L} + Y$ . The spontaneous symmetry breakdown is induced by the form of the potential  $V$ ,

$$V = \lambda(\Phi^\dagger \Phi - \frac{v^2}{2})^2, \quad (2.7)$$

with a minimum at  $\Phi^\dagger \Phi = v^2/2$ . Here "spontaneity" means that the minimum could be realized by a condensate  $v$  forming along any direction of the four dimensional space spanned by  $\vec{w}, H$ . We choose the components of  $\Phi$  so that the desired pattern of symmetry breaking occurs when the field  $H$  acquires the condensate  $v$ , i.e., for  $\vec{w} = 0$  and  $H = v$ . If we redefine  $H$  by  $H \rightarrow H + v$  so that it also vanishes classically at the minimum, then the potential can be rewritten as

$$V = \frac{\lambda}{4}(\vec{w}^2 + H^2)^2 + \lambda v H(\vec{w}^2 + H^2) + \lambda v^2 H^2. \quad (2.8)$$

Equation 2.8 illustrates Goldstone's theorem: before breakdown the potential, equation 2.7, had a four dimensional  $O(4)$  symmetry in the space spanned by  $\vec{w}, H$ , that is reduced to the  $O(3)$  symmetry of equation 2.8 under which  $\vec{w}$  is a triplet and  $H$  a singlet. The number of invariant generators is reduced from the six of  $O(4)$  to the three of  $O(3)$ , each broken generator giving rise to a massless Goldstone boson. In equation 2.8 we see that the Higgs field  $H$  has a mass

$$m_H^2 = 2\lambda v^2 \quad (2.9)$$

while the  $\vec{w}$  are massless — they are the expected Goldstone bosons.

In fact the model defined by equation 2.7 played a venerable role in the physics of the 1960's that led to QCD in the early 1970's: it is precisely the  $SU(2)$  sigma model<sup>(4)</sup> with  $\vec{w}$  replaced by the pions and  $H$  replaced by the scalar sigma field. The value of the sigma model is not as a comprehensive description of hadron physics — the existence of the sigma meson remains an enigma to this day — *but that it correctly embodies the symmetry structure of hadron physics*, an  $SU(2)_L \times SU(2)_R$  symmetry that breaks spontaneously to  $SU(2)_{L+R}$  (ordinary isospin) with three Goldstone bosons, the pions. It therefore embodies the low energy theorems for pion-pion scattering<sup>(8)</sup> which are the counterparts of the low energy theorems for longitudinally polarized  $W$  and  $Z$  scattering<sup>(1,2)</sup> to be discussed in Section 2.4 below. According to one of the original practitioners, the approach is inspired by a method of classical French cuisine: "We may compare this process to a method sometimes employed in French cuisine: a piece of pheasant meat is cooked between two slices of veal which are then discarded".<sup>(9)</sup> If  $\mathcal{L}_{SB}$  is strongly interacting then the minimal Higgs model will eventually be viewed like the sigma model (or like two slices of

veal).

The gauge boson mass is “transmitted” to the gauge bosons by the coupling of the scalars to the gauge bosons in equation 2.6, dictated by the gauge invariant minimal substitution prescription of equation 2.4. Since  $\Phi$  acquires a condensate  $v$ , equation 2.6 gives rise to mass terms for the gauge bosons  $\vec{W}$  and  $X$ . The charged components  $W^\pm = \frac{1}{\sqrt{2}}(W_1 \pm iW_2)$  acquire a mass

$$M_W = \frac{1}{2}gv \quad (2.10)$$

while the neutral components  $W^3$  and  $X$  acquire a mass matrix

$$M_{W_3, X}^2 = \frac{1}{4}v^2 \begin{pmatrix} g^2 & gg' \\ gg' & g'^2 \end{pmatrix}. \quad (2.11)$$

Since the determinant vanishes, the mass of one eigenstate vanishes — the photon — while the mass of the other is given by the trace,

$$M_Z = \frac{1}{2}\sqrt{g^2 + g'^2}v. \quad (2.12)$$

The eigenstates are related to  $W_3, X$  by a rotation

$$\begin{pmatrix} \gamma \\ Z \end{pmatrix} = \begin{pmatrix} \cos \theta_W & \sin \theta_W \\ -\sin \theta_W & \cos \theta_W \end{pmatrix} \begin{pmatrix} W^3 \\ X \end{pmatrix} \quad (2.13)$$

where the mixing angle is

$$\sin \theta_W = \frac{g'}{\sqrt{g^2 + g'^2}}. \quad (2.14)$$

Substituting equation 2.13 into equation 2.6 we discover that the electric charge is

$$e = g \sin \theta_W. \quad (2.15)$$

From the lowest order relation for the Fermi constant

$$G_F = \frac{g^2}{4\sqrt{2}M_W^2} \quad (2.16)$$

and from equation 2.10 we deduce the value of the condensate

$$v = (\sqrt{2}G_F)^{-1/2} = 246 \text{ GeV}. \quad (2.17)$$

Comparing the expressions for the  $W$  and  $Z$  masses and using equation 2.14 we learn that the rho parameter is equal to unity,

$$\rho \equiv \frac{M_W^2}{M_Z^2 \cos^2 \theta_W} = 1 \quad (2.18)$$

in excellent agreement with the most recent global fits<sup>(3,10)</sup> that give  $1.01 \pm .01$ .

Going beyond the minimal model, the success of equation 2.18 is an important clue to the symmetry structure of  $\mathcal{L}_{SB}$ . Returning to equations 2.10 and 2.11 we see with a little work that  $\rho = 1$  follows from the equality of the mass of  $W_3$  to that of  $W_1$  and  $W_2$ , which means it is a consequence of the unbroken  $SU(2)_{L+R}$  symmetry that survives the spontaneous breaking of  $SU(2)_L \times SU(2)_R$  in the minimal model, the analogue of ordinary isospin in the sigma model. Since this  $SU(2)_{L+R}$  protects equation 2.18 from potentially large  $O(\lambda_{SB})$  corrections from  $\mathcal{L}_{SB}$ , it is sometimes called the “custodial  $SU(2)$ ”.<sup>(11)</sup> In reference (2) it is shown that the validity of  $\rho = 1$  in the case of a strongly interacting  $\mathcal{L}_{SB}$  implies that the low (but not necessarily the high) energy interactions of the Goldstone bosons  $\vec{w}$  must be  $SU(2)_{L+R}$  symmetric — a limited converse to the observation of that  $SU(2)_{L+R}$  symmetry implies  $\rho = 1$ .

The third term,  $\mathcal{L}_f$ , in equation 2.1 is needed to transmit the symmetry breaking condensate to the fermions in order to induce fermion masses. In the minimal model these are the Yukawa couplings, which for the  $u$  and  $d$  quarks are given by

$$\mathcal{L}_f = \sqrt{2}\kappa_u \bar{\chi}_L \Phi u_R + \sqrt{2}\kappa_d \bar{\chi}_L \Phi^c d_R + h.c. \quad (2.19)$$

where  $h.c.$  denotes hermitian conjugate,  $\chi_L = \begin{pmatrix} u \\ d \end{pmatrix}_L = \frac{1 - \gamma_5}{2} \begin{pmatrix} u \\ d \end{pmatrix}$  is the weak isodoublet,  $\Phi$  is defined in equation 2.5 and  $\Phi^c$  is the charge conjugate doublet,

$$\Phi^c = \frac{1}{\sqrt{2}} \begin{pmatrix} (H - iw_3) \\ -(w_1 - iw_2) \end{pmatrix}. \quad (2.20)$$

Shifting  $H \rightarrow H + v$  to account for the vacuum condensate, the quarks  $q = u, d$  acquire masses

$$m_q = \kappa_q v \quad (2.21)$$

so that the Yukawa couplings are given by

$$\kappa_q = \frac{m_q}{v} = \frac{gm_q}{2M_W} \quad (2.22)$$

and are therefore much smaller than the gauge couplings for light quarks with  $m_q \ll M_W$ . The one generation model is completed by adding a similar coupling of  $e_R$  to  $(\nu_e, e)_L$  which generates the electron mass. In the absence of a right-handed neutrino no analogous neutrino coupling is possible.

Before concluding this brief review I want to emphasize one other feature of the minimal Higgs sector that we will see in Section 2.4 is perfectly general. From equations 2.9 and 2.17 we find that

$$\frac{\lambda}{4\pi} = \frac{m_H^2}{8\pi v^2} = \left( \frac{m_H}{1.25 \text{ TeV}} \right)^2 \quad (2.23)$$

so that the interaction is weak and can be analyzed perturbatively,  $\lambda/4\pi \ll 1$ , if  $m_H \ll 1 \text{ TeV}$ , while for  $m_H \gtrsim 1 \text{ TeV}$  the interaction is strong,  $\lambda/4\pi \gtrsim 1$ . The same conclusion emerges by computing the amplitudes for the scattering of longitudinal  $W$ 's and  $Z$ 's in the standard Higgs model at high energy,  $s \gg m_H^2$ , in tree approximation. For  $m_H \geq 1 \text{ TeV}$  the tree amplitudes violate partial wave unitarity, indicating the importance of loop corrections and the failure of perturbation theory.<sup>(12)</sup> Another indication is that the Higgs boson decay width is given approximately by

$$\Gamma_H \cong 0.5 \text{ TeV} \cdot \left( \frac{m_H}{1 \text{ TeV}} \right)^3 \quad (2.24)$$

with  $m_H$  given in TeV, so that for  $m_H \gtrsim 1 \text{ TeV}$  the width becomes of the same order as the mass, and  $H$  has no simple particle interpretation.

We will use low energy theorems in Section 2.4 to show that the relationship between coupling strength and mass scale holds for any symmetry breaking sector,  $\mathcal{L}_{SB}$ , not just for Higgs boson models. That is, the strength of the symmetry breaking interaction, which I will refer to as  $\lambda_{SB}$  in general, and the mass scale  $M_{SB}$  of the quanta that acquire the symmetry breaking vacuum condensate, must be related roughly as in equation 2.9.

## 2.2 Upper Limit on a Heavy Lepton Mass

In this section I will discuss the one loop corrections to the  $\rho$  parameter, equation 2.18, from a very heavy fermion  $f$ ,  $m_f \gg M_W$ . The result for a heavy charged lepton is that  $\rho$  is shifted by<sup>(13,14)</sup>

$$\delta\rho = \frac{G_F m_L^2}{8\sqrt{2}\pi^2} \quad (2.25)$$

provided the neutrino partner  $\nu_L$  is not too heavy. The experimental measurements of  $\rho$  imply<sup>(3,10)</sup> that  $\delta\rho < 0.013$  at the 90% confidence level, which then implies using equation 2.25 that

$$m_L \leq 350 \text{ GeV}. \quad (2.26)$$

We will see below how the bound is affected if the neutrino  $\nu_L$  is massive. For now I only remark that if  $m_{\nu_L} = 50 \text{ GeV}$  — so that the fourth generation would not be “counted” by the  $Z$  decay width — the bound 2.26 would only increase to 375 GeV. Therefore this constraint complements what we will learn from the  $Z$  width.

While a 350 GeV lepton would be copiously produced at the LHC or SSC, detecting it would not be a simple matter. The detection problem is reviewed in Section 3.

The discussion here uses an “old-fashioned” renormalization convention in which  $\sin \theta$  is defined to all orders by equation 2.15, i.e.,  $\sin \theta \equiv e/g$ ; as a result  $\rho = 1$  is corrected in higher orders,  $\delta\rho \neq 0$ . The “modern” convention defines  $\cos \theta \equiv M_W/M_Z$  so that  $\rho \equiv 1$  to all orders by definition in the standard model. Cahn follows the modern convention in his lectures at this workshop.<sup>(15)</sup> It has the practical advantage that the well-measured parameters  $M_W$  and  $M_Z$  are used as input parameters. My old-fashioned convention uses the less well-measured quantity  $g$  as an input parameter. However I prefer the old-fashioned convention here for a pedagogical reason: the result we obtain will have a simple intuitive explanation in terms of the “custodial”  $SU(2)_{L+R}$  symmetry discussed in Section 2.1.

I will now sketch the calculation of the one loop correction following reference (14). The lowest order gauge boson propagator in unitary gauge is

$$D_0^{\mu\nu}(p) = \frac{-i}{p^2 - M_0^2} \left( g^{\mu\nu} - \frac{p^\mu p^\nu}{M_0^2} \right) \quad (2.26)$$

where  $M_0$  is the lowest order mass of the  $W$  or  $Z$ . The one loop contribution to the gauge boson self energy is determined by the one loop contribution to the vacuum polarization tensor,

$$\Pi^{\mu\nu}(p) = - \int d^4x e^{-ip \cdot x} \langle T^* J^\mu(x) J^\nu(0) \rangle_0 \quad (2.27)$$

where  $J^\mu$  is the gauge current that couples to  $W$  or  $Z$  and  $T^*$  denotes the covariant time ordered product. Then the propagator to one loop order is given by

$$D^{\mu\nu} = D_0^{\mu\nu} + g^2 D_0^{\mu\alpha} \Pi^{\alpha\beta} D_0^{\beta\nu}. \quad (2.28)$$

Writing

$$\Pi^{\mu\nu} \equiv g^{\mu\nu} \Pi_1 + p^\mu p^\nu \Pi_2 \quad (2.29)$$

and expanding 2.28 as the first term in a geometric series we find

$$D^{\mu\nu} = \frac{-i}{p^2 - M_0^2 + ig^2 \Pi_1(p^2)} \left( g^{\mu\nu} - \frac{p^\mu p^\nu}{M_0^2} \right) + \dots \quad (2.30)$$

where the terms omitted in 2.30 are proportional to  $p^\mu p^\nu$  and will contribute to the renormalization of the longitudinal component. Renormalizing the propagator at  $p^2 = 0$ , we see from 2.30 that the correction to the mass is

$$\delta M^2 = -ig^2 \Pi_1(0). \quad (2.31)$$

(It is sufficient to consider  $p^2 = 0$  since the effect of renormalizing on shell,  $p^2 = M_{W,Z}^2$ , is a small correction, of order  $M_{W,Z}^2/m_f^2 \ll 1$ , to our result.)

The problem is now reduced to computing the one loop contribution to  $\Pi_1$ . We use dimensional regularization, which requires introduction of an arbitrary mass parameter  $\mu$  that is used to rescale the coupling constant  $g$  in order to maintain a lagrangian of the correct dimension as the dimension of space-time is continued. Following the minimal subtraction procedure, we simply discard the pole at  $n = 4$ . Then for a  $SU(2)_L$  doublet of heavy fermions,  $\begin{pmatrix} F_1 \\ F_2 \end{pmatrix}$ , with  $m_F \equiv m_i \gg M_{W,Z}$ , we find

$$\Pi_{1,W}(0) = -i \frac{\xi g^2}{32\pi^2} \left[ \left( \sum_{i=1}^2 m_i^2 \ln \frac{m_i^2}{\mu^2} \right) + \frac{m_1^2 m_2^2}{m_1^2 - m_2^2} \ln \frac{m_1^2}{m_2^2} - \frac{m_1^2 + m_2^2}{2} \right] \quad (2.32)$$

$$\Pi_{1,Z}(0) = -i \frac{\xi g^2}{32\pi^2} \frac{1}{\cos^2 \theta_W} \sum_{i=1}^2 m_i^2 \ln \frac{m_i^2}{\mu^2} \quad (2.33)$$

where  $\xi = 1$  for leptons and  $=3$  for quarks. Using equation 2.31 we can now compute the heavy fermion contribution to the rho parameter,

$$\delta\rho = \delta \left( \frac{M_W^2}{M_Z^2 \cos^2 \theta_W} \right)$$

$$\begin{aligned} &= \frac{1}{M_W^2} \left( \delta M_W^2 - \frac{\delta M_Z^2}{\cos^2 \theta_W} \right) \\ &= \xi \frac{G_F}{4\sqrt{2}\pi^2} \left( \frac{m_1^2 m_2^2}{m_1^2 - m_2^2} \ln \frac{m_2^2}{m_1^2} + \frac{m_1^2 + m_2^2}{2} \right). \end{aligned} \quad (2.34)$$

The arbitrary parameter  $\mu$  has cancelled in 2.34, as it must since there is no counterterm for  $M_W/M_Z$  and there are no  $O(g^2 m_f^2)$  corrections to  $\cos \theta_W$ .

It is instructive to consider two limits of 2.34. For  $m_1 = m_2$  we find after expanding the logarithm near  $m_1 = m_2$  that the correction vanishes,  $\delta\rho = 0$ . This has a simple physical explanation: for  $m_1 = m_2$  the fermions do not break the custodial  $SU(2)_{L+R}$  discussed in Section 2.1 and therefore  $\rho = 1$  continues to hold. The correction to  $\rho$  given by 2.34 can be understood as the consequence of the breaking of  $SU(2)_{L+R}$  when  $m_1 \neq m_2$ . It is for this insight that I have used the old-fashioned renormalization conventions in this discussion.

The second limit we consider is  $m_1 = 0$ , as would occur for a massless neutrino. Then for  $\xi = 1$  equation 2.34 implies the result for a heavy lepton given in 2.25. Assuming the experimental limit<sup>(3,10)</sup>  $\delta\rho < .013$  (90% C.L.) equation 2.34 implies  $m_L \lesssim 350$  GeV for a heavy lepton with  $m_\nu = 0$ . The limit continues to be strong even if the neutrino is not massless. For instance, for  $m_\nu = 50$  GeV, 100 GeV, or 200 GeV the corresponding upper limits on  $m_L$  are 375 GeV, 415 GeV, and 505 GeV respectively. Since  $m_b$  makes a negligible contribution to 2.34, the experimental limit on  $\delta\rho$  implies a limit on the top quark mass,  $m_t \lesssim 200$  GeV. It also implies that ultra heavy quark doublets cannot have large mass splitting. If we define  $\delta m \equiv m_U - m_D$  and expand 2.34 for  $m_U \gg \delta m$  we find

$$\delta\rho = \frac{G_F(\delta m)^2}{2\sqrt{2}\pi^2}. \quad (2.35)$$

For  $\delta\rho < .013$  this implies  $\delta m < 175$  GeV. The complete constraint including the top quark and a fourth generation with a light neutrino is

$$3m_t^2 + m_L^2 + 4(m_U - m_D)^2 < (350 \text{ GeV})^2. \quad (2.36)$$

Clearly if  $m_t$  approaches its upper limit of 200 GeV, the inequality leaves little room for a fourth generation.

### 2.3 Naturalness

There are two aspects of what is called the “naturalness” or “gauge hierarchy” problem. The first is the physical origin of the very small numbers  $M_W/M_{GUT} \cong 10^{-12}$  or  $M_W/M_{Planck} \cong 10^{-17}$ . The second is a technical problem that is specific to Higgs boson models: even if the gauge hierarchy problem has a natural solution in lowest order, the quadratic divergences associated with scalar fields induce one loop corrections that destroy the hierarchy. In ordinary Higgs boson models these corrections require an order by order fine tuning of the subtraction constants that seems physically unnatural. In this section I will concentrate on this technical naturalness problem.

Two strategies have been proposed to deal with the naturalness problem. One is to suppose that the symmetry breaking sector,  $\mathcal{L}_{SB}$ , does not contain elementary Higgs bosons. In particular, in technicolor models<sup>(16)</sup>  $\mathcal{L}_{SB}$  is presumed to be a confining gauge theory like QCD at a mass scale roughly  $v/F_\pi \sim 2700$  times greater than the GeV mass scale of QCD. Since QCD is known to undergo spontaneous symmetry breaking, with  $SU(2)_L \times SU(2)_R$  breaking to  $SU(2)_{L+R}$ , giving rise to three Goldstone bosons (the pions), it is plausible that a similar theory at a higher mass scale would contain the necessary ingredients for electroweak symmetry breaking.

The second strategy is to provide a principle for the cancellation of the quadratic divergences: supersymmetry.<sup>(17)</sup> In supersymmetric theories the quadratic divergences due to scalar boson loops are precisely cancelled by fermion loop contributions. The remaining finite difference is proportional to the scale of supersymmetry breaking, *e.g.*, the mass differences of the scalar and fermion superpartners. The absence of scalars degenerate with the known leptons and quarks tells us supersymmetry cannot be exact. Naturalness then implies an upper limit on the scale of supersymmetry breaking, since the naturalness problem returns if mass differences of fermion–boson superpartners are too large. To avoid fine-tuning at less than the few percent level, superpartners cannot be heavier than a few TeV.

Supersymmetry and technicolor are discussed in Sections 2.32 and 2.33. It is however important to recognize that nature may have found a way to solve the naturalness problem that has not yet occurred to us. For that reason we will also consider, in Section 3, the general properties of electroweak symmetry breaking that must hold in any theory because of unitarity and gauge invariance.

### 2.31 The Problem Defined

Consider the standard Higgs boson model, reviewed in Section 2.1. The potential  $V$  contains a wrong-sign (tachyonic) mass term for  $\vec{w}$  and  $h$ , given by the coefficient of  $\frac{1}{2}(\vec{w}^2 + h^2)$  in equation 2.7, equal to  $-\lambda v^2$ . Because of the tachyonic sign, the state of minimum energy has a condensate  $v$ , resulting in zero mass for the triplet  $\vec{w}$  and a mass  $+\sqrt{2}\lambda v^2$  for  $h$ . The one loop quantum correction is quadratically divergent,

$$\delta(\lambda v^2) = \frac{9\lambda}{2} \int \frac{d^4\ell}{(2\pi)^4} \frac{1}{\ell^2 + \lambda v^2}. \quad (2.37)$$

Though expressions like equation 2.37 are shocking to novices in field theory, they lose their shock value as the student masters (*i.e.*, is brainwashed by) the renormalization program, which shows that finite predictions can be extracted at the cost of a small number of subtractions or redefinitions. Most notably in the case of quantum electrodynamics this program has been extraordinarily successful. The divergence in equation 2.37 can be removed by introducing a counterterm that in effect shifts the initial value of  $\lambda v^2$  by an infinite constant cancelling the divergence generated in equation 2.37.

In the renormalization program we renounce any attempt to understand the physical origin of those parameters requiring subtraction — their values are simply fit to experiment — but we are then able to obtain finite predictions for all other physical quantities in the theory. To understand the naturalness problem it is necessary to go beyond this limited, though powerful, perspective and to ask questions about the origins of the subtracted quantities, assuming they will eventually be understood and calculable in the context of another theory formulated at a deeper level. The expectation is that the deeper theory introduces new physics at high energy that cuts off the divergent behavior of integrals like equation 2.37. Denoting the energy scale of the new physics by  $\Lambda$ , equation 2.37 would be replaced by

$$\delta(v^2\lambda) = C \frac{\lambda}{2\pi^2} \Lambda^2 \quad (2.38)$$

where  $C$  is a numerical constant of order unity.

Equation 2.38 tells us that the parameters of Higgs models are hypersensitive to the high energy scale of the deeper underlying theory. For example,

the Higgs boson mass, given in lowest order by  $m_H^2 = 2\lambda v^2$ , might reasonably range from tens of MeV to perhaps the TeV scale (see references (18) and (19) for reviews). The scale  $\Lambda$  of the deeper theory might be the scale of Grand Unified Theories,  $M_{\text{GUT}} = O(10^{14})$  GeV, or even the Planck scale suggested by superstring and supergravity models,  $M_{\text{Planck}} = O(10^{19})$  GeV. Writing the physical mass as the sum of a bare mass plus the one loop corrections

$$m_H^2 = m_{H,\text{bare}}^2 + \frac{C\lambda}{\pi^2} \Lambda^2 \quad (2.39)$$

we see that the bare mass must be tuned with exquisite precision to make the left side much smaller than the two terms on the right side. For instance, if  $m_H = 1$  TeV and  $\Lambda = M_{\text{Planck}}$  then the cancellation on the right side must work to one part in  $10^{17}$ ! Of course the renormalization program allows us to arrange the cancellation to any desired precision, but viewed from the perspective of the deeper theory such a cancellation seems extremely unnatural — one might even say, in the absence of any principle requiring or explaining such a cancellation, that it is absurdly implausible.

Though the term is also used in other ways, this is the naturalness problem that uniquely afflicts Higgs boson models. It may be thought of us as an instability of the energy scale of the theory against quantum corrections that tend naturally to drive the scale to violently larger values. The problem uniquely affects Higgs models because in 3 +1 dimensions the only renormalizable theories with quadratic divergences are those containing scalar fields. For instance in unbroken gauge theories like QED or QCD divergences are at most given by powers of logarithms. If instead of the quadratic dependence on  $\Lambda$  in equation 2.39 there were a logarithmic dependence,

$$m_H^2 = m_{H,\text{bare}}^2 + \frac{C\lambda}{\pi^2} m_{H,\text{bare}}^2 \ln \frac{\Lambda}{m_{H,\text{bare}}} \quad (2.40)$$

then no fine tuning would be needed even for  $\Lambda$  as large as  $M_{\text{Planck}}$ .

### 2.32 Supersymmetry

With only one known exception the discussion of Section 2.31 applies to all models with elementary Higgs bosons: in the absence of cancellation all have quadratic divergences that destabilize the electroweak scale, requiring finely tuned subtractions in each order of perturbation theory. The exception is provided by supersymmetric theories<sup>(20)</sup> in which the quadratic divergences cancel

between bosonic and fermionic loops, with only gentle logarithmic divergences remaining that do not require fine tuning.<sup>(17)</sup> The stabilizing mechanism is the combined consequence of chiral symmetry and supersymmetry. Chiral symmetric interactions at high energy cannot communicate their large intrinsic scales to fermion masses. Supersymmetry links scalar and fermion masses so that scalar masses are also protected by the chiral symmetry of the fermionic superpartners.

The hierarchy stability problem is the clue that supersymmetry may be discovered at the few hundred GeV scale of electroweak interactions. The quadratic divergences of the Higgs sector are cured by cancellation of loop contributions between the ordinary particles and their superpartners, *e.g.*, between contributions to the Higgs self energy from the  $W$  boson and its spin 1/2 partner the wino,  $\tilde{W}$ . Since supersymmetry is not an exact symmetry, the cancellation is not exact but leaves a finite contribution, proportional to the difference of the masses squared of particles and superpartners. Calculations show that if the supersymmetry breaking scale is much larger than 1 TeV then fine-tuning (to a few percent or less) again becomes necessary.<sup>(21)</sup> Therefore if supersymmetry is to solve the hierarchy stability problem, superpartner masses cannot be much greater than 1 TeV.

To be specific consider the minimal supersymmetric extension of the standard model.<sup>(22)</sup> It contains two Higgs doublets and the coupling constant  $\lambda$  is required by gauge invariance and supersymmetry to be equal to  $g^2$  (within factors of 2). Minimization of the Higgs potential and the condition  $M_W^2 = \frac{1}{4}g^2(v_1^2 + v_2^2)$ , where  $v_1$  and  $v_2$  are the vacuum expectation values of the two doublets then requires the tachyonic Higgs mass to be given in lowest order by

$$(\mu^2)_{\text{Tree}} = \frac{1}{2} M_W^2. \quad (2.41)$$

In the next order a heavy wino (the fermionic partner of the  $W$ ) would contribute a one loop correction to  $\mu^2$ . Using results from reference (14) I find it is given to leading order in  $M_{\tilde{W}}/M_W \gg 1$  by

$$\delta\mu^2 = \frac{\alpha M_{\tilde{W}}^2}{24\pi \sin^2 \theta_W} \left( 6 \ln \frac{M_{\tilde{W}}}{M_W} + 2 \right) \quad (2.42)$$

where I have set the arbitrary scale of the logarithm equal to  $M_W$ . Comparing 2.42 with 2.39 we see that  $M_{\tilde{W}}$  replaces the cutoff in simple Higgs models. If

$M_{\tilde{W}}$  gets too large we again encounter a fine-tuning problem: since there are no large (power-behaved) corrections to the gauge coupling constant  $g$ , the order of magnitude given by equation 2.41 must be maintained in higher orders to ensure vacuum expectation values of the right scale. If we want to restrict the tuning to  $\sim 50\%$  we require  $\delta\mu^2 < \mu_{T_{ree}}^2$  and 2.42 then implies  $M_{\tilde{W}} < 0.7$  TeV. If we are prepared to tolerate a 90% cancellation in the tuning,  $\delta\mu^2 < 10\mu_{T_{ree}}^2$ , than  $M_{\tilde{W}} < 2$  TeV. If we think a 97% cancellation is plausible,  $\delta\mu^2 < 30\mu_{T_{ree}}^2$ , then  $M_{\tilde{W}} < 3$  TeV. These bounds can be improved by adding loops due to other superparticles.

The conclusion is that if superpartners are much heavier than the TeV scale, then supersymmetry does not help us to understand the technical naturalness problem. Then if supersymmetry occurs in nature above the TeV scale there is no reason to prefer any scale below  $M_{Planck}$  as the mass scale of the superpartners. On the other hand, if supersymmetry does indeed stabilize the electroweak scale against quantum fluctuations then it must be discovered at or below the TeV scale.

### 2.33 Technicolor

Technicolor<sup>(16)</sup> is based on the knowledge of strong interaction dynamics acquired from the study of QCD. In technicolor models the symmetry breaking lagrangian  $\mathcal{L}_{SB}$  is presumed to be an unbroken, confining, non-abelian gauge theory, like  $\mathcal{L}_{QCD}$  but with an intrinsic mass scale of order  $v/F_\pi \cong 246 \text{ GeV}/92 \text{ MeV} \sim 2700$  times larger than in QCD (see reference (23) for a review). Technicolor models do not suffer from the technical naturalness problem because they do not have the quadratic divergences of theories with elementary scalar bosons but only the gentle logarithmic divergences of fermions interacting with massless gauge bosons. Viewed in isolation, the technicolor mass scale is just a parameter introduced to fit the weak scale  $G_F^{-1/2}$ , and as such no insight is gained into the deeper puzzle of the hierarchy between  $v$  and  $M_{Planck}$ . However a unified theory might some day relate both  $v$  and  $F_\pi$  to a higher scale, much as  $F_\pi$  (or  $\Lambda_{QCD}$ ) is related to  $M_{GUT}$  in grand unified theories encompassing  $SU(3)_{Color} \times SU(2)_L \times U(1)_Y$ . I will sketch an unrealistic calculation to show how this could come about.

Just as in QCD the parameter  $\Lambda_{QCD}$  that sets the scale of the strong interactions,  $\alpha_s(\Lambda_{QCD}) = O(1)$ , is of order  $F_\pi = 94 \text{ MeV}$ , similarly in a technicolor

theory we expect  $\alpha_{TC}(\Lambda_{TC}) = O(1)$  for  $\Lambda_{TC} = O(v) \cong O(250 \text{ GeV})$ . The relationship between  $\Lambda_{TC}$  and some higher scale, say  $\Lambda_{GUT}$ , is only logarithmically divergent, so no fine-tuning is needed. In fact the relationship suggests that we might even be able to understand the physics that determines the gauge hierarchy, the fundamental naturalness problem mentioned at the beginning of Section 2.

Suppose the technicolor theory is an  $SU(N_{TC})$  nonabelian gauge theory. Then the coupling constant evolves according to

$$\frac{dg_{TC}(E)}{d \ln E} = -b g_{TC}(E)^3 \quad (2.43)$$

where

$$b = \frac{3N_{TC} - 2n_f}{48\pi^2}. \quad (2.44)$$

Integrating from  $\Lambda_{GUT}$  to  $\Lambda_{TC}$  we get

$$\ln \frac{\Lambda_{GUT}}{\Lambda_{TC}} = \frac{1}{2b} \left( \frac{1}{g_{TC}^2(\Lambda_{GUT})} - \frac{1}{g^2(\Lambda_{TC})} \right). \quad (2.45)$$

The technicolor theory is asymptotically free, so the second term on the right side can be neglected. Then we compute the hierarchy

$$\frac{\Lambda_{GUT}}{\Lambda_{TC}} = \exp \left( \frac{1}{2bg_{TC}^2(\Lambda_{GUT})} \right). \quad (2.46)$$

The hierarchy is then a consequence of the asymptotic freedom of the technicolor theory: for  $2bg^2(\Lambda_{TC}) \ll 1$  the exponential in 2.46 ensures that  $\Lambda_{GUT}/\Lambda_{TC} \gg \gg \dots \gg \gg 1$ . As a specific example, suppose that  $N_{TC} = 4$  and  $n_f = b$ . Suppose also that the  $SU(4)_{TC}$  is unified with  $SU(3)_{Color} \times SU(2)_L \times U(1)_Y$  at  $\Lambda_{GUT}$ . Then  $\alpha_{TC}(\Lambda_{GUT}) = \alpha_{GUT} \cong 1/40$  and  $2bg_{TC}^2(\Lambda_{GUT}) \cong 1/25$  so that 2.46 yields  $\Lambda_{GUT} = 2 \cdot 10^{10} \Lambda_{TC}$  which is a bit small but in the right ballpark.

Unfortunately this toy calculation has a serious problem that I have hidden by setting  $n_f = 6$ . From the point of view of the technicolor sector there are typically many more flavors and the running of  $g_{TC}$  does not yield as encouraging a result as we obtained above.<sup>(24)</sup>

It is very instructive to consider the basic technicolor mechanism, because it reveals a more general view of the Higgs mechanism than comes from Higgs boson

models. We will see how the Higgs mechanism occurs without the existence of physical Higgs bosons.

Following Susskind<sup>(16)</sup> it is amusing and instructive to consider the  $SU(3)_{\text{Color}} \times SU(2)_L \times U(1)_Y$  model in the absence of an additional electroweak symmetry breaking sector,

$$\mathcal{L}_{SB} = 0. \quad (2.47)$$

Equation 2.47 is misleading since it suggests that  $SU(2)_L \times U(1)_Y$  is unbroken, i.e.,  $M_W = M_Z = 0$ . This is wrong — in fact electroweak symmetry would be spontaneously broken by QCD and instead of equation 2.47 we should write

$$\mathcal{L}_{SB} = \mathcal{L}_{\text{QCD}}. \quad (2.48)$$

To be precise consider QCD with two quark flavors,  $u$  and  $d$ , taken to be massless,  $m_u = m_d = 0$ . The theory then has an exact  $SU(2)_L \times SU(2)_R$  global symmetry that breaks spontaneously to the  $SU(2)_{L+R}$  isospin subgroup with three massless Goldstone bosons, the pions. The symmetry breaking vacuum condensate is the scalar quark bilinear

$$\langle \bar{u}_L u_R + \bar{d}_L d_R \rangle \neq 0 \quad (2.49)$$

with nonvanishing  $SU(2)_L$  and  $U(1)_Y$  charges. For pure QCD this would be the end of the story, but in the presence of the gauge sector of the electroweak lagrangian, equation 2.2, the Higgs mechanism occurs. The pions disappear from the meson spectrum while the  $W$  and  $Z$  bosons acquire longitudinal modes and masses,

$$M_W = \frac{g F_\pi}{2} = 29 \text{ MeV} \quad (2.50)$$

with  $M_Z = M_W / \cos \theta_W$  assured by the ordinary isospin symmetry (see Section 2.1).

To derive equation 2.50 consider the vacuum polarization tensor (with imaginary part proportional to the  $\bar{\nu}\nu$  annihilation cross section),

$$\Pi^{\mu\nu}(p) = - \int d^4x e^{-ip \cdot x} \langle T^* J_L^{+\mu}(x) J_L^{-\mu}(0) \rangle_0 \quad (2.51)$$

where  $J_L^{i\mu}$  is the weak current

$$J_L^{i\mu}(x) = \bar{\psi}_L(x) \frac{\tau^i}{2} \gamma^\mu \psi_L(x) \quad (2.52)$$

with  $\psi_L = (u, d)_L$  the weak quark doublet,  $\tau^i$  the conventional Pauli matrices, and  $J^+ = (J^-)^\dagger = J^1 + iJ^2$ . The pion decay constant is defined by

$$\langle 0 | J_L^{+\mu} | \pi^-(p) \rangle = i \frac{F_\pi}{\sqrt{2}} p^\mu. \quad (2.53)$$

Gauge invariance implies conservation of the polarization tensor,  $p_\mu \Pi^{\mu\nu}(p) = 0$ , so that  $\Pi^{\mu\nu}(p)$  is determined by a single Lorentz scalar  $\Pi(p^2)$ ,

$$\Pi^{\mu\nu}(p) = i(p^2 g^{\mu\nu} - p^\mu p^\nu) \Pi(p^2). \quad (2.54)$$

The pion pole contribution is

$$\Pi^{\mu\nu}(p) = -\frac{i}{p^2} p^\mu p^\nu \frac{F_\pi^2}{2} + \dots \quad (2.55)$$

where the factor  $1/p^2$  is the propagator of the massless pion. Consequently the scalar function  $\Pi(p^2)$  acquires a singularity at  $p^2 = 0$ ,

$$\Pi(p^2) = \frac{F_\pi^2}{2} \frac{1}{p^2} + \dots \quad (2.56)$$

The weak polarization tensor is of interest not because of any imminent proposal to build a  $\nu\bar{\nu}$  collider but because it controls the quantum corrections to the  $W$  and  $Z$  propagators and therefore the  $W$  and  $Z$  masses. Choosing Landau gauge, the lowest order  $W$  propagator is

$$D_0^{\mu\nu}(p) = -i(g^{\mu\nu} - \frac{p^\mu p^\nu}{p^2}) \frac{1}{p^2}. \quad (2.57)$$

In higher orders we sum the geometric series

$$\begin{aligned} D^{\mu\nu} &= D_0^{\mu\nu} + \frac{g^2}{2} D_0^{\mu\alpha} \Pi_{\alpha\beta} D_0^{\beta\nu} + \frac{g^4}{4} D_0^{\mu\alpha} \Pi_{\alpha\beta} D_0^{\beta\gamma} \Pi_{\gamma\delta} D_0^{\delta\nu} + \dots \\ &= -i(g^{\mu\nu} - \frac{p^\mu p^\nu}{p^2}) \frac{1}{p^2} \frac{1}{1 - \frac{1}{2} g^2 \Pi(p^2)}. \end{aligned} \quad (2.58)$$

The pole in  $\Pi(p^2)$  then induces a singularity at nonvanishing  $p^2$  in the  $W$  propagator,

$$\frac{1}{p^2(1 - \frac{1}{2} g^2 \Pi(p^2))} = \frac{1}{p^2 - \frac{1}{4} g^2 F_\pi^2}, \quad (2.59)$$



resulting in the  $W$  mass promised in equation 2.50. (Contributions to  $\Pi$  not singular at  $p^2 = 0$  are absorbed in the wave function renormalization or induce finite higher order corrections to the  $W$  propagator.)

In fact this derivation of equation 2.59 is a general derivation of the Higgs mechanism, more general than the one sketched in Section 2.1. It exhibits the essential features of the mechanism: a massless spin zero particle coupled to the gauge current gives a mass to the associated gauge boson. In particular, it is not necessary that there be a physical Higgs particle  $H$  with vacuum condensate  $v$ . Comparing equations 2.10 and 2.59 we see that the role of the vacuum condensate  $v$  in the Higgs boson model is played more generally by the coupling  $F_\pi$  of the Goldstone boson to the gauge current, equation 2.53. (Of course in the Higgs boson model the two are one and the same — a fact familiar to students of the sigma model.<sup>(4)</sup>) The QCD spectrum contains no scalar meson that is a strong candidate to identify with the physical Higgs boson in the world with  $\mathcal{L}_{SB} = \mathcal{L}_{QCD}$ . There must however be  $J = 0$  states with the correct couplings to ensure good high energy behavior of the  $W_L W_L$  scattering amplitudes discussed in Section 2.4 below, but they may be, and in this case probably are, predominantly broad resonances and/or multiparticle states. In QCD chiral symmetry breaking is induced by the condensate of the quark bilinear field, equation 2.49, rather than a scalar boson condensate, and good high energy behavior is assured by the hadron continuum that is dual<sup>(25)</sup> to the  $I = J = 0$  quark-antiquark continuum.

To turn this example into a model that correctly reproduces the  $W$  and  $Z$  masses we let  $\mathcal{L}_{SB}$  be a confining gauge theory with a spontaneously broken  $SU(2)_L \times SU(2)_R \rightarrow SU(2)_{L+R}$  symmetry and with Goldstone boson-gauge current coupling (defined as in equation 2.53 with  $\pi$  replaced by the Goldstone boson  $W$ ) given by

$$F_\pi^{TC} = v = 246\text{GeV}. \quad (2.60)$$

Our experience from QCD is most reliable if  $\mathcal{L}_{SB}$  has  $SU(N_{TC})$  gauge interactions. In that case we are most confident of the hypothesized global symmetry breaking, and in the large  $N_{TC}$  approximation we can naively estimate the technimeson masses. Technimeson masses are to leading order independent of  $N_{TC}$ <sup>(26)</sup> whereas  $F_\pi^{TC}$  is proportional to  $\sqrt{N_{TC}}$ . The  $N_{TC}$  dependence of  $F_\pi^{TC}$  (or the  $N_{QCD}$  dependence of  $F_\pi^{QCD}$ ) is easily deduced for equation 2.53,

since the electroweak gauge current is the sum of  $N_{TC}$  (or  $N_{QCD} = 3$ ) color diagonal terms while the color singlet Goldstone boson wave function is a sum of  $N_{TC}$  color diagonal  $\bar{q}_{TC} q_{TC}$  pairs normalized by a factor  $1/\sqrt{N_{TC}}$  (or  $1/\sqrt{3}$  for QCD.) Since  $F_\pi^{TC}$  and  $F_\pi \equiv F_\pi^{QCD}$  are normalized to their experimental values, 246 GeV and 92 MeV respectively, the result is

$$\frac{M_{\text{Technimeson}}}{M_{\text{Ordinary meson}}} \cong \sqrt{\frac{3}{N_{TC}}} \frac{F_\pi^{TC}}{F_\pi} \quad (2.61)$$

For example, for  $SU(4)$  technicolor the technirho mass is estimated at

$$m_{\rho T} = \sqrt{\frac{3}{4}} \frac{F_\pi^{TC}}{F_\pi} m_\rho = 1.8 \text{ TeV}. \quad (2.62)$$

Since meson widths scale like  $N_{TC}^{-1}$  for large  $N_{TC}$ ,<sup>(26)</sup> the corresponding width is

$$\Gamma_{\rho T} = \frac{3}{4} \frac{m_{\rho T}}{m_\rho} \Gamma_\rho = 260 \text{ GeV}. \quad (2.63)$$

As discussed in Section 3, a  $\sqrt{s} = 40 \text{ TeV}$  proton-proton collider with luminosity  $\mathcal{L} = 10^{33} \text{ cm}^{-2} \text{ sec}^{-1}$  is a minimal machine for observing the signal of the  $SU(4)$  technirho.

## 2.4 Implications of Unitarity and Gauge Invariance

Just as Lee and Yang and Ioffe, Okun and Rudik<sup>(27)</sup> showed using unitarity that the weak interaction quanta must modify Fermi theory scattering amplitudes below  $2\sqrt{2}\pi/G_F \cong (0.9 \text{ TeV})^2$ , similarly the requirements of gauge invariance and unitarity imply that the quanta of the symmetry breaking sector must affect  $W_L W_L$  scattering at or below a scale just twice as large, equation 1.1.<sup>(1,2)</sup> This conclusion is quite general, depending only on the assumption that electroweak interactions are due to a spontaneously broken  $SU(2)_L \times U(1)_Y$  gauge theory.

In this section we will review the derivation of this result and consider some of the consequences. Section 2.41 derives the low energy theorems for scattering of longitudinal  $W$  and  $Z$  bosons. The derivation makes use of the equivalence theorem and of the global symmetry that the symmetry breaking sector must have in order to avoid explicit breaking of the  $SU(2)_L \times U(1)_Y$  gauge symmetry. Section 2.42 concerns the implications of the low energy theorems. We show that

unitarity requires equation 1.1, that the symmetry breaking interaction must be strongly interacting if the associated quanta lie above 1 TeV, and that a general strategy to find the symmetry breaking quanta requires that we measure the  $W_L W_L$  scattering amplitude in the energy interval between 1 and 2 TeV.

### 2.41 Low Energy Theorems

In order to implement spontaneous symmetry breaking, the lagrangian of the symmetry breaking sector,  $\mathcal{L}_{SB}$ , must possess a global symmetry group  $G$  — analogous to the flavor symmetry of QCD — which breaks by asymmetry of the vacuum to a smaller group  $H$ ,

$$G \rightarrow H. \quad (2.64)$$

Gauge invariance requires that  $G$  include the electroweak  $SU(2)_L \times U(1)_Y$  and that  $H$  include the unbroken electromagnetic  $U(1)$ . For each broken generator of  $G$  there is a massless Goldstone boson in the spectrum of  $\mathcal{L}_{SB}$ . Three of these couple to the weak currents and are denoted  $w^\pm, z$ . Others, if any, are denoted by  $\{\phi_i\}$ . Including the electroweak gauge interactions, the Goldstone triplet  $w^\pm, z$  become longitudinal gauge boson modes  $W_L^\pm, Z_L$ , and the  $\{\phi_i\}$  acquire small masses  $O(gM_{SB})$ , becoming “pseudo-Goldstone” bosons.

As an example, for two flavor QCD with massless quarks the global symmetry  $G$  is  $SU(2)_L \times SU(2)_R$ . After spontaneous symmetry breaking the surviving invariance group is  $H = SU(2)_{L+R}$  which is just the isospin group. There are three broken generators, corresponding to the axial generators of  $SU(2)_{L-R}$ , so that three massless Goldstone bosons emerge,  $\pi^\pm$  and  $\pi^0$ . If there were no other symmetry breaking physics,  $\mathcal{L}_{SB}$ ,  $\pi^\pm$  and  $\pi^0$  would indeed become longitudinal modes of  $W^\pm$  and  $Z$ , which would however have masses of  $\sim 30$  MeV as shown in Section 2.33.

The statement that the longitudinal modes  $W_L^\pm, Z_L$  are identified with the Goldstone bosons  $w^\pm, z$  is given a precise meaning by the equivalence theorem,

$$M(W_L(p_1)W_L(p_2)\dots) = M(w(p_1)w(p_2)\dots)_R + O\left(\frac{M_W}{E_i}\right). \quad (2.65)$$

In eq. 2.65 the left side is a gauge-invariant S-matrix element involving longitudinal modes while the right side is the corresponding Goldstone boson amplitude in an  $R$  or renormalizable gauge. As indicated in eq. 2.65, the equivalence holds

at energies large compared to the  $W$  and  $Z$  masses. We can use the equivalence theorem to translate statements about Goldstone boson scattering amplitudes into statements about scattering of longitudinally polarized  $W$ 's and  $Z$ 's.

The equivalence theorem was proved in tree approximation in reference (28) and to all orders in both gauge and symmetry breaking interactions in reference (1) (see also reference (29)). The validity of the theorem to all orders in  $\lambda_{SB}$  is crucial since we wish to apply it when  $\mathcal{L}_{SB}$  is strongly interacting and perturbation theory in  $\lambda_{SB}$  fails. Intuitively the theorem is a plausible consequence of the Higgs mechanism that transmutes the Goldstone bosons  $w$  and  $z$  into the longitudinal gauge boson modes  $W_L$  and  $Z_L$ . This is seen explicitly by the gauge transformation from a renormalizable gauge — in which the Goldstone boson fields appear in the lagrangian — to the unitary gauge in which the Goldstone fields do not appear.<sup>(7)</sup> Nevertheless the proof to all orders<sup>(1)</sup> is lengthy and complicated, making use of the BRS identities which embody the full content of gauge invariance in spontaneously broken gauge theories. Here I will only state the theorem and illustrate it with a simple example.

In addition to being useful in the derivation of the  $W_L W_L$  low energy theorems, equation 2.65 greatly simplifies perturbative calculations for heavy — and therefore strongly coupled — Higgs systems (see Lee et al.<sup>(12)</sup> and references (1), (14), and (30)). For instance, to correctly evaluate heavy Higgs boson production and decay by  $WW$  fusion in unitary gauge requires evaluation of many diagrams with “bad” high energy behavior that cancel to give the final result.<sup>(31–33)</sup> But to leading order in the strong coupling  $\lambda = m_H^2/2v^2$  it suffices using equation 2.65 to compute just a few simple diagrams using the interactions of the scalar potential, equation 2.8. The result embodies the cancellations of many diagrams in unitary gauge and trivially has the correct high energy behavior. On the other hand, unitary gauge calculations of Higgs boson production in the  $s$ -channel pole approximation<sup>(34)</sup> have bad high energy behavior and overestimate the yield for heavy Higgs bosons,  $m_H \geq 800$  GeV.

As a simple example, consider the decay of a heavy Higgs boson to  $W_L^+ W_L^-$ . In unitary gauge the  $HW_L^+ W_L^-$  amplitude is

$$\mathcal{M}(H \rightarrow W_L^+ W_L^-) = gM_W \epsilon_L(p_1) \cdot \epsilon_L(p_2). \quad (2.66)$$

For  $m_H \gg M_W$  we neglect terms of order  $M_W/m_H$ , so that  $\epsilon_L^\mu(p_i) \cong p_i/M_W$

and similarly from  $m_H^2 = (p_1 + p_2)^2 \cong 2p_1 \cdot p_2$  we find

$$\mathcal{M}(H \rightarrow W_L^+ W_L^-) = g \frac{m_H^2}{2M_W} + O\left(\frac{M_W}{m_H}\right). \quad (2.67)$$

In a renormalizable gauge the corresponding amplitude can be read off (taking care with factors of 2) from the  $Hww$  vertex in the potential, equation 2.8,

$$\mathcal{M}(H \rightarrow w^+ w^-) = 2\lambda v. \quad (2.68)$$

Using equations 2.9 and 2.10 it is easy to see that equations 2.67 and 2.68 are indeed equal up to  $M_W/m_H$  corrections.

The accuracy of the equivalence theorem can be judged in figure (2) taken from reference (35). The scattering cross sections for  $W_L^+ W_L^- \rightarrow W_L^+ W_L^-$  and  $W_L^+ W_L^- \rightarrow Z_L Z_L$  are computed in the standard model with  $m_H = 1$  TeV. The exact calculations are compared with the result obtained from the equivalence theorem. For  $\sqrt{s} \gtrsim 800$  GeV the agreement is very good and above 1 TeV the two calculations are indistinguishable on the figure.

As an immediate application, consider the case<sup>(1)</sup> in which the global symmetry  $G$  includes  $SU(2)_L \times SU(2)_R$  and  $H$  includes an  $SU(2)_{L+R}$ . For such theories, which includes the case of the standard Higgs model as discussed in Section 2.1,  $\rho = 1$  up to electroweak corrections and we may immediately apply the pion low energy theorems that were derived from current algebra for just this case. For pions we have<sup>(8)</sup>

$$M(\pi^+ \pi^- \rightarrow \pi^0 \pi^0) = \frac{s}{F_\pi^2} \quad s \ll 1 \text{ GeV}^2 \quad (2.69)$$

and for  $\mathcal{L}_{SB}$  with no particles other than  $W, Z$  that are light compared to  $M_{SB}$  we would have

$$M(w^+ w^- \rightarrow zz) = \frac{s}{v^2} \quad s \ll M_{SB}^2 \quad (2.70)$$

where  $v = 0.246$  TeV. Using the equivalence theorem this becomes a statement about the scattering of  $W_L$  and  $Z_L$  in an intermediate energy domain:<sup>(1)</sup>

$$M(W_L^+ W_L^- \rightarrow Z_L Z_L) = \frac{s}{v^2} \quad M_W^2 \ll s \ll M_{SB}^2. \quad (2.71)$$

It is important to stress that the pion low energy theorems were derived before the discovery of QCD. This was possible because they depend only on the

symmetry and not on dynamics. Furthermore they are valid to all orders in the strong interactions. The low energy theorems and other current algebra results were important steps toward the discovery of QCD because they provided a reliable method to study the symmetries of a strongly coupled theory that could not be studied using perturbation theory.

The assumptions used above,  $G \supset SU(2)_L \times SU(2)_R$  and  $H \supset SU(2)_{L+R}$ , are sufficient to guarantee  $\rho = 1$  to all orders in  $\lambda_{SB}$  but they are not necessary conditions for  $\rho = 1$ . We are therefore motivated to derive the low energy theorems for all candidate groups  $G$  and  $H$  and for all values of  $\rho$ . The problem we face is equivalent to that of obtaining the pion-pion scattering low energy theorems in the absence of isospin symmetry. The low energy theorems are derived by three different methods:<sup>(2)</sup> a perturbative power counting analysis, nonlinear chiral lagrangians, and current algebra. I will sketch the current algebra derivation below. Along with the low energy theorems for general values of  $\rho$ , the derivation establishes a limited converse to the result quoted above: we find that if  $\rho = 1$  then the Goldstone boson sector consisting of  $w^\pm, z$  possesses an effective  $SU(2)_{L+R}$  symmetry ("custodial"  $SU(2)$ ) in the low energy domain  $s \ll M_{SB}^2$ .

Briefly the derivation is as follows. The global symmetry  $G$  must be at least as large as the gauge group,  $G \supset SU(2)_L \times U(1)_Y$ , so in particular we have the  $SU(2)_L$  charge algebra

$$[L_a, L_b] = i\epsilon_{abc} L_c \quad (2.72)$$

where the corresponding local currents  $L_a^\mu$  can generally be expanded in terms of the Goldstone triplet  $w^\pm, z$  as

$$L_a^\mu = \frac{1}{2} r_a \epsilon_{abc} w_b \partial^\mu w_c - \frac{1}{2} f_a \partial^\mu w_a + \dots \quad (2.73)$$

with terms involving heavy fields omitted. Since  $H \supset U(1)_{EM}$  we have  $f_1 = f_2$  and  $r_1 = r_2$ . The  $f_a$  are analogues of the PCAC constant and determine the gauge boson masses,

$$M_W = \frac{1}{2} g f_1, \quad (2.74)$$

$$\rho = (f_1/f_3)^2. \quad (2.75)$$

Corrections are suppressed by inverse powers of order  $M_{SB}$  or, because of quantum corrections, by inverse powers of  $4\pi f_a$ .

It is straightforward to show that the  $SU(2)_L$  algebra requires

$$r_1 = \frac{1}{\sqrt{\rho}}, \quad (2.76)$$

$$r_3 = 2 - \frac{1}{\rho}, \quad (2.77)$$

so that the parameters  $r_a$  and  $f_a$  in eq. 2.73 are completely determined in terms of  $G_F$  and  $\rho$ . In particular,  $\rho = 1$  implies  $f_1 = f_2 = f_3$  and  $r_1 = r_2 = r_3 = 1$  which means that the Goldstone boson contributions to  $L_a^\mu$  are the difference of  $SU(2)$  vector and axial vector currents. The existence of this vector  $SU(2)$  triplet of currents establishes the converse alluded to above.

The rest of the derivation is much like the usual current algebra derivation<sup>(8)</sup> except that we do not assume an  $SU(2)_{L+R}$  isospin invariance. Consequently pole terms which are forbidden by  $G$ -parity in the pion case are not forbidden here. Assuming that  $w^\pm$ ,  $z$  saturate these pole terms we find Goldstone boson low energy theorems such as

$$M(w^+ w^- \rightarrow zz) = \frac{s}{f_1^2} \frac{1}{\rho} \quad s \ll M_{SB}^2 \quad (2.78)$$

which using 2.74 reduces to 2.70 for the case  $\rho = 1$ . By the equivalence theorem we have then

$$M(W_L^+ W_L^- \rightarrow Z_L Z_L) = \frac{s}{v^2} \frac{1}{\rho} \quad M_W^2 \ll s \ll M_{SB}^2 \quad (2.79)$$

with  $v = f_1 \cong 2M_W/g$ . The other two independent amplitudes are

$$M(W_L^+ W_L^- \rightarrow W_L^+ W_L^-) = -\frac{u}{v^2} \left(4 - \frac{3}{\rho}\right), \quad (2.80)$$

$$M(Z_L Z_L \rightarrow Z_L Z_L) = 0, \quad (2.81)$$

and by crossing we have also

$$M(W_L^\pm Z_L \rightarrow W_L^\pm Z_L) = \frac{t}{v^2} \frac{1}{\rho}, \quad (2.82)$$

$$M(W_L^+ W_L^+ \rightarrow W_L^+ W_L^+) = M(W_L^- W_L^- \rightarrow W_L^- W_L^-) = -\frac{s}{v^2} \left(4 - \frac{3}{\rho}\right). \quad (2.83)$$

Like 2.79, eqs. 2.80 – 2.83 are valid in the intermediate domain  $M_W^2 \ll E_i^2 \ll M_{SB}^2, (4\pi v)^2$ .

It is also instructive to consider the perturbative power counting analysis. It does not use the equivalence theorem since it is carried out in unitary gauge. This derivation shows directly that the low energy theorems follow from the form of the  $SU(2)_L \times U(1)_Y$  gauge interactions. It reveals an amusing coincidence of the threshold behavior determined by the low energy theorems and the famous “bad” high energy behavior that a massive Yang-Mills theory would have if the masses were not “softly” generated by spontaneous symmetry breaking.

Consider first the minimal Higgs model. Though we are ultimately interested in working to order  $g^2$  in the electroweak gauge coupling and to all orders in the Higgs coupling  $\lambda_{SB}$ , we begin by examining  $W_L^+ W_L^- \rightarrow Z_L Z_L$  scattering to tree approximation in both couplings. The tree approximation amplitude in unitary gauge can be decomposed into the sum of a gauge sector term and a symmetry breaking sector term,

$$\mathcal{M}(W_L^+ W_L^- \rightarrow Z_L Z_L) = \mathcal{M}_{gauge} + \mathcal{M}_{SB}. \quad (2.84)$$

We will evaluate the amplitude for  $s \gg M_W^2$ . The first term,  $\mathcal{M}_{gauge}$ , is given by the sum of  $t$  and  $u$  channel  $W$  exchanges and by the four point contact interaction. Independent of the nature of the symmetry breaking sector it is a universal function of  $M_W$  and  $\rho$ ,

$$\mathcal{M}_{gauge} = \frac{g^2 s}{4\rho M_W^2}. \quad (2.85)$$

The second term,  $\mathcal{M}_{SB}$ , is in tree approximation just given by  $s$ -channel Higgs exchange,

$$\mathcal{M}_{SB} = -\frac{g^2 s}{4M_W^2} \frac{s}{s - m_H^2}. \quad (2.86)$$

$\mathcal{M}_{SB}$  has the famous “bad” high energy behavior that is cancelled at infinite  $s$  by  $\mathcal{M}_{gauge}$  (since  $\rho = 1$  in the minimal Higgs model). However for  $s \ll m_H^2$ ,  $\mathcal{M}_{SB}$  is negligible, so for the low energy domain  $M_S^2 \ll s \ll m_H^2$  we have

$$\begin{aligned} \mathcal{M}(W_L^+ W_L^- \rightarrow Z_L Z_L) &\cong \mathcal{M}_{gauge} \\ &\cong \frac{g^2 s}{4\rho M_W^2}. \end{aligned} \quad (2.87)$$

Using  $M_W = gv/2$  this agrees precisely with equation 2.79 obtained from the current algebra derivation. So the form of the low energy amplitude is determined by the “bad” ultraviolet behavior. Equations 2.80 – 2.83 can be derived by similar means.

Though to this point we have only obtained the theorems in tree approximation for the minimal Higgs model, we can extend the derivation to all orders in  $\lambda_{SB}$  for any symmetry breaking sector with no light particles. By power counting one can show that the only strong corrections to the low energy amplitudes are absorbed as renormalizations of  $M_W$  and  $\rho$ . All other quantum corrections due to the symmetry breaking sector are screened by an extra power of the electroweak coupling constant,  $\alpha_W/\pi = g^2/4\pi^2$ , or they are suppressed by powers of  $s/M_{SB}^2$ , where  $M_{SB}$  is the characteristic scale of the spectrum of the symmetry breaking sector. For details see reference (2).

If other light particles are present, such as pseudo-Goldstone bosons, they may or may not cause the low energy theorems to be modified. QCD is an example of a theory in which additional light particles do not cause modifications. That is, the  $\pi\pi$  low energy theorems obtained from  $SU(2)_L \times SU(2)_R$  symmetry are not affected by the existence of  $K$  and  $\eta$  Goldstone bosons if  $SU(2)_L \times SU(2)_R$  is embedded in a spontaneously broken  $SU(3)_L \times SU(3)_R$ .

### 2.42 Unitarity

Perhaps the most interesting application of the low energy theorems is to use them to estimate the generic signal we should expect if  $\mathcal{L}_{SB}$  is a strongly coupled sector at the TeV scale or above. The problem we face is like the one that physicists of the 1930's would have faced if they knew nothing of nuclei, baryons or other hadrons, but had discovered the pion, measured the PCAC constant  $F_\pi$ , and recognized (!?) the pion as an almost Goldstone boson. They would have then been able to derive the pion-pion low energy theorems, such as eq. 2.69, and the problem would be to use this information to reconstruct the scale of hadron physics. Though it would take a skilled writer of science fiction to make this a plausible plot line for the 1930's, it is precisely the situation we are in today if  $\mathcal{L}_{SB}$  is strongly coupled: our pions are the longitudinal modes of  $W$  and  $Z$ , our “PCAC” constant is  $v = 0.25$  TeV, and we have the low energy theorems eqs. 2.79 – 2.83.

The central ingredient in our considerations is unitarity. The linear growth in  $s, t, u$  of the amplitudes 2.79 – 2.83 cannot continue indefinitely or unitarity would be violated. For instance the  $W_L W_L \rightarrow Z_L Z_L$  amplitude 2.79 is pure  $s$ -wave. If we adopt the low energy amplitude 2.79 as a model of the absolute value of the scattering amplitude, then the  $J = 0$  partial wave amplitude is<sup>(1)</sup>

$$|a_0(W_L^+ W_L^- \rightarrow Z_L Z_L)| = \frac{s}{16\pi v^2} \quad (2.88)$$

where here and hereafter we set  $\rho = 1$ . Unitarity requires  $|a_0| \leq 1$  so we see that the growth of  $a_0$  must be cut off at a scale  $\Lambda$  with

$$\Lambda \leq 4\sqrt{\pi}v = 1.75 \text{ TeV}. \quad (2.89)$$

Using  $v^2 = 1/\sqrt{2}G_F$  this is equivalent to equation 1.1. At the cutoff  $\sqrt{s} = \Lambda$  the order of magnitude of the amplitude is

$$|a_0(\Lambda)| = \frac{\Lambda^2}{16\pi v^2}. \quad (2.90)$$

For  $\Lambda \lesssim \frac{1}{2}$  TeV we have  $|a_0(\Lambda)| \ll 1$  indicating a weakly interacting theory for the symmetry breaking dynamics  $\mathcal{L}_{SB}$ , while for  $\Lambda \gtrsim 1$  TeV we have  $|a_0(\Lambda)| \cong O(1)$ , the hallmark of a strong interaction theory. The most likely dynamics is that the cutoff scale  $\Lambda$  is of the order of  $M_{SB}$ , the mass scale of the new quanta. Then for  $\Lambda \cong O(M_{SB})$  eq. 2.90 generalizes the Higgs model relationship, eq. 2.9, between the mass scale of the new quanta and the strength of the new interactions: weak coupling for  $M_{SB} \ll 1$  TeV and strong coupling for  $M_{SB} \gtrsim O(1)$  TeV.

A weak coupling example is provided by the standard Higgs model with a light Higgs boson,  $m_H \ll 1$  TeV, which can be treated perturbatively. Then  $a_0(W_L W_L \rightarrow Z_L Z_L)$  is given in tree approximation by (where I neglect  $M_W^2/s$ )

$$a_0 = \frac{-s}{16\pi v^2} \frac{m_H^2}{s - m_H^2}. \quad (2.91)$$

For  $s \ll m_H^2$  this agrees with the low energy theorem 2.88 while for  $s \gg m_H^2$  it saturates at the constant value  $m_H^2/16\pi v^2$ . Comparing with 2.90 we see that  $m_H$  indeed provides the scale for  $\Lambda$  in the standard Higgs model.

A strong interaction example is provided by hadron physics. For the  $J = I = 0$  partial wave, the low energy theorem gives

$$a_{00}(\pi^+ \pi^- \rightarrow \pi^0 \pi^0) = \frac{s}{16\pi F_\pi^2} \quad (2.92)$$

with  $F_\pi = 92$  MeV. Eq. 2.92 saturates unitarity at  $4\sqrt{\pi}F_\pi = 650$  MeV which is indeed the order of the hadron mass scale. The  $a_{11}$  and  $a_{02}$  amplitudes saturate at 1100 and 1600 MeV.

The two generic possibilities are illustrated in figure (3). For weak coupling the partial wave amplitudes saturate at values small compared to 1 giving rise to narrow resonances at masses well below 1 TeV. For strong coupling they saturate the unitarity limit with broad resonances in the TeV range.

These results suggest a general experimental strategy to search for the symmetry breaking sector.  $W_L W_L$  fusion at a pp collider probes the interaction of the symmetry breaking sector as shown in figure (4). Since the initial  $W_L W_L$  pair are off mass shell, they must rescatter to appear in the final state as real on-shell particles. Therefore this process measures the strength of the  $W_L W_L$  interaction which we know from the equivalence theorem is essentially the strength of the interaction of the symmetry breaking sector  $\mathcal{L}_{SB}$ . Counting powers the  $W_L W_L$  fusion amplitude is  $O(g^2 \lambda_{SB})$ . It must be compared to the  $O(g^2)$  background due to  $\bar{q}q \rightarrow WW$ . The gauge bosons produced in this way are predominantly transversely polarized, but they cannot be efficiently separated from the longitudinal pairs at the necessary statistical level. Therefore the  $W_L W_L$  fusion signal can be visible above the  $\bar{q}q \rightarrow WW$  background only if  $\lambda_{SB} = O(1)$ , that is, if  $\mathcal{L}_{SB}$  is strongly interacting.

We will see in detail in Section 3 that for the  $ZZ$ ,  $WZ$ , and  $W^+W^-$  channels, the signal can only emerge over the  $\bar{q}q$  annihilation backgrounds for  $M_{WW} > 1$  TeV. This in turn requires a pp collider of at least the SSC design parameters,  $\sqrt{s} = 40$  TeV and  $\mathcal{L} = 10^{33} \text{cm}^{-2} \text{sec}^{-1}$ . It is unlikely that lower energy can be compensated by higher luminosity for this particular physics, as discussed in Section 3.

The strategy then is to look for an excess of gauge boson pair events with  $M_{WW}$  between 1 and 2 TeV. If there is no excess then we learn that  $\mathcal{L}_{SB}$  is weakly interacting and that the new physics, probably Higgs bosons, lies below 1 TeV. If an excess is found we learn that  $\mathcal{L}_{SB}$  is strong and that the new quanta lie above 1 TeV. Then at the SSC we would have a good chance to find the lightest resonances of this new world of particles, since the unitarity bound 1.1 suggests that they cannot be much heavier than  $\sim 2$  TeV.

This can be summarized by the “No-Lose Corollary” to the low energy theorems. It applies for a collider that is able to produce an observable 1 - 2 TeV  $W_L W_L$  signal if  $\mathcal{L}_{SB}$  is strongly interacting. For such a collider we have the

*No-Lose Corollary:*

*Either there are light ( $\ll 1$  TeV) particles from  $\mathcal{L}_{SB}$  that can be produced and studied directly*

*and/or*

*Excess  $WW$ ,  $WZ$ ,  $ZZ$  production is observable, signaling strongly-coupled  $\mathcal{L}_{SB}$  with  $M_{SB} \gtrsim 1$  TeV.*

In Section 3.4 we will discuss the one known exception: the standard model Higgs boson if  $2m_t < m_H < 2M_W$ . However even in this case the absence of the 1-2 TeV  $W_L W_L$  scattering signal conveys useful information. Usually a negative search leaves us wondering whether we must search at higher energies. But the absence of the 1-2 TeV signal would be an unambiguous indication to search the sub-TeV region as carefully and completely as possible.

### 3. PHYSICS SIGNALS AT MULTI-TeV pp COLLIDERS

In this section I want to present a rough idea of the signals that could be observed at the SSC or LHC corresponding to the physics topics discussed in Section 2. I will begin with a very brief and incomplete discussion of the QCD backgrounds. Then I will discuss what I call "reconnaissance", i.e., open-ended searches for new physics where there are typically no strong theoretical landmarks to tell us whether or at what scale such physics might occur. The topics under this heading are composite structure of quarks and leptons, heavy charged or neutral gauge bosons, and further generations of quarks and leptons. The second topic is supersymmetry, which must emerge at or below the TeV scale if SUSY is part of the solution to the naturalness problem, as discussed in Section 2.3. The final topic is the symmetry breaking sector — Higgs bosons or a new world of strong quanta above 1 TeV — that must emerge at or below the  $\sim 2$  TeV unitarity scale derived in Section 2.4.

I will typically assume an instantaneous luminosity  $\mathcal{L} = 10^{33} \text{cm}^{-2} \text{sec}^{-1}$ . Then a typical experiment of  $10^7$  sec will acquire an integrated luminosity of  $10^{40} \text{cm}^{-2} = 10^4 \text{pb}^{-1}$ , meaning that a cross section of  $1 \text{pb} = 1$  picobarn =  $10^{-36} \text{cm}^2$  will correspond to  $10^4$  events.

In addition to more specialized papers I will draw heavily on the EHLQ review,<sup>(36)</sup> the LHC La Thuile study,<sup>(37)</sup> the Snowmass series of SSC studies,<sup>(38-39)</sup> and the 1987 SSC detector workshop.<sup>(40)</sup> The interested reader would do well to browse these references to become familiar with the range of studies. Though a great deal of work has been done, much more remains to be done, by theorists and experimenters. As the remainder of this section will show, many important questions remain about the observability of the physics signals. New ideas and more careful studies are badly needed.

#### 3.1 QCD

QCD phenomena at the LHC and SSC form an enormous and complex subject that is essential for the extraction of *all* new physics. This is already clear from the extent that QCD based Monte Carlo have been crucial to the analysis of the data obtained by UA-1/2 and more recently by CDF. In these talks there is neither the time nor the expertise to do more than scratch the surface. More theoretical work together with the analysis of data from the SPS

and Tevatron  $\bar{p}p$  colliders will be essential for effective utilization of the SSC and LHC.

#### 3.11 Structure Functions

Given the proton-proton luminosity, we need the proton structure functions to compute the corresponding quark-quark, quark-gluon, and gluon-gluon luminosities. We define  $f_i(x, Q^2)$  as the probability distribution  $dP_i/dx$  to find parton "i" in the proton probed at momentum scale  $Q$  with momentum fraction  $x = p_i/P$  of the total proton momentum. Then for a collision of partons 1 and 2 the parton center of mass energy is  $W^2 \equiv s_{12} = (p_1 + p_2)^2 \cong 2p_1 \cdot p_2 = x_1 x_2 (2P \cdot P')$  where  $P$  and  $P'$  are the four-momenta of the colliding protons. Therefore we have  $W^2 = x_1 x_2 s$ . The quantity  $\tau$  is defined by  $\tau \equiv W^2/s$ , so  $\tau = x_1 x_2$  if parton and proton masses can be neglected.

The effective luminosity for collisions of parton  $i$  with parton  $j$  is then

$$\begin{aligned} \frac{d\mathcal{L}_{ij}(Q^2)}{dW^2} &= \int dx_1 dx_2 \delta(W^2 - x_1 x_2 s) f_i(x_1, Q^2) f_j(x_2, Q^2) \\ &= \frac{1}{s} \int \frac{dx_1}{x_1} f_i(x_1, Q^2) f_j\left(\frac{W^2}{x_1 s}, Q^2\right). \end{aligned} \quad (3.1)$$

The inclusive cross section to produce a partonic final state  $f$  is obtained by summing over all relevant partonic subprocesses  $ij \rightarrow f$ ,

$$\frac{d\sigma(pp \rightarrow f + \dots)}{dW^2} = \sum_{ij} \frac{d\mathcal{L}_{ij}(Q^2)}{dW^2} \hat{\sigma}(ij \rightarrow f)_W. \quad (3.2)$$

The structure functions are determined by using low energy deep inelastic scattering data to obtain fits to the  $f_i(x, Q_0^2)$  at some rather small value of  $Q_0$  and then evolving to higher  $Q^2$  using either the renormalization group or, equivalently, the Altarelli-Parisi equations. In practice  $\nu$  and  $\bar{\nu}$  scattering data is used to determine the  $f_i(x, Q_0^2)$ , since it provides the largest statistics and best accuracy.

For instance, the EHLQ<sup>(36)</sup> distributions use CDHS  $\nu$  and  $\bar{\nu}$  data at  $Q_0^2 = 5 \text{GeV}^2$  and  $x > .01$ . The data determine the distribution functions for the valence  $u$  and  $d$  quarks and for the sea quark components consisting of  $u, d, s, \bar{u}, \bar{d}, \bar{s}$ . The  $s$  and  $\bar{s}$  components are extracted by analyzing dimuon events due to charm and anti-charm production in charged current scattering from  $s$  and  $\bar{s}$  quarks.

Assuming the  $u$  and  $d$  sea components to be isosinglet, the result is a fit to the six distribution functions  $u, d, s, \bar{u}, \bar{d}, \bar{s}(x, Q_0^2)$ . The gluon distribution function  $g(x, Q_0^2)$  is then determined by introducing an ansatz for its form as a function of  $x$  and using the momentum sum rule to determine the normalization. At  $Q_0^2 = 5 \text{ GeV}^2$  the proton is assumed to have negligible components of  $c, b,$  and  $t$  quarks; they appear in the proton wave function at larger  $Q^2$  by perturbative evolution via  $g \rightarrow \bar{c}c, \bar{b}b, \bar{t}t$ .

There are three principal sources of uncertainty in this procedure:

- the form of the  $x$  dependence assumed for  $g(x, Q_0^2)$
- the value of  $\Lambda_{QCD}$
- the absence of low  $Q_0^2$  data for  $x < .01$

It is of course necessary to explore the sensitivity of the results to these uncertainties. The lack of low  $x$  data will be alleviated when HERA data is available. Fortunately there is a tendency for the structure functions to “converge” as they are evolved to large  $Q^2$  despite variations in the form assumed for  $g(x, Q_0^2)$  at low  $Q_0^2$ , as we will see below.

The Altarelli-Parisi equations<sup>(41)</sup> are useful computationally and for providing an intuitive picture of the large  $Q^2$  evolution. Consider quark “ $i$ ” at some scale  $Q^2$  with distribution function  $q_i(x, Q^2)$ . At a larger scale  $Q^2 + dQ^2$  it has an amplitude to dissociate into a quark and gluon, determined by the simple bremsstrahlung Feynman diagram for  $q_i \rightarrow q_j + g$ . The probability of dissociation is just the square of that amplitude, the “splitting function”,  $\alpha_s \gamma_{ji}(x/x')$ , where  $x'$  is the proton momentum function of the “parent” quark  $i$  and  $x$  of the “child”  $j$ . The Altarelli-Parisi equation for the evolution of  $q_i$  is then

$$\frac{\partial q_j(x, Q^2)}{\partial \ln Q^2} = \alpha_s(Q^2) \int_x^1 \frac{dx'}{x'} \sum_j \gamma_{ij} \left( \frac{x}{x'} \right) f_j(x', Q^2) \quad (3.3)$$

where the sum is over all possible parton “parents”  $j$  that can give rise to the “child”  $i$ .

We see from this algorithm that  $f_i(x, Q^2)$  is determined by the  $f_j(x', Q_0^2)$  in the domain  $x' > x$ , so we cannot directly compute the  $f_i(x, Q^2)$  for values

of  $x$  below the  $x$  range of the initial value data set at  $Q_0^2$ . We also see that as  $Q^2$  increases the  $f_i(x, Q^2)$  evolve toward small  $x$ . This behavior is shown in figures (5) and (6) for the valence  $u$  quark and gluon distributions.<sup>(36)</sup> It explains the relative insensitivity of the high  $Q^2$  gluon structure function to the form assumed at low  $Q_0^2$ .

Convoluting the distribution functions according to equation 3.1 we obtain the partonic luminosity functions, which are crucial for establishing the discovery potential of the pp colliders. The ratio of several luminosity functions for  $\sqrt{s} = 40 \text{ TeV}$  compared to  $17 \text{ TeV}$  are shown in figure (7), taken from the La Thuile workshop.<sup>(37)</sup> The greatest dependence on collider energy occurs in the  $gg$  and  $W_L W_L$  luminosity functions, corresponding to the dominant production channels for heavy squark/gluino production and for heavy Higgs boson production respectively. At  $\sqrt{s} = 1 \text{ TeV}$  the ratio of these luminosities is of order 10 and it rises steeply for larger values of  $\hat{s}$ .

### 3.12 Calibration Studies

Fortunately we are not completely at the mercy of theorists for knowledge of the distribution functions. One of the most important initial tasks at the LHC and SSC will be to make measurements to test and tune the distribution functions. We might call these “calibration” studies. By studying a variety of known processes, we will be able to isolate and check different components of the proton wave function. Some examples are given below for the case of the SSC.

Once assured that the distribution functions are sufficiently under control, we can use them to look for new physics from the symmetry breaking sector (and elsewhere). Of course, one person’s calibration is another’s physics: the processes considered here are certainly of interest *per se* and could themselves be windows to surprising new physics. Many of the results quoted in this section are taken from the paper of EHLQ.<sup>(36)</sup>

The two jet cross section at large  $p_T$  is a straightforward measurement that probes the strength of quark and gluon distributions at large  $Q^2$ . From figure (8) we see that the cross section is dominated by  $gg$  scattering at  $M_{jj} = 1 \text{ TeV}$ , with a tremendous event rate of  $O(10^8)$  events/SSC year in a mass interval of width  $\Delta M_{jj} = 0.1 \text{ TeV}$ . For  $M_{jj} = 3 \text{ TeV}$  there are  $O(10^5)$  events in a 0.1



TeV  $M_{jj}$  interval, dominated equally by  $gg$  and  $gq$  scattering. For  $M_{jj} > 7$  TeV, of order  $O(10^4)$  events are predicted, with  $gq : gg : qq$  roughly in the ratio 3 : 1 : 1.

If the prediction for  $d\sigma/dM_{jj}$  is verified, it does not verify the relative weights assigned to  $gg$ ,  $gq$ , and  $qq$  scattering but only the sum. We want especially to isolate the  $qq$  component, since the  $qq$  luminosity controls the scale of  $WW$  fusion, crucial for the discussion of Section 3.4. Unfortunately there is no kinematical region accessible at the SSC where large  $p_T$   $qq$  scattering dominates the two jet cross section, so we will have to rely on the other measurements described here to fix the  $qq$  luminosity.

Production of high mass  $e^+e^-$  and  $\mu^+\mu^-$  pairs (Drell-Yan) measures the  $\bar{q}$  content of the proton. For  $0.9 < M_{e^+e^-} < 1.1$  TeV and  $|y_e| < 2.5$  we expect of order 250 events/SSC year in each channel. For the ratio of up to down quarks,  $f_u : f_d$ , we consider production of  $\mu^\pm\nu$  at large invariant mass. That is, we require a large  $p_T$  muon and large missing  $p_T$  on the opposite side. We expect<sup>(42)</sup>  $O(500)$  events/SSC year for  $0.45 < p_T(\mu) < 0.55$  TeV and  $|y_\mu| < 2.5$ . Production of  $e^\pm\nu$  can also be used.

Another process probing  $f_u/f_d$  is production of  $W^\pm + \text{jet}$  at large  $W$ -jet invariant mass. For  $0.9 < M_{Wj} < 1.1$  TeV and  $|y_{Wj}| < 1.5$  we expect  $O(10^5)$  events/SSC year. The  $W^+j$  events are predominantly due to  $ug \rightarrow W^+d$  and  $\bar{d}g \rightarrow W^+\bar{u}$  while the  $W^-j$  events arise chiefly from the charge conjugate reactions. If only muon decays are used to measure the  $W^+ : W^-$  ratio, we expect  $O(10^3)$  events/SSC year.  $Z + \text{jet}$  events, produced chiefly from  $gq$  and  $\bar{q}g$  scattering, occur at comparable rates.

The cross sections to produce two gauge bosons will also be useful for ‘‘calibration’’ purposes. If the gauge sector is correctly described by the  $SU(2) \times U(1)$  theory, then the  $ZZ, WZ$ , and  $W^+W^-$  cross sections allow us to calibrate various combinations of  $\bar{q}q$  luminosities, except for possible new physics from other sources such as the symmetry breaking sector. In the minimal Higgs model, there are no large effects in the  $WZ$  channel, while effects in the  $WW$  and  $ZZ$  channel are restricted to  $WW$  and  $ZZ$  masses around the mass of the Higgs. For instance, for  $m_H = 1$  TeV there is little effect on the  $WW$  and  $ZZ$  yields for  $M_{WW} < 0.5$  TeV. In more general models with strongly interacting symmetry breaking sectors, there may be measureable enhancements of  $WW$ ,

$ZZ$ , and  $WZ$  for  $M_{WW} \gtrsim O(1)$  TeV) but little effect on the contribution from  $\bar{q}q$  annihilation below  $\frac{1}{2}$  TeV. The  $W\gamma$  and  $Z\gamma$  cross sections could also be useful for calibration purposes, since they cannot be significantly affected by symmetry breaking physics.

By such means it is likely that the error in cross section predictions due to uncertainties in the distribution functions will be no larger than 20 or 30% — see for example the discussion of the heavy Higgs boson working group<sup>(43)</sup> at the 1987 SSC detector workshop.

### 3.13 Jets and Hadronization

QCD is central to pp collider physics not only through the proton wave function but also through the process of hadronization by which partons become observable hadronic final states. If we had a deeper and more precise understanding of hadronization, we would be much better able to reject strong interaction backgrounds to many interesting new physics signals.

As an example consider the problem of detecting a 1 TeV Higgs boson, discussed in Section 3.4 below. One observable leptonic decay channel is  $H \rightarrow ZZ \rightarrow e^+e^-/\mu^+\mu^- + \bar{\nu}\nu$ , which has a QCD background from  $Z + \text{jets} \rightarrow e^+e^-/\mu^+\mu^- + \cancel{E}_T$ . That is, the recoil jets in the background could give much of their energy to neutrinos (e.g., if the jet contains a leading  $t$  quark that decays semileptonically) and possibly simulate a  $Z \rightarrow \bar{\nu}\nu$  decay. Of course these background events would also have significant visible transverse energy,  $E_T$ , which can be used to distinguish them from the signal. With a sufficiently hermetic detector it seems that we will be able to overcome this background at the SSC.<sup>(43)</sup>

A second example is the ‘‘mixed’’ hadron-lepton decay of a heavy Higgs boson,  $H \rightarrow WW \rightarrow \ell\bar{\nu} + \bar{q}q$ . The QCD background from  $W + jj$  is 100 times larger even if we make a very optimistic assumption about the jet-jet mass resolution.<sup>(44)</sup> Much work has been done on how this background might be overcome — see Section 3.4. Here I only want to remark that the dijet system consists dominantly of one or two gluons. If we understood very well how gluon jets hadronize we might find a way to separate at least some of the background from the  $W \rightarrow \bar{q}q$  signal.

In general improved understanding of jets and hadronization will increase

our ability to find the signals of new physics at the SSC and LHC. Analysis and theoretical studies of jet data from the SPS and TeVatron colliders will be very important for effective use of the higher energy colliders.<sup>(45)</sup>

### 3.2 Reconnaissance

Exploratory “reach” for a broad variety of possible new physics is important not just for the sake of the specific examples considered but as an indication of capability to make the most important discoveries — the completely unexpected. In this section we will consider three examples of what we might expect:

- Compositeness
- New gauge forces —  $W', Z'$
- New matter —  $Q, L$

We will see that compositeness and new gauge forces can be explored straightforwardly into the multi-TeV domain with no serious background problems. To find heavy quarks in the TeV range we will have to work harder against backgrounds. Most difficult is the search for a fourth generation charged lepton in the few hundred GeV range allowed by the rho parameter (see Section 2.2), for which the backgrounds are very large.

#### 3.21 Compositeness

As Chairman Mao’s “straton” theory suggests, it is natural to speculate that quarks and leptons may be composite. Almost everything else is composite — molecules, atoms, nuclei, nucleons. Why shouldn’t quarks and leptons also be? Compositeness would be an elegant solution to the generation puzzle if we could understand the second and third generations as excitations of the first, though it is hard to understand then why we have not yet seen any orbital excitations. Composite technicolor models<sup>(46)</sup> solve many of the problems of ordinary technicolor models; if they are correct then composite structure will be found at no more than the few TeV scale and the effects will be obvious at the LHC and SSC.

If quarks and leptons are composite they have form factors that can be observed at short distances in high momentum transfer interactions.<sup>(47)</sup> For instance, the elementary electron-photon interaction vertex  $e\bar{u}(p')\not{A}u(p)$  would be

multiplied by a form factor  $F(Q^2)$  where  $Q^2 = -(p' - p)^2$ . For  $Q$  small compared to the scale of the bound state,  $\Lambda \cong R^{-1}$ ,  $F(Q^2)$  is approximated by the leading terms in the Taylor expansion

$$F(Q^2) \cong 1 + \frac{Q^2}{\Lambda^2}. \quad (3.4)$$

We then expect deviations by powers from scaling in deep inelastic scattering, in  $e^+e^-$  annihilation, and in Drell-Yan production of lepton pairs at hadron colliders. Since the elementary quark-gluon vertex would also acquire structure, we would also expect power law deviations from the usual predictions for quark-quark and quark-gluon scattering.

Another and, in most cases, larger signal of composite structure would be contact interactions,<sup>(48)</sup> that is, four-fermion effective interactions that would show up at energies below the compositeness scale,  $s \ll \Lambda^2$ . At the very least, flavor diagonal contact interactions would be generated by the preon binding force and also by preon exchange. While the chirality structure is completely unknown, we could consider a purely left-handed, vectorial interaction at  $s \ll \Lambda^2$ ,

$$\mathcal{L} = \frac{g^2}{\Lambda^2} \bar{\psi}_L \gamma^\mu \psi_L \bar{\psi}_L \gamma_\mu \psi_L. \quad (3.5)$$

Since the preon binding force is likely to be strong when  $s \ll \Lambda^2$ , it is customary to assume  $g^2 = 4\pi$ . Of course this really just amounts to a definition of  $\Lambda$ . Notice that  $1 \text{ TeV}^{-1} \cong 2 \cdot 10^{-17} \text{ cm}$  so that in probing the multi-TeV domain in  $\Lambda$  we are exploring distance scales of order  $10^{-18} \text{ cm}$ , five orders of magnitude smaller than hadrons.

Using the model of equation 3.5 we can compute the differential cross section for  $uu$  elastic scattering,<sup>(49)</sup>

$$\begin{aligned} \frac{d\sigma}{d\Omega}(uu \rightarrow uu) &= \frac{\alpha_s^2}{9s} \left[ \frac{s^2 + u^2}{t^2} + \frac{s^2 + t^2}{u^2} - \frac{2s^2}{3tu} \right] \\ &\quad \pm \frac{2\alpha_s s}{9\Lambda^2} \left[ \frac{1}{u} + \frac{1}{t} \right] + \frac{2}{3} \frac{s}{\Lambda^4}. \end{aligned} \quad (3.6)$$

The first term is the usual QCD interaction while the second is the interference term with the sign customarily left unspecified. For a vector interaction we expect constructive interference<sup>(50)</sup> corresponding to the negative sign in 3.6

(since  $u$  and  $t$  are negative). The interference term in 3.6 is larger by one power of  $\alpha_s$  than the effect due to a form factor in the quark-gluon vertex at large  $|t|$  or  $|u|$ . Figure (9) shows the resulting two jet cross section at the SSC,  $d\sigma/dM_{jj}$  for values of  $\Lambda$  ranging from 15 TeV to infinity (i.e., pure QCD). The figure assumes flavor-diagonal  $qq$  interactions of the form of equation 3.6 plus analogous flavor off-diagonal interactions such as  $u_L d_L \rightarrow u_L d_L$ .<sup>(49)</sup> The dashed lines are for constructive and the solid lines for destructive interference. The authors of reference (49) find that  $\Lambda = 25$  TeV would result in an observable signal at the SSC for  $10^4 \text{pb}^{-1}$ , with 1) at least 100 events due to the contact interactions and 2) fewer events due to the QCD background than the contact interaction. Using somewhat different criteria, figure (10) from reference (36) shows the sensitivity to  $\Lambda$  as a function of collider energy  $s$  for  $10^4 \text{pb}^{-1}$  and also for  $10^2 \text{pb}^{-1}$ . Another approach which achieves similar sensitivity is based on the angular distribution of two jet events.<sup>(51)</sup>

Quark-lepton contact terms must also occur if quarks and leptons have constituents in common and may occur even if they do not. We would then expect anomalous production of massive dilepton pairs from  $\bar{q}q$  annihilation. Relative to dijet production this method loses because the  $\bar{q}q$  luminosity is smaller than the  $qq$  luminosity at large  $\hat{s}$  but wins back one or two factors of  $\alpha_s/\alpha$  because of the smaller standard model background (i.e., one power of  $\alpha_s/\alpha$  if the interference term dominates and two powers at large  $\hat{s}$ ). With conservative criteria (at least 100 events per 500 GeV bin in  $M_{e^+e^-}$ , at least half due to the contact interactions) the authors of reference (49) find for a left-left interaction that an effect would be seen at the SSC with  $10^4 \text{pb}^{-1}$  for  $\Lambda = 15$  TeV (constructive interference) or 12.5 TeV (destructive). Using different criteria, the EHLQ<sup>(36)</sup> study finds a sensitivity up to 28 TeV at the SSC and 15 TeV at the LHC. In particular, references (36) and (49) disagree as to whether dileptons or dijets are more sensitive. The important conclusion however is that the two methods have comparable sensitivity and are both worth pursuing.

### 3.22 New Gauge Forces

The power of multi-TeV pp colliders is clearly exhibited by the ability to discover heavy gauge bosons to masses of several TeV. The experimental signals in leptonic channels are spectacular and have no significant backgrounds. The cross section to produce a heavy right-handed  $W_R$  boson is shown in figure

(11) for  $\sqrt{s} = 10, 20,$  and  $40$  TeV pp and  $\bar{p}p$  colliders,<sup>(52)</sup> assuming the same strength couplings to quarks and leptons as the usual  $W$  of  $SU(2)_L$ . For the decay  $W_R \rightarrow e + \bar{\nu}_e/N_e$  when  $N_e$  is a possible heavy neutrino assumed to be much lighter than  $W_R$ , the signal is at least two orders of magnitude larger than the standard model background. Requiring  $\geq 10$  events in the electron channel the  $W_R$  “reach” is 9 TeV at the SSC and 5 TeV at the LHC.

For heavy neutral gauge bosons decaying leptonically, the background is again negligible, at least two orders of magnitude below the signal. If we consider the  $Z'$  predicted in  $SO(10)$  models then the reaches are 6 TeV at the SSC and 3 TeV at the LHC for a minimum of  $10 e^+e^-$  events.

If we do discover a heavy  $Z'$  it could provide us with crucial information about a possible grand unified theory. Since the proton lifetime might be undetectably long, this could be one of the few if not only window on the GUT scale in the foreseeable future. The grand unified groups predict the couplings of the  $Z'$  to quarks and leptons. As shown in figure (12) from reference (52), those couplings can be studied by measuring front-back decay asymmetries. The technique makes use of the fact that in  $\bar{q}q$  collisions at a pp collider the quark is likely to be more energetic than the antiquark, so that the  $Z'$  tends to move in the laboratory along the direction of the initial quark. The front-back asymmetries for the negative lepton are then defined in the  $Z'$  rest frame with “front” defined as the  $Z'$  direction of motion in the lab frame. Figure (12) shows the predicted asymmetries for the  $Z_\chi$  of  $SO(10)$  and for a heavy  $Z^0$  assumed to be a replica of the standard  $Z$  of  $SU(2)_L \times U(1)_Y$ . We see that the asymmetries are dramatically different for the two models at a pp collider, with opposite correlations between the sign of the asymmetry and the laboratory rapidity of the produced  $Z$ . If we require 200 events to make a  $4\sigma$  determination of the asymmetry, then the determination is possible for a 3 TeV  $Z_\chi$  at the SSC and a 2 TeV  $Z_\chi$  at the LHC.

### 3.23 Fourth Generation Quarks and Leptons

The one loop quantum corrections imply tight constraints on the masses of a possible fourth generation, as discussed in Section 2.2. Soon we will also learn from measurement of the  $Z$  decay width whether there may be more than three light neutrinos. However if  $m_U \cong m_D$  and  $m_L \cong m_{\nu_L} > M_Z/2$ , then both of these constraints become useless. Though these two conditions may seem

unrealistic — especially  $m_{\nu_L} > M_Z/2$  — we should consider that we really know *absolutely nothing* about the origin of fermion mass. Therefore we cannot exclude the possibility that such conditions for a fourth generation might have a natural explanation, *e.g.*, if all four fourth generation fermions acquire a large mass from some single common scale while the first three generations' masses arise by a very different mechanism such as by radiative corrections. Consequently there is no substitute for direct searches for the fourth generation quarks and leptons.

Consider first the fourth generation quarks. In hadronic interactions the  $c$  and  $b$  quarks were first observed by producing the  $\bar{c}c$  and  $\bar{b}b$  quarkonium states,  $J/\psi$  and  $\Upsilon$  and observing their leptonic decays to  $e^+e^-$  or  $\mu^+\mu^-$ . The same technique cannot be used for the fourth generation, since  $\Gamma(\psi(\bar{Q}Q) \rightarrow e^+e^-) \propto m_Q$  and  $\Gamma(Q \rightarrow W_q) \propto m_Q^5$  so that the weak decays of the constituent  $\bar{Q}Q$  pair dominate and  $BR(\psi(\bar{Q}Q) \rightarrow e^+e^-) \ll 1$  is unobservably small. Instead we must search for the weak decays of  $Q$  and  $\bar{Q}$ .

The production mechanisms are  $gg \rightarrow \bar{Q}Q$  and  $\bar{q}q \rightarrow \bar{Q}Q$  with gluon fusion dominant. The yields are large and depend strongly on the collider energy. For  $m_Q = 0.5$  TeV and requiring central rapidity,  $|y_Q| < 1.5$ , there are  $4 \cdot 10^4$  events at LHC and  $4 \cdot 10^5$  at the SSC per  $10^4 \text{pb}^{-1}$ .<sup>(36)</sup> For  $m_Q = 1.0$  TeV the corresponding yields are  $1 \cdot 10^3$  at the LHC and  $2 \cdot 10^4$  at the SSC. Careful Monte Carlo analyses are needed to devise detection strategies and to estimate the likely detection efficiency.

For instance, a fourth-generation down quark decays by

$$D\bar{D} \rightarrow tW^- + \bar{t}W^+.$$

Purely hadronic decay modes are lost in the multi-jet QCD background, as shown in figure (13). The most promising strategy<sup>(53)</sup> is to use the  $\ell^+\ell^- + \cancel{E}_T$  signature. That is, consider events in which the  $t$  and  $W$  from one quark both decay leptonically

$$D \rightarrow tW^- \rightarrow b\ell^+\nu + \ell^-\nu$$

while the other quark decays hadronically,

$$\bar{D} \rightarrow \bar{t}W^+ \rightarrow b\bar{q}q + \bar{q}q.$$

The background from

$$gg \rightarrow \bar{t}t \rightarrow \bar{b}\bar{q}q + b\bar{\ell}\nu; b \rightarrow c\bar{\ell}\nu$$

can be eliminated by  $p_T(\ell)$  cuts (that is, cuts on the transverse momentum of the leptons with respect to the jet axes) and by requiring  $n_{jet} \geq 3$  for the quark on the hadronic side (since Monte Carlo studies show that  $t \rightarrow b\bar{q}q$  does not usually result in detection of three well-separated jets). The jets from the hadronically decaying  $D$  can then be used to measure the quark mass. It appears that this strategy could be used to discover a  $D$  quark as heavy as 1 TeV at the SSC.<sup>(53)</sup> For  $m_D > 1$  TeV the method is rate-limited and it is necessary to consider single lepton decay modes which suffer from larger backgrounds.<sup>(54)</sup>

Contrary to the initial optimism<sup>(51)</sup> it appears that detection of a fourth generation charged lepton will be very difficult.<sup>(55)</sup> The problem is that in the simplest decay modes there are too many neutrinos, so that much of the total missing energy cancels. The diluted missing energy signal must then compete against backgrounds which arise from final states with smaller invariant mass and consequently larger cross sections.

For instance, consider a 300 GeV charged lepton with a much lighter neutrino partner,  $m_{\nu_L} \ll m_L = 300$  GeV. There is then a significant rate for production of  $L\bar{\nu}_L + \bar{L}\nu_L$  via an intermediate virtual  $W$  boson. For  $10^4 \text{pb}^{-1}$  and  $|y_L| < 1.5$  there are 3000 events at the LHC (17 TeV) and 7000 events at the SSC.

Consider the  $L\bar{\nu}_L$  final state. The  $L$  decays by  $L \rightarrow W\nu_L$ . If we use the most readily identifiable  $W$  decays,  $W \rightarrow \ell\nu_\ell$  where  $\ell = e$  or  $\mu$ , then the final state

$$L\bar{\nu}_L \rightarrow \ell\nu_\ell\bar{\nu}_L\nu_L$$

has three neutrinos and cannot be distinguished from the background due to

$$\bar{q}q \rightarrow W^* \rightarrow \ell\nu_\ell.$$

Because of the dilution of missing energy in the signal, the  $\hat{s}$  of the background reaction is smaller so that the cross section is larger. The result, shown in figure (14) for 100 and 200 GeV leptons, is that the background is much larger than the signal.

We must therefore consider the hadronic  $W$  decays,  $W \rightarrow \bar{q}q$ . The final state is then

$$L\bar{\nu}_L \rightarrow \nu_L\bar{\nu}_L + \bar{q}q.$$

The signal is defined by a dijet with  $M_{jj} = M_W$  at large  $p_T$  with large missing  $p_T$  on the opposite side. The dominant background is QCD production of  $Z+2$  jets, for instance  $gg \rightarrow Z\bar{q}q$ , followed by  $Z \rightarrow \bar{\nu}\nu$ . A calculation<sup>(56)</sup> using the complete lowest order QCD matrix elements<sup>(57)</sup> shows that the background is more than an order of magnitude larger than the signal assuming a 10 GeV dijet mass resolution, *i.e.*,  $m_{jj} = M_W \pm 10$  GeV. The signal might be improved by using cuts devised to detect the hadronic decays of  $W$ 's resulting from heavy Higgs boson decay,<sup>(58)</sup> discussed in Section 3.4. For now the detectability of a heavy lepton signal remains uncertain.

### 3.3 Looking for Supersymmetry

The principal low energy motivation for supersymmetry, reviewed in Section 2.3, is that it can solve the technical naturalness problem, one aspect of the gauge hierarchy problem. This motivation requires that supersymmetry breaking cannot be much larger than 1 TeV. Of course supersymmetry might exist in nature and be unrelated to the problem of  $SU(2)_L \times U(1)_Y$  breaking, *e.g.*, at the Planck scale where it might account for the unification of gravity with the other forces. Supersymmetry would then be immeasurably more difficult to establish then if, as we consider here, it is relevant to the breaking of the electroweak symmetry.

An important goal for the next generation of colliders is to provide a definitive test of whether SUSY is relevant to the electroweak scale. At the SSC there are large production cross sections for squarks and gluinos as heavy as 1 TeV; the cross sections for 1 TeV squarks and gluinos at the LHC are smaller by about a factor of 25.<sup>(59,60)</sup> However if squarks and gluinos are heavier than a few hundred GeV the experimental search is complicated by large branching ratios to complex final states that are more difficult to analyze than the relatively simple final states that dominate within the ranges of the SPS and TeVatron colliders.<sup>(61,60,59)</sup> More work needs to be done on the backgrounds and the signals of these complex decays in order to determine the mass ranges we can study definitively at the SSC and LHC.

Interactions between the ordinary particles and their superpartners are uniquely determined by gauge invariance and supersymmetry. For example, from the electron photon vertex,  $\bar{e}e\gamma$ , we can uniquely deduce the form and strength of the interactions between the electron  $e$ , the photon  $\gamma$ , the selectron  $\tilde{e}$  and the

photino  $\tilde{\gamma}$ . The additional interaction vertices are  $\tilde{e}\tilde{e}\gamma$ ,  $\tilde{e}\tilde{e}\tilde{\gamma}$ ,  $\tilde{e}\tilde{e}\tilde{\gamma}$ , and  $\tilde{e}\tilde{e}\gamma\gamma$ . Unlike the interactions the masses of the sparticles are not known at all on general grounds. They are unknown with respect to one another and with respect to the masses of the ordinary particles. Therefore we cannot make model independent predictions of the sparticle decay modes, and the experimental search must be organized with all possibilities in mind.

The minimal SUSY extension of the standard model just adds the minimal complement of superparticles required to complete the  $N = 1$  supersymmetry representations. Each chirality quark or lepton acquires a scalar partner,  $\{\tilde{u}_L, \tilde{d}_L, \tilde{u}_R, \tilde{d}_R, \tilde{e}_L, \tilde{e}_R, \tilde{\nu}_L\}$ . Each transverse gauge boson degree of freedom acquires a two component fermionic gaugino partner,  $\{\tilde{\gamma}, \tilde{Z}, \tilde{W}^\pm, \tilde{g}\}$ . The chirality structure of the Higgs-fermion interaction together with supersymmetry requires at least two complex Higgs boson doublets. The minimal SUSY extension has precisely these two Higgs doublets

$$\begin{pmatrix} H_1^+ \\ H_1^0 \end{pmatrix}, \begin{pmatrix} H_2^0 \\ H_2^- \end{pmatrix}$$

of which one gives mass to  $T_{3L} = +\frac{1}{2}$  fermions and the other to  $T_{3L} = -\frac{1}{2}$  fermions. The fermionic Higgsino partners are then

$$\begin{pmatrix} \tilde{H}_1^+ \\ \tilde{H}_1^0 \end{pmatrix}, \begin{pmatrix} \tilde{H}_2^0 \\ \tilde{H}_2^- \end{pmatrix}.$$

The four neutral gauginos and Higgsinos are two-component Majorana fermions; they mix to form four Majorana fermion eigenstates known as "neutralinos",

$$\tilde{\gamma}, \tilde{Z}, \tilde{H}_1^0, \tilde{H}_2^0 \rightarrow \chi_1^0, \chi_2^0, \chi_3^0, \chi_4^0.$$

Similarly the wino and charged Higgsinos (and their antiparticles) mix to form two four-component Dirac fermions, the "charginos",

$$\tilde{W}^+, \tilde{H}_1^+ \rightarrow \tilde{\chi}_1^+, \tilde{\chi}_2^+.$$

In most models there is a conserved  $R$ -parity, defined by  $R(\text{particle}) = 0$  and  $R(\text{sparticle}) = \pm 1$ .  $R$ -parity conservation implies stability of the lightest supersymmetric particle or LSP. Decay modes and experimental signatures depend strongly on the identity of the LSP. A common though unjustified assumption

is that the LSP is the photino (which in general is not even an eigenstate). It is however quite possible that the LSP is the lightest neutralino. If it is (or if the LSP is a sneutrino  $\tilde{\nu}$ ), missing energy will be a characteristic experimental signature of supersymmetry since the LSP will have interactions with ordinary matter of weak strength or less. Consider for example elastic photino-quark scattering,  $\tilde{\gamma}q \rightarrow \tilde{\gamma}q$ , which occurs by  $s$ - and  $u$ -channel squark exchange. As the photino slows, the low energy amplitudes are of order  $O(e^2/m_q^2)$ . The existing lower limits on the  $\tilde{q}$  mass imply that  $e^2/m_q^2 \lesssim g^2/M_W^2 \cong O(G_F)$ , so photinos interact in ordinary matter with cross sections of order or less than neutrino cross sections. The same is true of the other possible components of a neutral LSP. (It is assumed that the gluino is not the LSP since its color charge tends to give it higher mass than the color-singlet neutralinos; it would be surprising and interesting if this assumption were wrong.)

The widely quoted limits on SUSY particles from  $\bar{p}p$  collisions assume that  $LSP = \tilde{\gamma}$ . Then if the squark and gluino are not too heavy they decay predominantly into simple final states:

$$\text{if } m_{\tilde{q}} > m_{\tilde{g}} : \quad \tilde{g} \rightarrow \bar{q}q\tilde{\gamma}, \quad \tilde{q} \rightarrow q\tilde{g} \quad (3.7)$$

$$\text{if } m_{\tilde{g}} > m_{\tilde{q}} : \quad \tilde{g} \rightarrow \bar{q}\tilde{q}, \quad \tilde{q} \rightarrow q\tilde{\gamma}. \quad (3.8)$$

For example, with  $m_{\tilde{g}} > m_{\tilde{q}}$  production of squark-antisquark pairs results in events with two jets plus missing transverse energy,

$$pp \rightarrow \bar{q}\tilde{q} + \dots \rightarrow jj + \cancel{E}_T.$$

Assuming that the photino is the LSP and that  $m_{\tilde{\gamma}} < 20$  GeV, searches with the UA-1 detector have given 90% confidence level lower limits<sup>(62)</sup> on squark and gluino masses,  $m_{\tilde{q}} > 45$  GeV and  $m_{\tilde{g}} > 53$  GeV (the latter assumes  $m_{\tilde{q}} < 1$  TeV). At the TeVatron collider it should be possible to search up to the 150-200 GeV mass range.

Searches above 200 GeV will require the LHC and SSC. Above 500 GeV these searches are more difficult because heavier squarks and gluinos have more complicated decay modes than the simple decays 3.7 and 3.8.<sup>(61)</sup> For instance a heavy gluino could decay via an intermediate wino by the sequence

$$\begin{aligned} \tilde{g} &\rightarrow \bar{q}q \tilde{W} \\ \tilde{W} &\rightarrow W\tilde{\gamma} \\ W &\rightarrow \ell\nu, q\bar{q}. \end{aligned} \quad (3.9)$$

Depending on how the  $W$  decays, 3.9 results in  $4j + \cancel{E}_T$  or  $2j + \ell + \cancel{E}_T$ . The multijet signals suffer from QCD backgrounds. The proliferation of neutrinos and LSP's results in cancelling  $E_T$  with a subsequently smaller signal, as for the problem of heavy lepton detection reviewed in Section 3.23. Such complicated decays become important for  $m_{\tilde{g}}$  and  $m_{\tilde{q}}$  above 500 GeV. For instance, for a broad range of parameters in the minimal SUSY model with  $m_{\tilde{q}} > m_{\tilde{g}} \geq 600$  GeV the branching ratio for the simple gluino decay to the lightest neutralino,  $\tilde{g} \rightarrow \bar{q}q \chi_1^0$ , is never bigger than  $\sim 14\%$ .<sup>(60)</sup> The probability that both gluinos in a produced  $\tilde{g}\tilde{g}$  pair will decay to  $\bar{q}q \chi_1^0$  is therefore less than  $\sim 2\%$ . A similar result is typically true of heavy left-handed squarks because of their  $\tilde{W}$  and  $\tilde{Z}$  couplings. Only heavy right-handed squarks have dominant direct decays to the LSP for an appreciable range of the minimal SUSY model parameters, though there is also a significant range of parameters for which their direct LSP decays are as small as those of the left-handed squarks and gluinos. Therefore we must be prepared to deal with the possibility that complex decays such as 3.9 are dominant for all heavy squarks and gluinos.

Because the decay branching ratios are very dependent on the details of the SUSY model and in particular on the several undetermined parameters in the minimal SUSY model, a comprehensive discussion cannot be approached in these lectures. Furthermore, as of this summer there is no comprehensive analysis of the signals and backgrounds. Here I will just mention a few illustrative examples which suggest the kind of analysis that is needed and give an idea of what the discovery prospects may be.

Since they are produced by strong interactions the squark and gluino cross sections are sizeable. For instance figure (15) from reference (63) shows the  $\bar{q}\tilde{q}$  cross section at the SSC assuming  $m_{\tilde{g}} = m_{\tilde{q}}$ . The 10 pb cross section for  $m_{\tilde{q}} = 1$  TeV corresponds to  $10 \cdot 10^{-36} \cdot 10^{33} \cdot 10^7 = 10^5$  events in an experimental "year" of  $10^7$  sec at  $10^{33} \text{cm}^{-2} \text{sec}^{-1}$  luminosity. The cross section at the LHC

is considerably smaller; for instance, for a 1 TeV gluino the  $\tilde{g}\tilde{g}$  production cross section is 25 times smaller<sup>(59,60)</sup> at  $\sqrt{s} = 17$  TeV than at 40 TeV.

If the simple decays 3.7 and 3.8 dominate then probably both the LHC and SSC would suffice to discover gluinos or squarks as heavy as 1 TeV. With this assumption a high statistics ISAJET study<sup>(64)</sup> for the LHC,  $\sqrt{s} = 17$  TeV, found about  $\sim 750$  detectable  $\tilde{g}\tilde{g}$  events per LHC-year for  $m_{\tilde{g}} = 1$  TeV. The background was 180 or 80 events for  $m_t = 40$  GeV or 200 GeV respectively. Assuming  $\tilde{g} \rightarrow \bar{q}q + \text{LSP}$ , the  $\tilde{g}\tilde{g}$  signal would be  $\sim 4$  jets +  $\cancel{E}_T$ . The backgrounds considered were ( $Z \rightarrow \bar{\nu}\nu$ ) + jets, ( $W \rightarrow \bar{\ell}\nu$ ) + jets, and  $\bar{t}t$  or  $\bar{t}t\tilde{g}$  with semileptonic decays of  $t$  and  $\bar{t}$ . Backgrounds were reduced by rejecting events with an isolated lepton, by cuts on the number of jets, and by cuts on the event “topology”, i.e., on angles between the various jets and the missing-transverse-energy vector.

However, as emphasized above, these results would not apply to the minimal SUSY model since for  $m_{\tilde{g}} = 1$  TeV the upper limit<sup>(60)</sup> on the branching ratio for the minimal decay  $\tilde{g} \rightarrow \bar{q}q + \text{LSP}$  is  $\leq 14\%$ . Therefore instead of 750 signal events we expect at most  $750 \cdot (0.14)^2 = 15$  events, which is far too small to observe over the above quoted background. It is clearly important to reanalyze the signal and background assuming that just one gluino decays directly to the LSP, since in that case the signal is only reduced by  $2 \cdot (.14) - (.14)^2 = 0.26$  to  $\sim 200$  events.

We are left with two possible strategies for the discovery of heavy squarks and gluinos. One is to study whether the direct decays to the LSP are observable despite the reduced branching ratios. The other strategy is to examine the sequential decays such as 3.9. Neither strategy has been comprehensively studied though work has begun for both.<sup>(59–64)</sup> The SSC, and perhaps also the LHC, may be able to discover squarks and gluinos into the TeV range, corresponding to the upper limit suggested by the considerations of Section 2.3. But we cannot be certain until the necessary studies of the signals and backgrounds are completed. In particular, without detailed, comprehensive studies we cannot know whether even the SSC cross sections are sufficiently large and, if so, whether the factor 25 advantage of the SSC is essential for the discovery of TeV superpartners.

### 3.4 $SU(2)_L \times U(1)_Y$ Breaking: Higgs or Whatever

Electroweak symmetry breaking is the clearest target of the next gener-

ation colliders. Unlike other physics that *might* be, it *must* be — as long as we are correct in believing that the electroweak interactions are described by a spontaneously broken gauge theory. In Section 2.33 we learned an important general lesson from the technicolor example: the Higgs mechanism does not require the existence of a physical Higgs boson. The analysis reviewed in Section 2.4, based only on unitarity and general symmetry properties, shows that we can expect either Higgs bosons below 1 TeV or a new world of strongly interacting particles above 1 TeV. This new world would reveal its presence by strong  $W_L W_L$  scattering between 1 and 2 TeV.  $WW$  fusion would then lead to additional production of longitudinally polarized gauge boson pairs in all channels:  $ZZ, W^\pm Z, W^+W^-, W^+W^+, W^-W^-$ . For a collider powerful enough to observe this signal we have a No-Lose Corollary: if the signal is not present we learn that the symmetry breaking sector is below 1 TeV, probably in the form of one or more Higgs bosons.

In this section we will review some of the possible experimental signals. We will see that a collider with the SSC energy and luminosity is a minimal configuration for the 1-2 TeV signals. A pp collider with half the energy would not suffice, nor is it practicable to compensate the lower energy with higher luminosity. (The necessary luminosity upgrade is an unlikely factor of 600 to  $6 \cdot 10^{35} \text{cm}^{-2} \text{sec}^{-1}$  as discussed below and in more detail in my contribution to the discussion session, also reproduced in the proceedings of this workshop.)

#### 3.41 Higgs Boson Searches

First consider the standard model Higgs boson. Existing constraints are essentially negligible.<sup>(18,19)</sup> The cosmological lower limit<sup>(65)</sup> fails if the top quark is heavy enough,  $m_t \gtrsim 80$  GeV. Nuclear physics experiments imply  $m_H \gtrsim 10$  MeV. Existing limits from  $\Upsilon$  decay are not sure because of large uncertainties in the theoretical predictions. For someone with a very cautious view, almost nothing is ruled out.

Where can we look? For  $m_H < m_{J/\psi}$  or  $< m_\Upsilon$  we can look for  $J/\psi \rightarrow \gamma H$  or  $\Upsilon \rightarrow \gamma H$ .<sup>(66)</sup> With enough statistics BEPC could contribute. Supersymmetric Higgs bosons could show up at bigger rates than the standard model Higgs boson.<sup>(67)</sup> Despite the uncertainties in the theoretical predictions, these are very interesting channels to consider. Though negative results may be difficult to interpret, a positive result would be spectacular.

For  $m_H \lesssim 40$  GeV we can look in  $Z$  boson decays,<sup>(68)</sup>  $Z \rightarrow HZ^*$ , where the virtual  $Z^*$  decays to  $e^+e^-$ ,  $\mu^+\mu^-$ , or  $\bar{\nu}\nu$ . If  $H$  is heavy enough, it will decay chiefly to  $\bar{b}b$  quarks. The experimental signatures are quite distinctive. With  $\sim 5 \cdot 10^6$   $Z$  decays it should be possible to search up to 40 GeV in the Higgs boson mass.

LEP 200 will be able to search for Higgs bosons up to 70 GeV using the process  $e^+e^- \rightarrow Z^* \rightarrow HZ$ .<sup>(69)</sup> The virtual  $Z^*$  decays to a real  $Z$  and  $H$  which are observed as in the case of  $Z \rightarrow HZ^*$  discussed above.

For more detailed discussions of light Higgs boson searches the reader can consult more detailed reviews.<sup>(18,19)</sup> Here we are principally concerned with Higgs bosons heavier than 70 GeV, requiring higher energy  $e^+e^-$  colliders than LEP 200 and/or multi-TeV pp colliders like the LHC and SSC.

Unless the top quark mass nearly saturates the upper bound obtained from the rho parameter,  $m_t \lesssim 200$  GeV,  $WW$  fusion<sup>(70,71)</sup> is the principal mechanism for production of the 1 TeV Higgs boson at pp or  $e^+e^-$  colliders. (For  $e^+e^-$  collisions  $WW$  fusion dominates regardless of the value of  $m_t$ .) In  $e^+e^-$  scattering,  $e^+e^- \rightarrow e^+e^-WW$ ,  $WW \rightarrow H$ , or in quark collisions,  $qq \rightarrow qqWW$ ,  $WW \rightarrow H$ , the scattering fermions persevere into the final state. As in the more familiar photon-photon scattering process at  $e^+e^-$  colliders, the kinematics favors collisions in which the final state fermions retain a large fraction of the total energy and the cross section grows logarithmically with energy at fixed  $m_H$ . Therefore beam energy is at a premium. Even more than for other physics signals, not only the signal but also the signal to background ratio is rapidly enhanced by increasing the available energy.<sup>(72)</sup>

To extend the Higgs boson search to  $m_H = 1$  TeV with colliders of luminosity  $\mathcal{L} = 10^{33} \text{cm}^{-2} \text{sec}^{-1}$  requires at least a  $\sqrt{s} \cong 40$  TeV proton-proton collider or a  $\sqrt{s} \cong 2$  TeV electron-positron collider, as discussed below. The first corresponds to the design parameters of the SSC<sup>(73)</sup> while the second is a goal of design studies for CLIC.<sup>(74)</sup>

A preliminary study has been performed to determine whether the Higgs boson reach of a  $\sqrt{s} = 16$  TeV pp collider (i.e., the LHC with 10 Tesla magnets<sup>(75)</sup>) could be extended to  $m_H = 1$  TeV by increasing the luminosity to  $\mathcal{L} = 5 \cdot 10^{34} \text{cm}^2 \text{sec}^{-1}$ .<sup>(76)</sup>

The study concludes that it may be possible provided both electrons and muons can be detected and identified. However, as the authors are careful to observe, rate-associated problems such as radiation hardening and data acquisition already stretch the imagination at luminosities of  $10^{33} \text{cm}^{-2} \text{sec}^{-1}$ . It is by no means clear that the associated problems at  $\mathcal{L} = 5 \cdot 10^{34} \text{cm}^{-2} \text{sec}^{-1}$  could be solved by the mid 1990's. In a contribution to the discussion section reprinted elsewhere in this volume I estimate that in order to obtain equivalent statistical significance for Higgs discovery, a 16 TeV collider must have a luminosity from  $1.5 \cdot 10^{35}$  to  $6 \cdot 10^{35} \text{cm}^{-2} \text{sec}^{-1}$  (depending on whether electron detection is possible) to be equivalent to a 40 TeV collider with  $\mathcal{L} = 10^{33} \text{cm}^{-2} \text{sec}^{-1}$ . The estimate includes a factor for leptonic signals with missing energy (e.g.,  $ZZ \rightarrow \bar{\ell}\ell + \bar{\nu}\nu$ ) that according to reference (76) cannot be observed for luminosities above  $10^{34} \text{cm}^{-2} \text{sec}^{-1}$ .

At the multi-TeV pp colliders the two principal production mechanisms are gluon-gluon fusion<sup>(77)</sup> and  $WW$  fusion<sup>(71)</sup> while only the latter is relevant at the TeV  $e^+e^-$  colliders. (For pp colliders  $WW$  fusion is shorthand for the sum of  $WW$  and  $ZZ$  fusion.) In the case of the pp colliders the magnitude of the gluon-gluon fusion contribution scales quadratically with the mass of the heaviest quark, since the  $ggH$  coupling is mediated by a quark loop. The amplitude is proportional to  $m_q$  for  $m_q$  less than the largest external scale,  $m_H$  in this case, and is independent of  $m_q$  for heavier quarks, which it therefore "counts". The  $gg$  fusion contribution is significant because of the very large gluon luminosity at the relevant energy scale, much larger than quark-quark luminosities at the same subprocess energy.<sup>(36)</sup> For three generations with  $m_t \cong 40$  GeV and  $\sqrt{s} = 40$  TeV,  $gg \rightarrow H$  dominates over  $WW \rightarrow H$  for  $m_H \lesssim 300$  GeV but quickly becomes negligible for larger  $m_H$ .<sup>(71)</sup> For  $m_t = 200$  GeV  $gg \rightarrow H$  dominates all the way up to  $m_H = 1$  TeV where it is almost twice the  $WW$  fusion contribution<sup>(78)</sup> (see figure (16)). For this discussion a 40 GeV top quark mass is usually assumed.

At TeV  $e^+e^-$  colliders  $WW$  fusion is far more important than  $e^+e^- \rightarrow ZH$ . For  $\sqrt{s} \gg m_H$  the former grows logarithmically<sup>(79)</sup>

$$\sigma(e^+e^- \rightarrow \nu\bar{\nu}H) \cong \frac{\alpha^3 \ln\left(\frac{s}{m_H^2}\right)}{16M_W^2 \sin^6\theta_W} = 0.13 \ln\left(\frac{s}{m_H^2}\right) \text{ pb.} \quad (3.10)$$



while the latter falls like  $1/s$ ,  $\sigma \cong (.01/s)$  in picobarns for  $s$  in  $\text{TeV}^2$ . In the regime of interest with  $m_H$  and  $\sqrt{s}$  of the same order of magnitude,  $WW$  fusion is still dominant. For instance, for  $m_H = 400$  GeV it dominates over  $e^+e^- \rightarrow ZH$  for  $\sqrt{s} \geq 500$  GeV.<sup>(79)</sup>

The  $WW$  fusion cross sections for pp and  $e^+e^-$  colliders of various energies are shown in figure (17) taken from Reference (80). For  $m_H = 1$  TeV the pp cross section at  $\sqrt{s} = 40$  TeV is a factor ten larger than at  $\sqrt{s} = 15$  TeV and about  $\sim 40$  times larger than the  $e^+e^-$  cross section at  $\sqrt{s} = 2$  TeV. However the advantage in rate of the 40 TeV pp collider over the  $e^+e^-$  collider is offset by the ability to utilize more of the  $e^+e^-$  signal. It is not known if a  $\sqrt{s} = 2$  TeV  $e^+e^-$  collider can also match the sensitivity of the SSC for the  $WW$  continuum signals of symmetry breaking physics above 1 TeV. It certainly cannot match the reach of the SSC for resonances at  $\sim 2$  TeV in the  $WW$  fusion channel.

The first calculations of  $WW$  fusion were done by numerical methods.<sup>(70,71)</sup> Subsequently analytical expressions were derived for the double differential cross section in the final state fermion energies<sup>(81)</sup> (useful for tagging) and for the differential cross section with respect to the Higgs boson three momentum.<sup>(80)</sup> In addition a computationally simple approximation was derived, the effective  $W$  approximation,<sup>(82,1)</sup> analogous to the more familiar Weiszacker-Williams approximation for photon-photon scattering.<sup>(83)</sup> The effective  $W$  approximation is a small angle approximation that provides no information on the sometimes important transverse momentum distributions of the fermions and Higgs bosons. It is however generally adequate (see below) for calculating yields of heavy Higgs bosons.

The result is an effective luminosity function for the probability to find colliding "beams" of longitudinally polarized gauge bosons  $V_1$  and  $V_2$  in incident fermions  $f_1$  and  $f_2$ ,

$$\frac{\partial \mathcal{L}}{\partial z} \Big|_{V_1 V_2 / f_1 f_2} = \frac{\alpha^2 \chi_1 \chi_2}{\pi^2 \sin^4 \theta_W} \frac{1}{z} \left[ (1+z) \ln \left( \frac{1}{z} \right) - 2 + 2z \right] \quad (3.11)$$

where  $z \equiv s_{VV}/s_{ff}$  and the  $\chi_i$  are the  $f_i$ - $V_i$  couplings, e.g.,  $\chi_W = 1/4$  for all fermions,  $\chi_{Zu\bar{u}} = (1 + (1 - \frac{8}{3} \sin^2 \theta_W)^2)/16 \cos^2 \theta_W$ , etc. ... Equation 3.11 must be convoluted with the desired  $V_1 V_2$  subprocess cross section, e.g.,  $\sigma(V_1 V_2 \rightarrow H)$  if a narrow width approximation is appropriate for  $H$ , and also with the quark

distribution functions in the case of pp collisions.

The effective  $W$  approximation has been compared with analytical<sup>(80)</sup> and numerical evaluations<sup>(81,84,32)</sup> of Higgs boson production. The most definitive results are probably the analytical calculations of Reference (80). They show good agreement for  $WW \rightarrow H$  for  $m_H \geq 500$  GeV, with errors  $\lesssim O(10\%)$  and decreasing with  $m_H$  and  $\sqrt{s}$ , while for the relatively less important process  $ZZ \rightarrow H$  the errors are roughly twice as large.

Care must also be taken in evaluating the subprocess cross section, sometimes characterized by  $\sigma(VV \rightarrow H)$  in narrow width approximation, e.g., Reference (36). At large values of  $m_H$ , the width  $\Gamma_H$  is very large and  $\sigma(VV \rightarrow H)$  must be replaced by a calculation of what is actually measured,  $VV \rightarrow VV$  (i.e.,  $W^+W^- \rightarrow W^+W^-$ ,  $W^+W^- \rightarrow ZZ$ , etc. ...). There are then two possible ways of proceeding. Using the equivalence theorem (cf. Section 2) the scattering amplitudes for longitudinally polarized gauge bosons can be evaluated in an  $R$  gauge from the corresponding Goldstone boson amplitudes, including Higgs boson  $s, t$ , and  $u$  channel exchange contributions.<sup>(1)</sup> This procedure is computationally simple and automatically assures the correct high energy behavior. It provides a good approximation for  $m_H$  and  $\sqrt{s}_{VV}$  above 800 GeV, as shown for instance in figure (2) taken from Reference (35). The alternative is to use the unitary gauge, in which good high energy behavior requires the cancellation of many diagrams involving gauge sector and Higgs sector exchanges, e.g., References (32), (80), (84), and (85).

All the above approximations must be approached with caution to be sure that they are applied within their domains of validity. They can then be very useful, providing needed checks on more exact computations. In particular the equivalence theorem is useful computationally at high energy as a check on the cancellations of the much more complicated  $U$  gauge calculations and as a source of physical intuition (cf. Section 2).

Methods of searching for heavy Higgs bosons at the SSC and LHC have been extensively studied during the last few years, though much more remains to be done. Recent results are summarized in References (19), (43), and (72). Leptonic decay modes,  $H \rightarrow ZZ \rightarrow \ell^+ \ell^- \ell^+ \ell^-$  and  $H \rightarrow ZZ \rightarrow \ell^+ \ell^- \bar{\nu} \nu$  with  $\ell = e$  or  $\mu$ , are the most straightforward, though the latter has at least one potential background that is not yet fully analyzed. Larger rates and, unfortunately,

much larger backgrounds occur in mixed hadron-lepton decay modes such as  $H \rightarrow WW \rightarrow \bar{q}q\ell\bar{\nu}$ . The purely hadronic decays are hopelessly overwhelmed by the four jet QCD background.

The cleanest and rarest channel is  $H \rightarrow ZZ \rightarrow \ell^+\ell^-\ell^+\ell^-$  with  $\ell = e$  or  $\mu$ . With  $BR(Z \rightarrow e^+e^-) = .033$ , the branching ratio is  $(4/3) \cdot (.033)^2 = 1.5 \cdot 10^{-3}$ . The background is from  $\bar{q} \rightarrow ZZ$  and  $gg \rightarrow ZZ$ , the latter<sup>(77)</sup> proceeding by a quark loop. Recent Monte Carlo simulations suggest that the Higgs boson can be detected in this channel for  $m_H \leq 300$  GeV at the LHC<sup>(51)</sup> and for  $m_H \leq 600$  GeV at the SSC.<sup>(43)</sup> (Here and elsewhere unless otherwise stated both SSC and LHC are assumed to operate at  $\mathcal{L} = 10^{33} \text{cm}^{-2} \text{sec}^{-1}$ .) At these values of  $m_H$  the Higgs boson appears as a recognizable peak above the continuum background.

The 1 TeV Higgs boson cross section,  $d\sigma/dM_{ZZ}$ , is shown in figure (18) for pp colliders of 10, 20, 30, and 40 TeV. It is shown again over the  $\bar{q}q \rightarrow ZZ$  background in figure (19) for  $\sqrt{s} = 40$  TeV. At  $m_H = 1$  TeV the width is  $\Gamma_H = 0.5$  TeV and the Higgs boson appears as a broad enhancement over the background. One strategy at this mass is to impose cuts  $|y_Z| < 1.5$  and  $m_{ZZ} > 1$  TeV to optimize the signal to background ratio while retaining a large fraction of the signal.<sup>(1)</sup> With these cuts a calculation using the effective  $W$  approximation and the equivalence theorem yields 4 signal events over a background (augmented by 50% for  $gg \rightarrow ZZ$ ) of  $1\frac{1}{2}$  events for an integrated luminosity of  $10^4 \text{pb}^{-1}$  at the SSC.<sup>(72)</sup> (Here and below unless otherwise stated yields are quoted per  $10^4 \text{pb}^{-1}$  corresponding to  $\mathcal{L} = 10^{33} \text{cm}^{-2} \text{sec}^{-1}$  for  $10^7 \text{sec}$ .) At the LHC the corresponding signal is a factor ten times smaller while the background is about four times smaller. Such a signal at the SSC would not be statistically significant, but augmented by additional years of running and/or results from several experiments it would become significant. It would also be a valuable confirmation of larger signals detected in other channels.

Of course to detect such a structureless signal it is necessary to know the magnitude of the background, requiring a variety of calibrations *in situ* at the SSC to confirm knowledge of the relevant distribution functions and couplings (Section 3.1). After such calibration studies are completed the  $ZZ$  background should be known to within 30% uncertainty,<sup>(43)</sup> sufficient accuracy given the expected 3:1 signal to background ratio.

Ascending the ladder of rates while descending on the scale of "purity" of

signal, we come next to the decay  $H \rightarrow ZZ \rightarrow \bar{\ell}\ell\bar{\nu}\nu$ .<sup>(1,86)</sup> The branching ratio is six times larger than the previous decay,  $1/3 \times 2 \times .066 \times .195 = .0086$ , nearly 1%. Monte Carlo simulations have suggested a reach in this channel to  $m_H \lesssim 600$  GeV at the LHC<sup>(51)</sup> and to at least 800 GeV at the SSC<sup>(43)</sup> (A comparable Monte Carlo study for  $m_H > 800$  GeV at the SSC has not yet been done). The two studies are not directly comparable because while both considered the  $\bar{q}q \rightarrow ZZ$  and  $gg \rightarrow ZZ$  backgrounds, only the SSC study considered the background from  $Z + \text{jet}$  where the jet generates large missing energy, faking a  $Z \rightarrow \bar{\nu}\nu$  decay. This background is sharply reduced by cutting on visible hadronic transverse energy on the side opposite to the observed  $Z \rightarrow \ell^+\ell^-$ . A very hermetic detector was found to be critical. The analysis may be improved in the future by adding cuts involving event topology and the rapidity distribution of the visible hadronic clusters. The same background may be more dangerous at the LHC because of the less favorable signal to background ratio.

The 1 TeV Higgs boson should be observable at the SSC in this mode. Requiring the observed  $Z \rightarrow \ell^+\ell^-$  to satisfy  $p_T > 0.45$  TeV and  $|y| < 1.5$ , the estimated yield is a signal of 27 events over a  $(\bar{q}q \text{ or } gg) \rightarrow ZZ$  background of  $\sim 12$  events.<sup>(72)</sup>

The mixed decay mode,  $H \rightarrow WW \rightarrow \bar{\ell}\nu\bar{q}q$  with  $\ell = e$  or  $\mu$  and  $\bar{q}q = u\bar{d}$  or  $c\bar{s}$ , has a large branching ratio,  $2 \times \frac{1}{6} \times \frac{1}{2} = 1/6$ . However the QCD background from  $Wjj$  is two orders of magnitude bigger than the signal even if we optimistically assume a 5% measurement of the dijet mass.<sup>(44)</sup> Two approaches have been taken to attempt to winnow the signal from this enormous background. One method is to cut on the  $p_T$  of the jets, using the tendency of the longitudinally polarized  $W$ 's from the signal to decay into jets transverse to the  $W$  line of flight, unlike the QCD dijets and the transversely polarized  $W$ 's that both tend to produce jets along the line of flight. Applying this approach to the SSC for  $m_H = 800$  GeV a parton level calculation results in a signal of 500 events over an equal background.<sup>(58)</sup> Smaller but still encouraging yields have been reported based on Monte Carlo studies.<sup>(87)</sup> The prospects to follow this strategy in the real world are more difficult to assess than for the purely leptonic decays, being more sensitive to detailed aspects of jet physics and detector performance.

The second approach to the mixed modes borrows a trick from photon-

photon scattering experiments at  $e^+e^-$  colliders where detecting an  $e^\pm$  near the forward direction is a powerful way to isolate a clean sample of two photon events. The analogous idea<sup>(34)</sup> is to tag the forward jets that occur in  $WW$  fusion,  $qq \rightarrow qqWW$ , with transverse momentum of order  $M_W$ . Of course tagging suffers its own QCD background, due to processes with a real  $W \rightarrow \ell\bar{\nu}$  plus a dijet to fake the second  $W \rightarrow \bar{q}q$  and one or two jets near the forward direction that fake the tagged quark or quarks. The necessary background calculation has not yet been performed. A recent calculation assuming 100% efficient tagging for a 700 GeV Higgs boson resulted in 20 events for an LHC year and 160 events for an SSC year<sup>(88)</sup> (a “year” is always  $10^7$  seconds). The QCD backgrounds after tagging were estimated at 12 and 140 events respectively, however the authors remark that their background estimates will probably prove to be small by a factor of 2. Highly segmented forward calorimeters would be essential.

An additional serious background would occur if  $m_t > M_W$  so that the top quark decays by  $t \rightarrow Wb$ .<sup>(89)</sup> For  $100 \text{ GeV} \leq m_t \leq 200 \text{ GeV}$  the contribution to the  $W^+W^-$  continuum from  $t\bar{t} \rightarrow W^+W^-\bar{b}b$  would be two orders of magnitude larger than  $\bar{q}q \rightarrow W^+W^-$ , eliminating any hope of detecting  $H \rightarrow W^+W^-$ . The leptonic decay signals from  $H \rightarrow ZZ$  would not be affected.

Heavy Higgs boson searches at TeV  $e^+e^-$  colliders do not have to contend with the fierce backgrounds found in pp colliders. As a result detection of the purely hadronic decays  $H \rightarrow WW \rightarrow \bar{q}q\bar{q}q$  is feasible at an  $e^+e^-$  collider though unimaginable at a pp collider. The  $e^+e^-$  colliders can therefore afford to give up an appreciable factor in raw cross section, as figure (17) shows they indeed do for the collider energies under consideration. See reference (90) for a discussion of heavy Higgs boson detection at  $e^+e^-$  colliders, with references to the original literature.

### 3.42 Signals of Dynamical Symmetry Breaking above 1 TeV

Even within the framework of an  $SU(2)_L \times U(1)_Y$  gauge theory broken spontaneously by the Higgs mechanism, there is no guarantee that the Higgs boson exists at all, and there are models in which it does not (Section 2.33). Many of these models predict other quanta below 1 TeV but their properties are uncertain, they may be difficult to find, and to recognize and interpret if they are found. Furthermore at least one model exists without such quanta — technicolor with two flavors. It may not be viable but neither are the multi-flavored tech-

nicolor models that predict light quanta (i.e., pseudogoldstone bosons). Since there are no satisfactory dynamical models it is dangerous to rely heavily on the existing models for guidance.

The analysis reviewed in Section 2.4 uses only unitarity and symmetry properties valid in any spontaneously broken  $SU(2)_L \times U(1)_Y$  gauge theory. Two alternatives emerge, classified according to the strength of the interaction of the symmetry breaking sector. If the symmetry breaking force is weak then new weakly coupled quanta exist in the  $J = 0$  channel below 1 TeV i.e., Higgs bosons.

The second alternative is that the symmetry breaking force is strong in which case the new quanta are to be found above 1 TeV and, probably, not far beyond 2 TeV. Whether the quanta exist below 2 TeV or not, the presence of the strong force will be revealed by strong scattering of longitudinally polarized  $W$  and  $Z$  bosons at  $WW$  center of mass energies between 1 and 2 TeV. If, as we have learned from the study of hadron physics, resonances form when strong scattering occurs, then there will be resonances in at least some of the  $WW$ ,  $WZ$ , and  $ZZ$  channels near 2 TeV. In any case the presence or absence of the continuum signals is a general test of whether the symmetry breaking sector is strongly coupled, regardless of the detailed nature of the spectrum. In this subsection we consider the  $ZZ$ ,  $WZ$ , and  $WW$  continuum signals of strong interactions and one example of a resonance near 2 TeV.

The estimate of the continuum signal is based on the low energy theorems, equations 2.79-2.83, valid to all orders in the interactions of the symmetry breaking sector.<sup>(1,2)</sup> As the analogous  $\pi\pi$  low energy theorems,<sup>(8)</sup> e.g., equation 2.69, are probably applicable for  $\sqrt{s} \cong 300 \text{ MeV}$ , we might expect equations 2.79-2.83 to apply at  $\lesssim 300 \text{ MeV} \times v/F_\pi \cong 1 \text{ TeV}$ . A crude model<sup>(1)</sup> of the strong continuum consists of extrapolating above 1 TeV, using equations 2.79-2.83 as a model for the absolute value of the relevant partial wave amplitudes which are  $a_{JI} = a_{00}, a_{11}, a_{02}$  where  $I$  denotes the effective low energy custodial  $SU(2)$ . Above the energy at which partial wave unitarity is saturated, the amplitudes are set equal to one. For  $a_{00}$  saturation occurs at  $\sqrt{16\pi v^2} = 1.7 \text{ TeV}$ , equation 2.89, so in that case the model is

$$|a_{00}(s)| = \frac{s}{16\pi v^2} \theta(16\pi v^2 - s) + 1 \cdot \theta(s - 16\pi v^2). \quad (3.12)$$

The detailed form is not critical, the essential point being to extrapolate smoothly from the known behavior at low energy into the domain above 1 TeV where the amplitude becomes strong, of order 1, without assuming enhanced resonant behavior. Continuum cross section signals are then computed from  $WW$ ,  $WZ$ , and  $ZZ$  fusion. The  $ZZ$  signals for 10, 20, 30, and 40 TeV colliders are shown in figure (20). The signal at 40 TeV is seen with the  $\bar{q}q \rightarrow ZZ$  background in figure (19).

The model is conservative in that it assumes no resonant behavior. For instance, the  $ZZ$  continuum signal for  $M_{ZZ} > 1$  TeV is only half the corresponding signal from the 1 TeV Higgs boson. Comparatively little is gained from the high energy region where  $|a_J| = 1$  because of the rapidly falling luminosities at the relevant collider energies. The model is also conservative in that only the leading partial waves ( $I, J = (0, 0), (1, 1), (2, 0)$ ) are kept while higher partial waves are set to zero.

Figure (21) from reference (91) shows how well the model fits  $\pi\pi$  scattering data. The ‘‘dictionary’’ is that  $\sim 650$  MeV corresponds to the unitarity limit at 1.75 TeV. Our model corresponds to curve  $a$  in  $|T_0^0|$ ,  $|T_1^1|$ , and  $\text{Re } T_0^2$  (since  $T_0^2$  is exotic in QCD, the imaginary part is negligible below 1 GeV). The model describes the trend of the 0, 0 channel well. In the 1, 1 channel it underestimates the data by a large factor, as a result of the rho meson. In the 2, 0 channel there is considerable disagreement between different experiments; the model interpolates the data out to  $\sim 600$  MeV beyond which it overestimates the data. This is not as serious as it might seem since  $\sqrt{s}_{\pi\pi} > 600$  MeV corresponds to  $\sqrt{s}_{WW} > 1.7$  TeV where the  $WW$  luminosity at the SSC is small so that  $WW$  yields are not very sensitive to the model in this region.

The experimental yields for this model have been estimated for pp colliders<sup>(1,72)</sup> and  $e^+e^-$  colliders.<sup>(35,92)</sup> (Below unitarity saturation energies the  $m_H \rightarrow \infty$  limit considered in Reference (92) is equivalent to the model described here.) Since the continuum signal is shifted to larger values of  $M_{ZZ}$  relative to the 1 TeV Higgs boson, it puts even greater stress on the beam energy. The most promising leptonic signal for the  $ZZ$  channel is  $ZZ \rightarrow \ell^+\ell^-\bar{\nu}\nu$  with  $\ell = e$  or  $\mu$ . Requiring the observed  $Z$  to satisfy  $|y| < 1.5$  and  $p_T > 0.45$  TeV, the yield at  $\sqrt{s} = 40$  TeV is 15 events over a background of  $\sim 12$  including  $gg \rightarrow ZZ$ .<sup>(72)</sup> The corresponding signal at  $\sqrt{s} = 16$  TeV is 1 event over a background of 4 or 5.

The possible background from  $Z$ +jet has not yet been examined but is probably less pernicious than for the 800 GeV Higgs boson considered in Reference (43).

Unlike the standard Higgs boson signal, strong interaction continuum signals also occur in the  $W^\pm Z$  and like-charge  $WW$  channels.<sup>(1)</sup>  $WZ$  can be detected in clean leptonic decays  $WZ \rightarrow \ell\nu\ell\bar{\ell}$ ,  $\ell = e$  or  $\mu$ , with a  $\sim 1\%$  branching ratio, augmented to  $\sim 1.5\%$  if  $W \rightarrow \tau\nu$  is also feasible. Assuming only  $e$ 's and  $\mu$ 's the expected signal is  $\sim 7-1/2$  events over a  $\bar{q}q \rightarrow WZ$  background of  $\sim 3$  after cuts of  $|y_{W,Z}| < 1.5$  and  $M_{WZ} > 1$  TeV.

If either of the methods discussed in Section 3.41 to detect the mixed decay modes  $WW \rightarrow \ell\bar{\nu}\bar{q}q$  prove practicable, they can also be applied to the  $WW$  continuum signal. Including  $W^+W^-$ ,  $W^+W^+$ , and  $W^-W^-$ , the net  $WW$  continuum signal with  $|y_W| < 1.5$  and  $M_{WW} > 1$  TeV is  $\sim 2/3$  of the  $H \rightarrow W^+W^-$  signal for  $m_H = 1$  TeV.<sup>(1)</sup>

The like-charge signal,  $W^+W^+ + W^-W^-$ , not accessible to  $e^+e^-$  colliders, is of special interest because it is free of the  $\bar{q}q$  and/or  $gg$  annihilation backgrounds that occur in the  $W^+W^-$ ,  $W^\pm Z$ , and  $ZZ$  channels at pp colliders. This means that the signal for lower mass gauge boson pairs may be observable, with the benefit of increased rate from higher quark effective luminosities. It also means that more of the signal comes from the domain of validity of the low energy theorems. Of course the charge can only be determined in leptonic decays so that  $M_{WW}$  cannot be measured. Taking only  $\ell = e, \mu$  the branching ratio for  $WW \rightarrow \ell\bar{\nu}\ell\bar{\nu}$  is 0.028. The true physics background,  $pp \rightarrow (W^+W^+ \text{ or } W^-W^-)X$ , occurs in leading order by gluon exchange. It was recently computed; correcting an error in the original paper,<sup>(93)</sup> this background<sup>(94)</sup> is of the same order as the continuum model signal. Other backgrounds, primarily from heavy quark decays, can be rejected by requiring the leptons to be isolated and by cutting against events with high  $p_T$  hadronic jets.

Because the equivalence theorem imposes a lower limit on the domain of validity of the low energy theorems,  $M_{WW}^2 \gg M_W^2$ , equation 2.65, the signal is computed with  $M_{WW} > 500$  GeV imposed. In fact lower values of  $M_{WW}$  will contribute and increase the signal considerably, defined operationally by cuts on the observed leptons of  $|y_\ell| < 3$  and  $p_T(\ell) > 50$  GeV. The corresponding signal yield is 40 events at  $\sqrt{s} = 40$  TeV and  $\sim 4$  at  $\sqrt{s} = 15$  TeV.<sup>(93)</sup> For a light Higgs boson,  $m_H < 200$  GeV, the signal would be entirely negligible, while for  $m_H =$

1 TeV it is  $\sim 1/4$  of the value for the continuum model. A model based on the  $I = 2 \pi\pi$  scattering data gives a yield of about 25 events.<sup>(93)</sup> The required  $e$  and  $\mu$  charge determinations are well within the range of experimental feasibility.<sup>(95)</sup>

Though we have pessimistically concentrated here on continuum signals of strong  $WW$  scattering, where there are strong interactions there are probably also resonances. As a concrete example consider the techni-rho meson of  $N_c = 4$  technicolor, with a mass of 1.8 TeV and width of 260 GeV — see equations 2.62 and 2.63. In pp colliders both  $\bar{q}q \rightarrow \rho_T^{(36)}$  and  $WW \rightarrow \rho_T^{(1)}$  contribute comparably to the production cross section. In analogy to the hadronic  $\rho$  we expect the charged  $\rho_T$  to decay predominantly to  $WZ$ ,  $\rho_T^\pm \rightarrow W^\pm Z$ , which can be detected in the leptonic decay mode  $WZ \rightarrow \ell\bar{\nu}\ell\bar{\ell}$  that occurs with a 1% branching ratio for  $\ell = e$  or  $\mu$ . Then at the SSC with  $10^4 \text{ pb}^{-1}$  the signal in the central region,  $|y_W|$  and  $|y_Z| < 1.5$ , is 12 events over a  $\bar{q}q \rightarrow WZ$  background of only 1 event, while the LHC signal is 1 event over a somewhat smaller background.<sup>(1,72)</sup>

In this and the preceding section on heavy Higgs boson detection I have not made much of the fact that the signals are dominated by longitudinally polarized  $W$ 's and  $Z$ 's while the backgrounds are predominantly transverse. The decay angular distributions do not differ sharply enough and the statistics are typically too low to use polarization as an effective discriminant against the background. However it will be important to analyze the  $W$  and  $Z$  polarizations of any potential signal to confirm the expected predominance of longitudinal modes.

#### 4. CONCLUSION

The TeV scale is not just the next energy scale that we will be able to study in the laboratory but it defines the outer boundary of an energy region certain to contain a crucial missing element of the standard model. We are very lucky to soon be able to study it experimentally, since the only other sure landmark is the unimaginably distant Planck mass at  $10^{19}$  GeV.

The missing element that we are certain to learn about in the TeV region is  $\mathcal{L}_{SB}$ , the unknown lagrangian of electroweak symmetry breaking. A collider with enough energy and luminosity to study strong  $WW$  scattering between 1 and 2 TeV is sure to show us where to look for  $\mathcal{L}_{SB}$  and is likely to allow direct observation of the new quanta. This is true whether strong  $WW$  scattering occurs or not. If it is observed not to occur we will learn that symmetry breaking is due to a Higgs boson or bosons below 1 TeV. They will be copiously produced at any collider sufficient to observe the strong scattering signal. If the strong scattering signal is observed, we will learn that  $\mathcal{L}_{SB}$  is a strongly-coupled lagrangian with quanta above 1 TeV. The strong scattering signal will occur even if the new quanta are much heavier than 1 TeV, though it is far more likely that they will be found near the 1.7 TeV unitarity scale, equation 1.1. A collider able to see the 1-2 TeV continuum signal of a strongly coupled  $\mathcal{L}_{SB}$  would also suffice to discover the low-lying resonances expected near the  $\sim 1.7$  TeV unitarity limit.

At  $\mathcal{L} = 10^{33} \text{ cm}^{-2} \text{ sec}^{-1}$  the LHC can reach<sup>(51)</sup> to perhaps 600 GeV in the mass of the standard model Higgs boson, using the leptonic channel  $H \rightarrow ZZ \rightarrow e^+e^-/\mu^+\mu^- + \bar{\nu}\nu$ . At the same luminosity and in the same channel the SSC can reach to  $m_H = 1$  TeV.<sup>(72)</sup> With the SSC but not the LHC we could also observe the 1-2 TeV strong  $WW$ ,  $WZ$ , and  $ZZ$  scattering signals in leptonic decay channels. Detection capability of the SSC would be further enhanced if observation of mixed modes,  $WW \rightarrow \ell\bar{\nu} + \bar{q}q$ , proves practicable. At least with the tagging strategy discussed in Section 3.43, it appears that mixed modes do not improve the LHC reach beyond 600 GeV.<sup>(76)</sup>

As discussed elsewhere,<sup>(96)</sup> in order for the LHC to have a reach for strong  $WW$  scattering statistically equivalent to that of the SSC using all feasible leptonic decay modes, we would require an LHC luminosity of  $6 \cdot 10^{35} \text{ cm}^{-2} \text{ sec}^{-1}$ . This estimate is based exclusively on the all-muon decay mode for the high- $\mathcal{L}$  LHC,  $ZZ \rightarrow \mu^+\mu^- + \mu^+\mu^-$ , since that is the only surely detectable mode at

such luminosities. The study of the LHC high luminosity option<sup>(76)</sup> reported that  $ZZ \rightarrow \ell^+ \ell^- \bar{\nu} \nu$  and  $WW \rightarrow \ell \bar{\nu} q \bar{q}$  could not be utilized. It is not clear whether electron identification is feasible above  $10^{34} \text{cm}^{-2} \text{sec}^{-1}$ , since, for example, event pile-up causes overlapping  $\pi^\pm - \gamma$  pairs that fake an  $e^\pm$  signal (not to mention the problems of radiation damage and data acquisition). If electrons could be identified  $\mathcal{L} = 1.5 \cdot 10^{35} \text{cm}^{-2} \text{sec}^{-1}$  would suffice.

If strong  $WW$  scattering does not occur,  $\mathcal{L}_{SB}$  is weakly coupled and we expect Higgs bosons below 1 TeV. There is then a theoretical prejudice for supersymmetry since it is the only *known* weak-coupling solution of the technical naturalness problem. (Of course the only *known* solution need not be the *only* solution.) The solution requires that the superpartners are not much heavier than the 1 TeV scale. Production cross sections for 1 TeV squarks and gluinos are large at both the LHC and SSC, but the decay modes are complicated and may be difficult to observe over backgrounds. Though the problem has not been completely analyzed, it seems likely that discovery strategies will be found. Careful study is needed to decide whether the factor 25 cross section advantage at the SSC is essential or whether the LHC energy could suffice. In any event an additional factor 25 in cross section would certainly be welcome to study the new phenomena, whether needed for their discovery or not.

Searches for fourth generation quarks are possible to at least 1 TeV at the SSC and perhaps beyond. The reach at the SSC is about twice that of the LHC for heavy quarks. Unless the fourth generation neutrino is surprisingly heavy — in the multi-hundred GeV range — the bound from the rho parameter implies that the charged lepton is no heavier than  $\sim 350$  GeV. Despite sizeable cross sections it is not clear that a 350 GeV charged lepton could be observed at the LHC or SSC (see Section 3.2).

As discussed in Section 3, the SSC and LHC can probe for composite quark and lepton structure to scales of order  $10^{-18} \text{cm}$ ., five orders of magnitude smaller than hadron sizes. The SSC can reach to  $O(10)$  TeV for heavy  $W$ 's and to half that for heavy  $Z$ 's, while the LHC reach is about half that of the SSC in both cases. The leptonic signals are spectacular and background-free.

Perhaps more important than the topics I have discussed are those I have not. Multi-TeV pp colliders will open up a tremendous phase space for completely unanticipated and revolutionary discoveries. The prospects are exciting,

both for what we are sure to find and for what we cannot now imagine. But nothing (or almost nothing) will be easy, and the requirements to discover many of the signals are very demanding. There is plenty of work for all high energy physicists, both theorists and experimenters, to ensure that we make the most effective use of these powerful instruments.

#### Acknowledgements

I wish to express my gratitude to Professors K.T. Chao, C.S. Gao, D. Qin, Y. Zhu for their kindness and superb hospitality and for arranging a very enjoyable meeting. I am grateful for the support of Peking University, the Institute of Modern Physics, and the Chinese Center for Advanced Science and Technology.

## References

1. M. Chanowitz and M. Gaillard, Nucl. Phys. B261: 379 (1985).
2. M. Chanowitz, M. Golden, and H. Georgi, Phys. Rev. D36: 1490 (1987); Phys. Rev. Lett. 57: 2344 (1986).
3. U. Amaldi *et al.*, Phys. Rev. D36: 1385 (1987).
4. M. Gell Mann and M. Levy, Nuovo Cim. 16: 705 (1960); B.W. Lee, *Chiral Dynamics*, New York, Gordon & Breach (1972).
5. S.L. Glashow, Nucl. Phys. 22: 579 (1961).
6. S. Weinberg, Phys. Rev. Lett. 19: 1264 (1967); A. Salam, in *Proc. 8th Nobel Symp.*, ed. N. Svartholm, p. 367, Stockholm: Almqvist & Wiksells (1968).
7. E.S. Abers and B.W. Lee, Phys. Rep. 9C: 1 (1973).
8. S. Weinberg, Phys. Rev. Lett. 17: 616 (1966).
9. M. Gell Mann, Physica 1: 63 (1964).
10. G. Costa *et al.*, Nucl. Phys. B297: 244 (1988).
11. P. Sikivie *et al.*, Nucl. Phys. B173: 189 (1980).
12. D. Dicus and V. Mathur, Phys. Rev. D7: 3111 (1973); B.W. Lee, C. Quigg, and H. Thacker, Phys. Rev. D16: 1519 (1977).
13. M. Veltman, Nucl. Phys. B123: 89 (1977).
14. M. Chanowitz, M. Furman, I. Hinchliffe, Phys. Lett. 78B: 285 (1978); Nucl. Phys. B153: 402 (1979).
15. R.N. Cahn, LBL-26433 and these proceedings (1988).
16. S. Weinberg, Phys. Rev. D13: 974 (1976); D19: 1277 (1979); L. Susskind, Phys. Rev. D20: 2619 (1979).
17. J. Wess and B. Zumino, Phys. Lett. 49B: 52 (1974).

18. R.N. Cahn, LBL-25092, to be published in *Reports on Progress in Physics* (1988).
19. M.S. Chanowitz, Ann. Rev. Nucl. Part. Sci. 38: 323 (1988).
20. Y.A. Golfand and E.P. Likhtman, JETP Lett. 13: 373 (1971); D.V. Volkov and P.V. Akulov, Phys. Lett. 46B: 109 (1973); J. Wess, B. Zumino, Nucl. Phys. B70: 379 (1974).
21. R. Barbieri, G.F. Giudice, Nucl. Phys. B203: 75 (1988); J. Ellis *et al.*, Mod. Phys. Lett. A1: 57 (1986).
22. P. Fayet, Nucl. Phys. B90: 104 (1975); R. Kaul, P. Majumdar, Nucl. Phys. B199: 38 (1982).
23. E. Farhi, L. Susskind, Phys. Rep. 74: 277 (1981).
24. P. Frampton, Phys. Rev. Lett. 43: 1912 (1979).
25. E. Bloom, F. Gilman, Phys. Rev. D4: 2901 (1970); Phys. Rev. Lett. 25: 1140 (1971).
26. G. 't Hooft, Nucl. Phys. B72: 461 (1974).
27. T.D. Lee, C.N. Yang, Phys. Rev. Lett. 4: 307 (1960); B. Ioffe, L. Okun, A. Rudik, Sov. Phys. JETP Lett. 20: 1281 (1965).
28. M. Cornwall, D. Levin, G. Tiktopoulos, Phys. Rev. D10: 1145 (1974).
29. G. Gounaris, R. Kogerler, H. Neufeld, Phys. Rev. D34: 3257 (1986).
30. C. Vayonakis, Lett. Nuovo Cim. 17: 383 (1976).
31. M. Duncan, G. Kane, W. Repko, Nucl. Phys. B272: 571 (1986).
32. D. Dicus, R. Vega, Phys. Rev. Lett. 57: 1110 (1986).
33. J. Gunion, J. Kalinowski, A. Tofighi-Niakis, Phys. Rev. Lett. 57: 2351 (1986).
34. R.N. Cahn *et al.*, Phys. Rev. D35: 1626 (1987).

35. M.C. Bento, C.H. Llewellyn-Smith, Nucl. Phys. B289: 36 (1987).
36. E. Eichten *et al.*, Rev. Mod. Phys. 56: 579 (1984).
37. *Proc. Workshop on Physics at Future Accelerators*, ed. J. Mulvey, CERN 87-07 (1987).
38. *Proc. 1984 Summer Study on Design and Utilization of the SSC*, eds. R. Donaldson, J. Morfin, APS/DPF (1984).
39. *Proc. Summer Study on Physics of the Superconducting Super Collider*, eds. R. Donaldson, J. Marx, APS/DPF (1986).
40. *Proc. Workshop on Experiments, Detectors, and Experimental Areas for the SSC, July 7-17, 1988, Berkeley*, eds. R. Donaldson, M. Gilchriese, (World Scientific, Singapore, 1988).
41. G. Altarelli and G. Parisi, Nucl. Phys. B126: 298 (1977).
42. J. Gunion, p. 147, reference (38).
43. R. Cahn *et al.*, p. 20, reference (40).
44. W. Stirling *et al.*, Phys. Lett. 163B: 261 (1985); J. Gunion *et al.*, Phys. Lett. 163B: 389 (1985).
45. See for example J. Collins, p. 287, reference (40).
46. R.S. Chivukula, H. Georgi, Phys. Lett. 188B: 99 (1987); R.S. Chivukula, L. Randall, H. Georgi, Nucl. Phys. B292: 93 (1987); R.S. Chivukula, H. Georgi, Phys. Rev. D36: 2102 (1987).
47. M.S. Chanowitz, S.D. Drell, Phys. Rev. D9: 2078 (1974); Phys. Rev. Lett. 30: 807 (1973),.
48. E. Eichten, K. Lane, M. Peskin, Phys. Rev. Lett. 50: 811 (1983).
49. V. Barnes *et al.*, p. 235, reference (40).
50. Private discussion with M. Suzuki.
51. D. Froidevaux *et al.*, p. 61, reference (37).

52. P. Langacker, R. Robinett, J. Rosner, Phys. Rev. D30: 1470 (1984).
53. S. Dawson *et al.*, p. 144, reference (40).
54. S. Dawson, S. Godfrey, p. 165, reference (40).
55. V. Barger, T. Han, J. Ohnemus, Phys. Rev. D37: 1174 (1988).
56. G. Anderson and I. Hinchliffe, p. 282, reference (40).
57. K. Ellis and R. Gonsalves in *Supercollider Physics*, ed. D. Soper (World Scientific, Singapore, 1985).
58. J. Gunion and M. Soldate, Phys. Rev. D34: 826 (1986).
59. R.M. Barnett *et al.*, p. 178, reference (40).
60. R.M. Barnett *et al.*, Phys. Rev. Lett. 60: 401 (1988).
61. H. Baer and E. Berger, Phys. Rev. D34: 1361 (1986) and D35: 406 (E)(1987); G. Gamberini, Z. Phys. C30: 605 (1986); H. Baer *et al.*, Phys. Rev. D36: 96 (1987).
62. C. Albajar *et al.* (UA1 collaboration), Phys. Lett. 198B: 261 (1987).
63. H. Baer *et al.*, p. 210, reference (40).
64. R. Batley, Vol. II, p. 109, reference (37).
65. S. Weinberg, Phys. Rev. Lett. 36: 294 (1976); A. Linde, JETP Lett. 19: 296 (1976); Phys. Lett. 63B: 435 (1976).
66. F. Wilczek, Phys. Rev. Lett. 39: 1304 (1977).
67. H. Haber, G. Kane, Phys. Lett. 135B: 196 (1984); R.M. Barnett *et al.*, Phys. Lett. 136B: 191 (1984); Phys. Rev. D30: 1529 (1984); R. Willey, Phys. Rev. Lett. 52: 585 (1984).
68. B. Ioffe, V. Khoze, Leningrad report 274 (1976); J.D. Bjorken in *Proc. SLAC Summer Inst. on Particle Physics, SLAC-198*, ed. M. Zipf, p. 1 (1976).
69. J. Ellis, M. Gaillard, D. Nanopoulos, Nucl. Phys. B106: 292 (1976).



70. D. Jones, S. Petcov, Phys. Lett. 84B: 440 (1979); Z. Hioki, S. Midorikawa, H. Nishiura, Prog. Theor. Phys. 69: 1484 (1983).
71. R. Cahn and S. Dawson, Phys. Lett. 136B: 196 (1984) and 138B: 464 (E)(1984).
72. M. Chanowitz, in *Results and Perspectives in Particle Physics*, ed. M. Greco, p. 335 (Editions Frontieres, Gif-sur-Yvette, 1987).
73. Conceptual Design of the SSC, ed. J. Jackson, SSC-SR-2020 (1986).
74. K. Johnsen, p. 16, reference (37).
75. G. Brianti, p. 6, reference (37).
76. The Feasibility of Experiments at High Luminosity at the LHC, ed. J. Mulvey, CERN 88-02 (1988).
77. H. Georgi *et al.*, Phys. Rev. Lett. 40: 692 (1978).
78. J. Gunion *et al.*, Nucl. Phys. B294: 621 (1987).
79. G. Altarelli, p. 36, reference (37).
80. G. Altarelli, B. Mele, F. Pitolli, Nucl. Phys. B287: 205 (1987).
81. R. Cahn, Nucl. Phys. B255: 341 (1985).
82. M.S. Chanowitz, M.K. Gaillard, Phys. Lett. 142B: 85 (1984); S. Dawson, Nucl. Phys. B29: 42 (1985); G. Kane, W. Repko, W. Rolnick, Phys. Lett. 148B: 367 (1984).
83. See e.g., *Classical Electrodynamics*, J.D. Jackson, N.Y./London: Wiley, 2nd ed. (1975).
84. J. Gunion *et al.*, p. 156, reference (39); Phys. Rev. Lett. 57: 2351 (1986).
85. M. Duncan, G. Kane, W. Repko, Nucl. Phys. B272: 571 (1986).
86. R. Cahn and M. Chanowitz, Phys. Rev. Lett. 56: 1327 (1986).
87. A. Savoy-Navarro, p. 68, reference (40).

88. R. Kleiss, W. Stirling, Phys. Lett. 200B: 193 (1988).
89. G. Herten, p. 103, reference (40).
90. F. Richard, p. 23, Vol. II, reference (37); J. Gunion, A. Tofighi-Niaki, Phys. Rev. D36: 2671 (1987).
91. J. Donoghue, C. Ramirez, G. Valencia, Phys. Rev. D38: 2195 (1988).
92. J. Gunion, A. Tofighi-Niaki, reference (90).
93. M. Chanowitz, M. Golden, Phys. Rev. Lett. 61: 1053 (1988); the gluon exchange background reported here is incorrect due to a programing error (see ref. (94)).
94. D. Dicus and R. Vega, U.C. Davis preprint (1988).
95. G. Hanson *et al.*, p. 340, reference (40).
96. M. Chanowitz, contribution to the INFN Eloisatron Project Workshop Summary Report, Erice (1988).

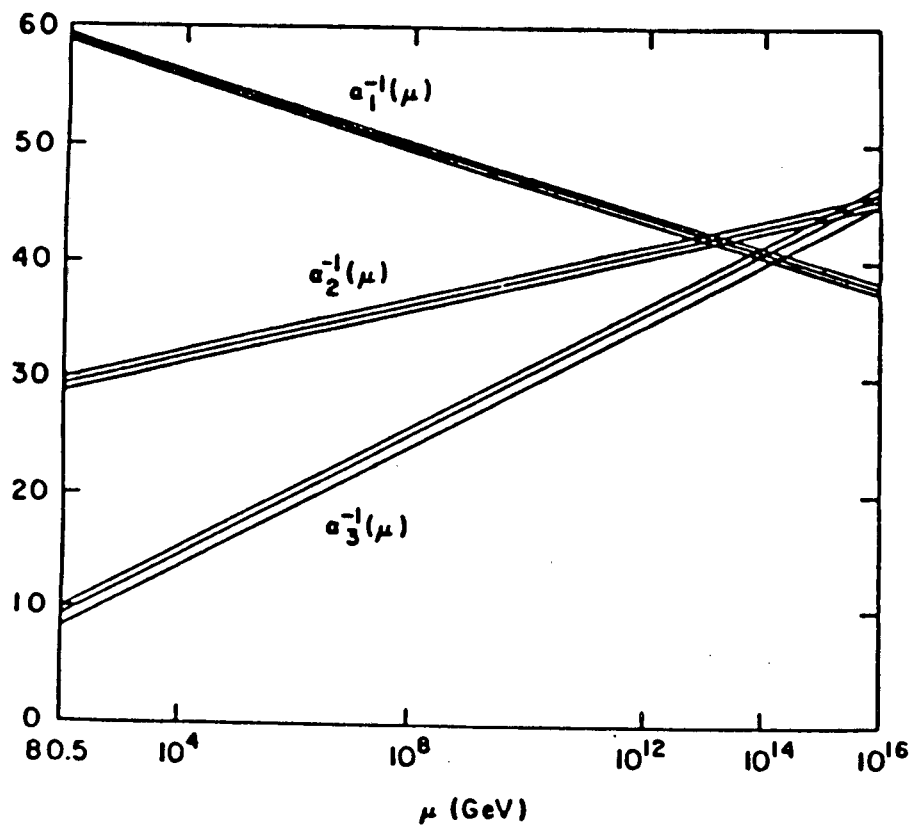


Figure 1: Evolution of  $SU(3)_C \times SU(2)_L \times U(1)_Y$  gauge coupling constants (from ref. 3). In the absence of new physics the couplings seem not to intersect at a point.

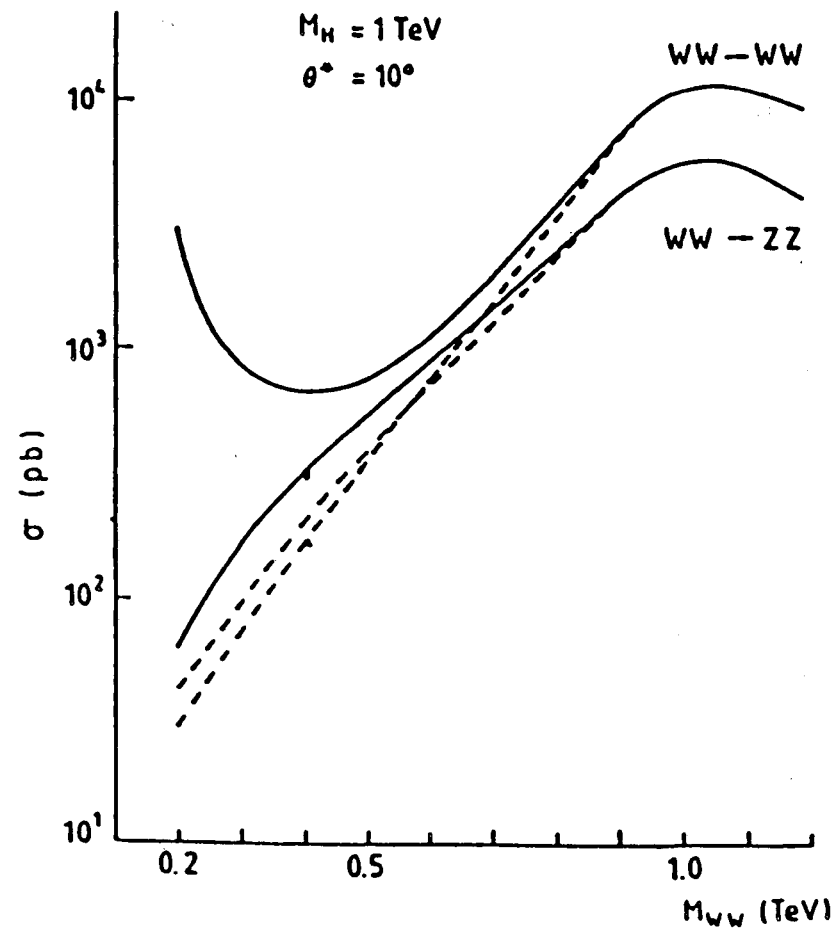


Figure 2: Comparison of  $WW$  cross sections in unitary gauge and with use of the equivalence theorem (from ref. 35).

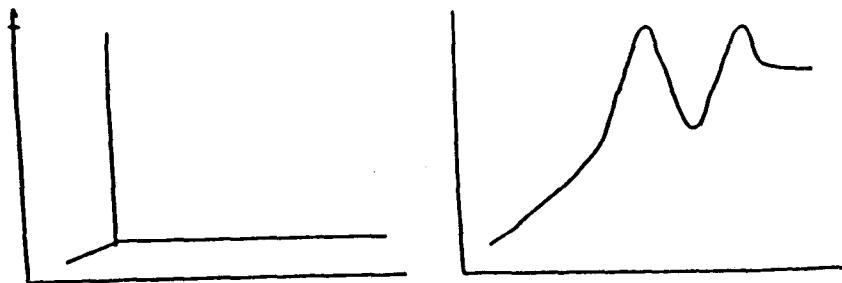


Figure 3: Typical behavior of partial wave amplitudes for  $W_L W_L$  scattering. The plot on the left represents a weak coupling model with a narrow (Higgs) resonance below 1 TeV. The plot on the right shows strong coupling behavior, with saturation of unitarity and broad resonances in the 1-2 TeV region.

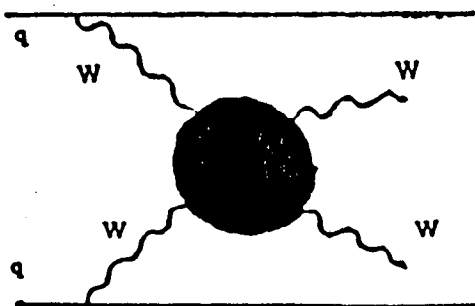


Figure 4: Production of  $WW$  pairs by  $WW$  fusion.

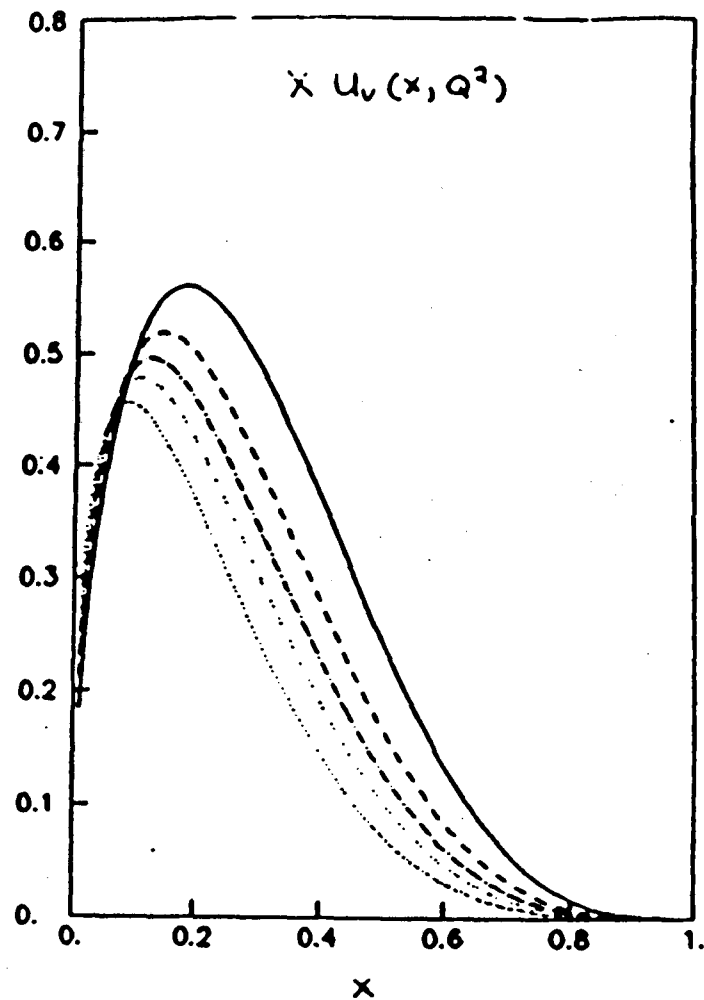


Figure 5: The valence up quark distribution of the proton,  $x u_v(x, Q^2)$ , as a function of  $x$  for various  $Q^2$ . The solid, dashed, dot-dashed, sparse dot, and dense dot lines correspond to  $Q^2 = 10, 10^2, 10^3, 10^4$ , and  $10^6$  (GeV)<sup>2</sup> respectively (from ref. 36).

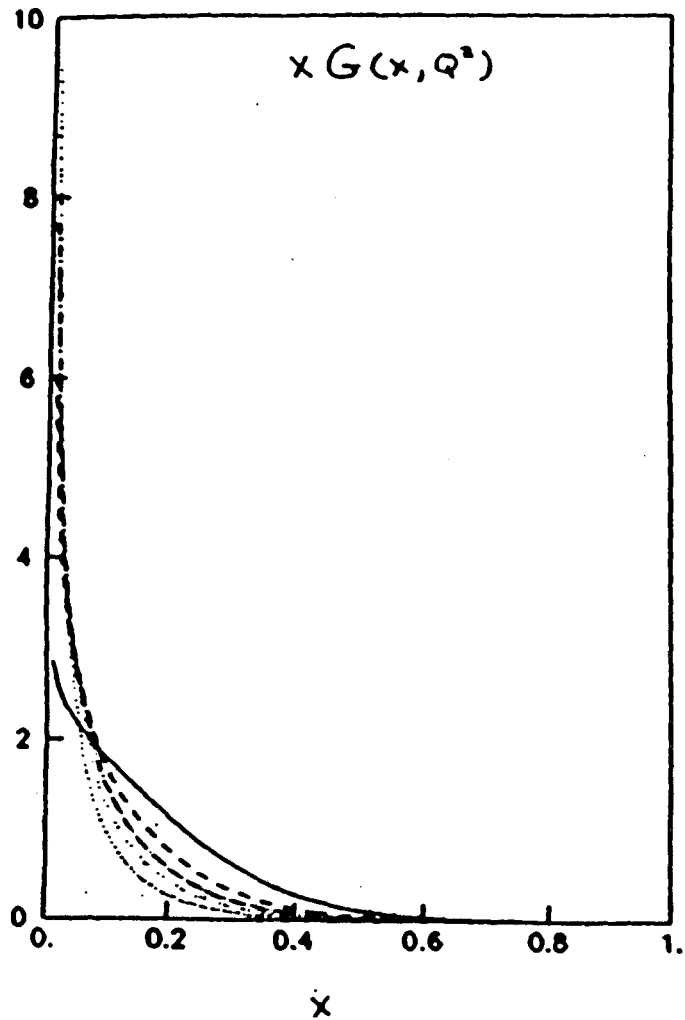


Figure 6: The gluon distribution of the proton,  $xG(x, Q^2)$ , as a function of  $x$  for various  $Q^2$ . The solid, dashed, dot-dashed, sparse dot, and dense dot lines correspond to  $Q^2 = 10, 10^2, 10^3, 10^4$ , and  $10^5$  (GeV) $^2$  respectively (from ref. 36).

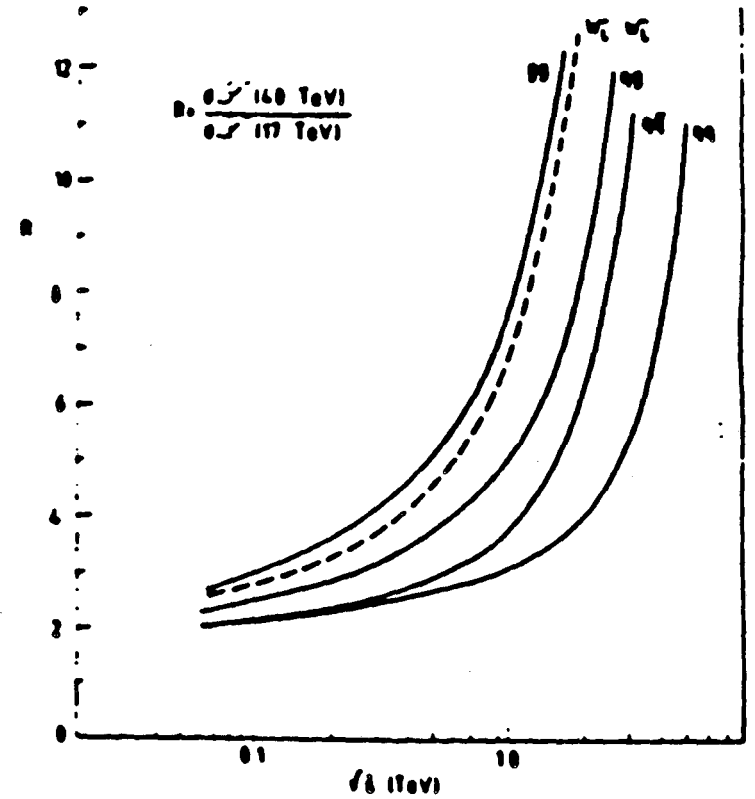


Figure 7: The ratio of luminosity distributions,  $R = \mathcal{L}(40 \text{ TeV})/\mathcal{L}(17 \text{ TeV})$  for (from left to right)  $gg$ ,  $W_L^- W_L^-$ ,  $qg$ ,  $q\bar{q}$ , and  $qq$  scattering (from the contribution of Z. Kunzst, ref. 37).

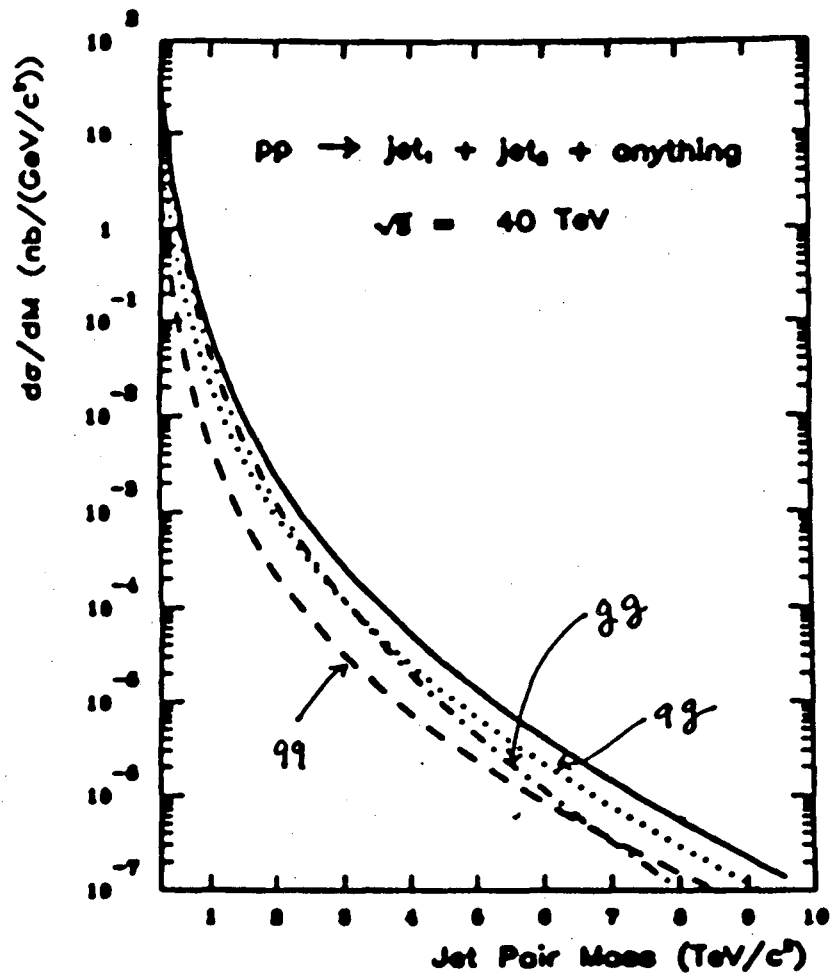


Figure 8: The inclusive dijet differential cross section with respect to the dijet mass at  $\sqrt{s} = 40 \text{ TeV}$  (from ref. 36).

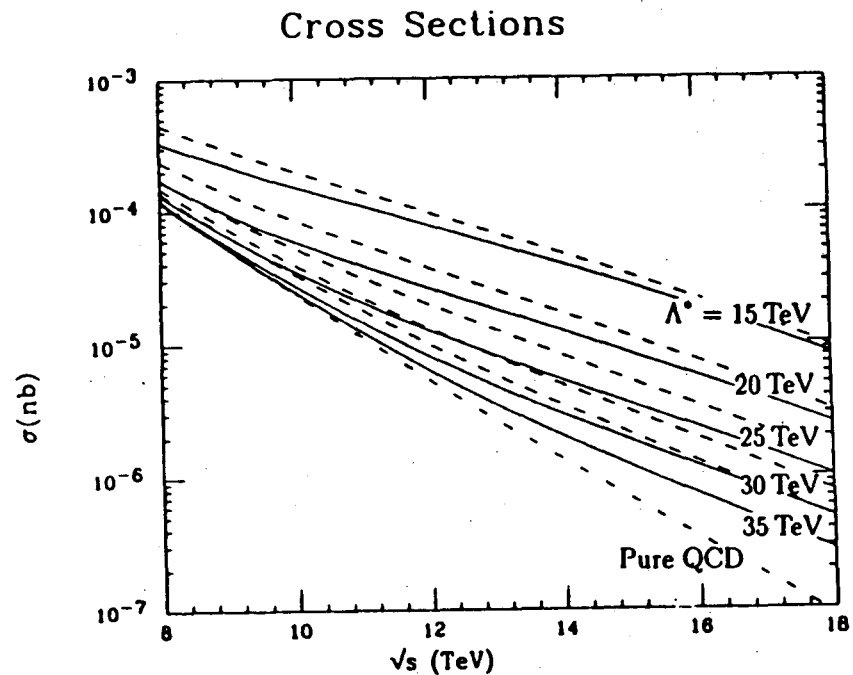


Figure 9: The cross section at the SSC to produce a jet-jet pair with invariant mass greater than  $\sqrt{\hat{s}}$ , with a scattering angle between  $60^\circ$  and  $120^\circ$  in the jet-jet c.m., as a function of  $\sqrt{\hat{s}}$ . The dashed line is for production by QCD only. The cross section increases as the value of  $\Lambda^*$  is decreased progressively, with the values 35, 30, 25, 20, 15 TeV. The dotted curves are for constructive interference between QCD and the compositeness interaction, the solid curves for destructive interference (from ref. 49).

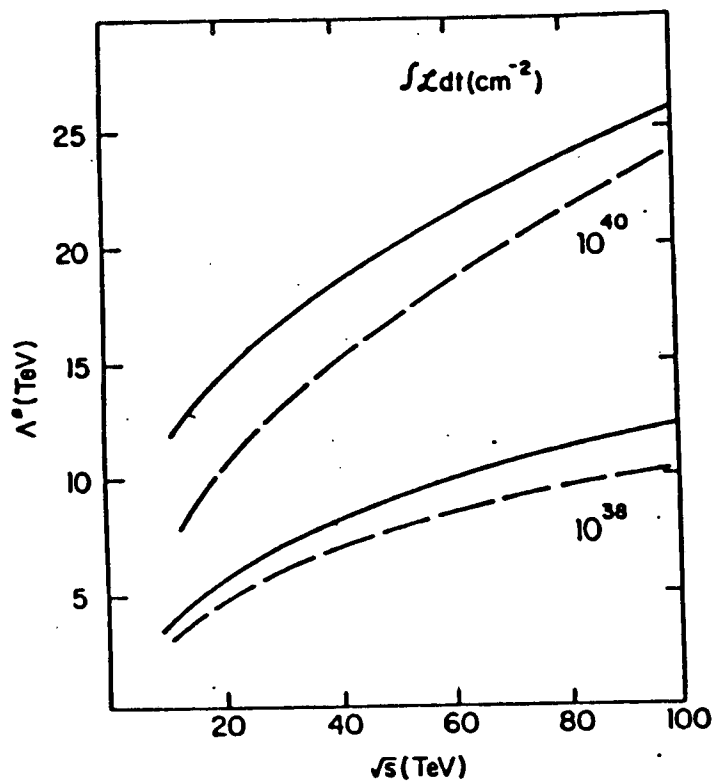


Figure 10: The ability to observe a compositeness scale  $\Lambda^*$  as a function of  $\sqrt{s}$  for integrated luminosities of  $10^{38}$  and  $10^{40}$   $\text{cm}^{-2}$ . Solid and dashed curves correspond to constructive and destructive interference (from ref. 36).

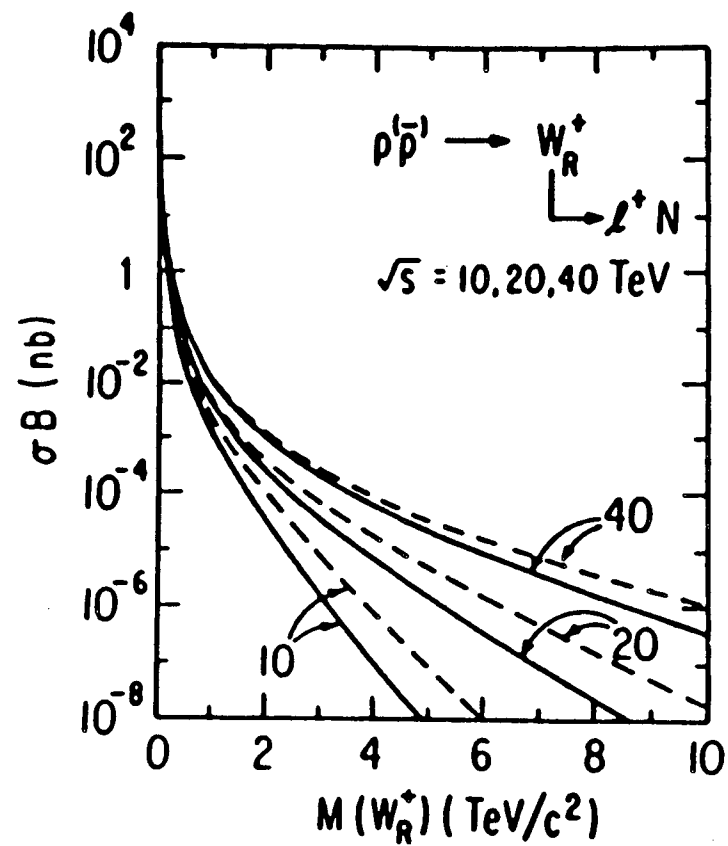


Figure 11: Cross sections  $\sigma$  times branching ratio  $B$  to  $eN$  ( $B = 8.3\%$ ) for  $W_R^+$  in  $pp$  (solid curves) and  $p\bar{p}$  (dashed curves) collisions. The three sets of curves refer to  $\sqrt{s} = 10, 20, \text{ and } 40$  TeV, in ascending order (from ref. 52).

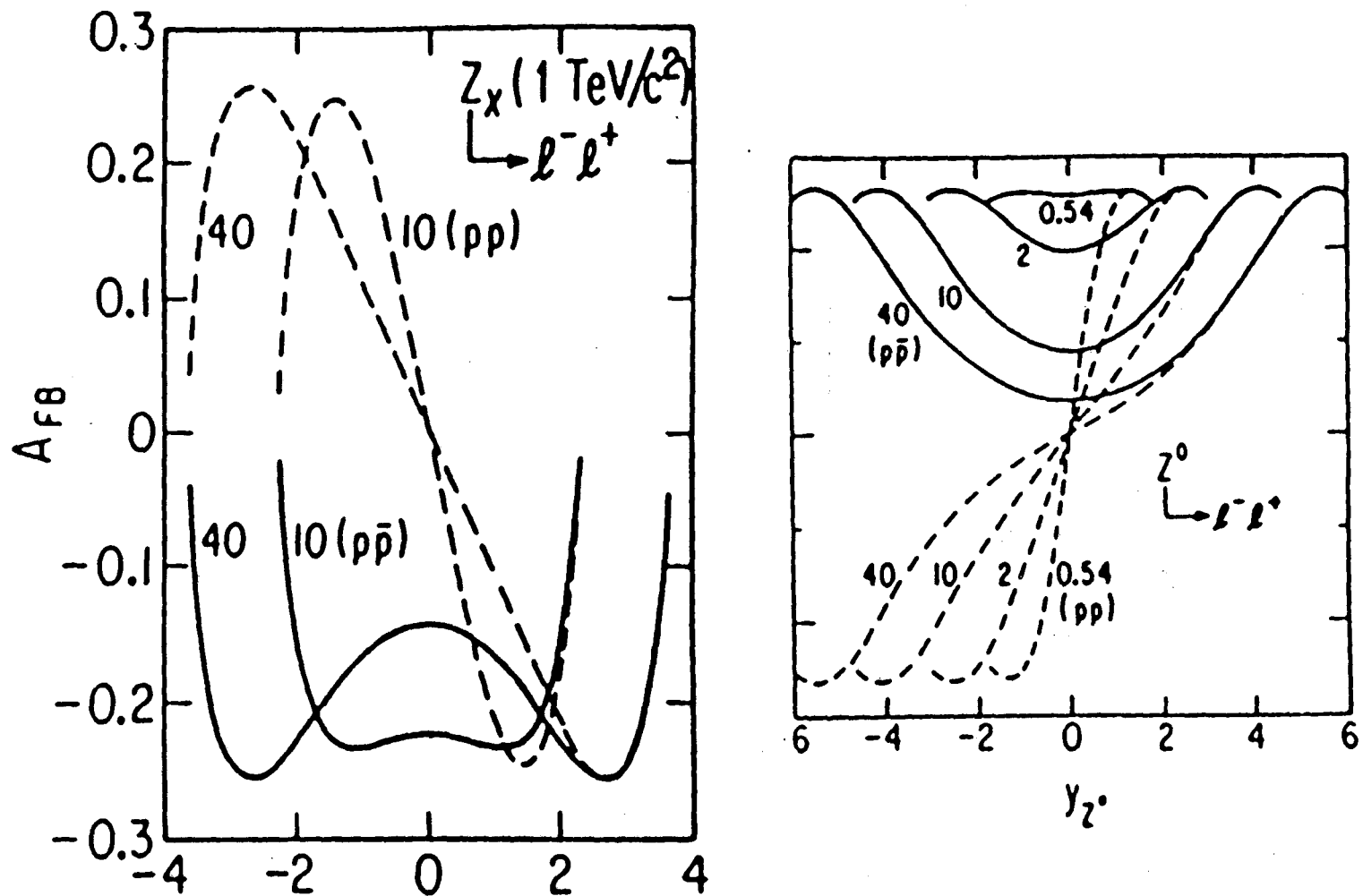


Figure 12: Front-back asymmetries for 1 TeV  $Z_x(SO(10))$  and  $Z^0$  (heavy replica of the standard  $SU(2) \times U(1)$   $Z^0$ ), plotted versus the  $Z$  rapidity for various  $pp$  and  $p\bar{p}$  collider energies (from ref. 52). See text for how the asymmetry is defined.

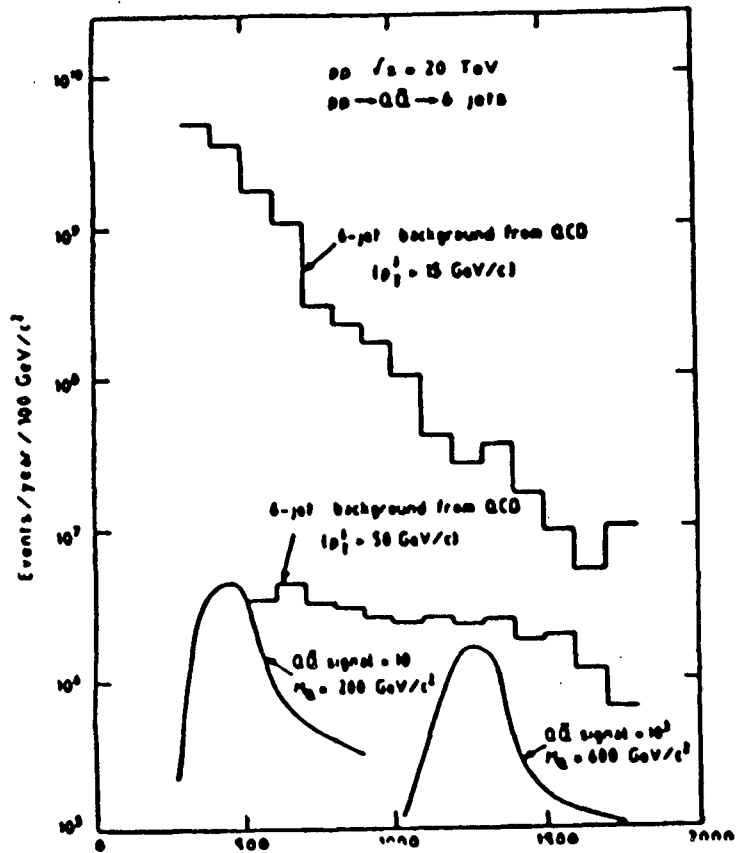


Figure 13: QCD backgrounds overwhelm the signal from nonleptonic decays of heavy  $Q\bar{Q}$  pairs (from ref. 51).

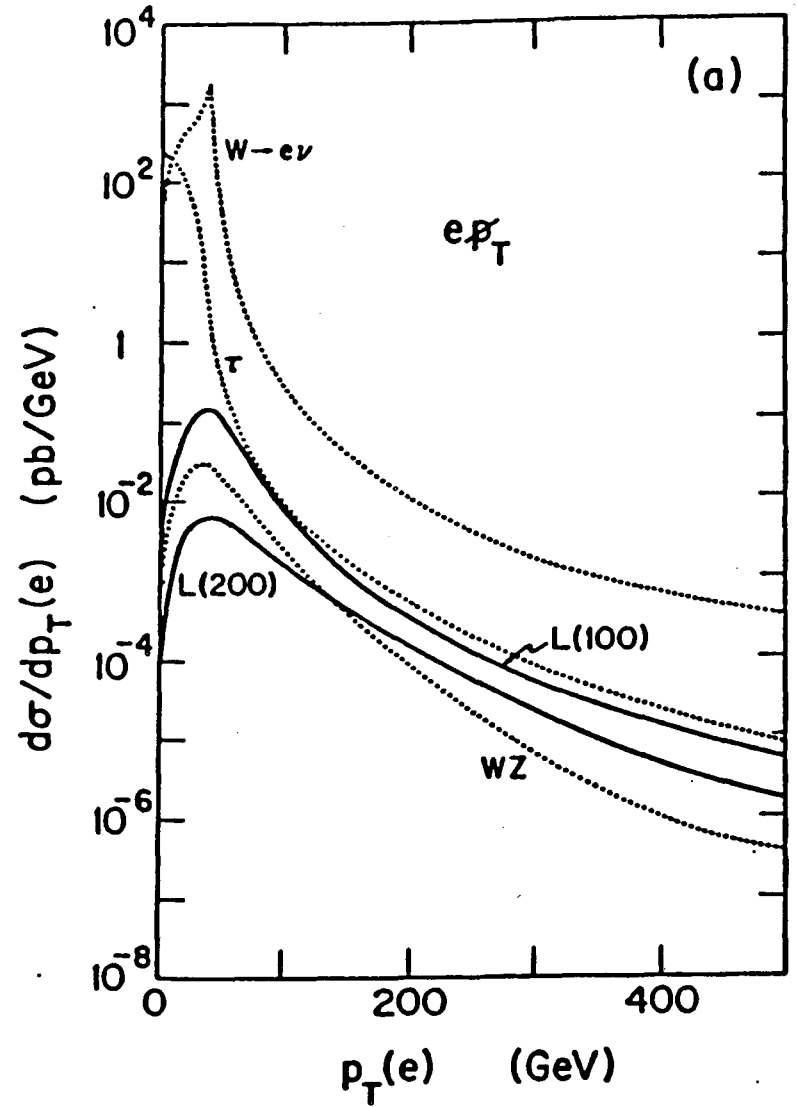


Figure 14: Signals and backgrounds for the single charged lepton decay mode of heavy  $L\bar{\nu}_L$  pairs (from ref. 55).



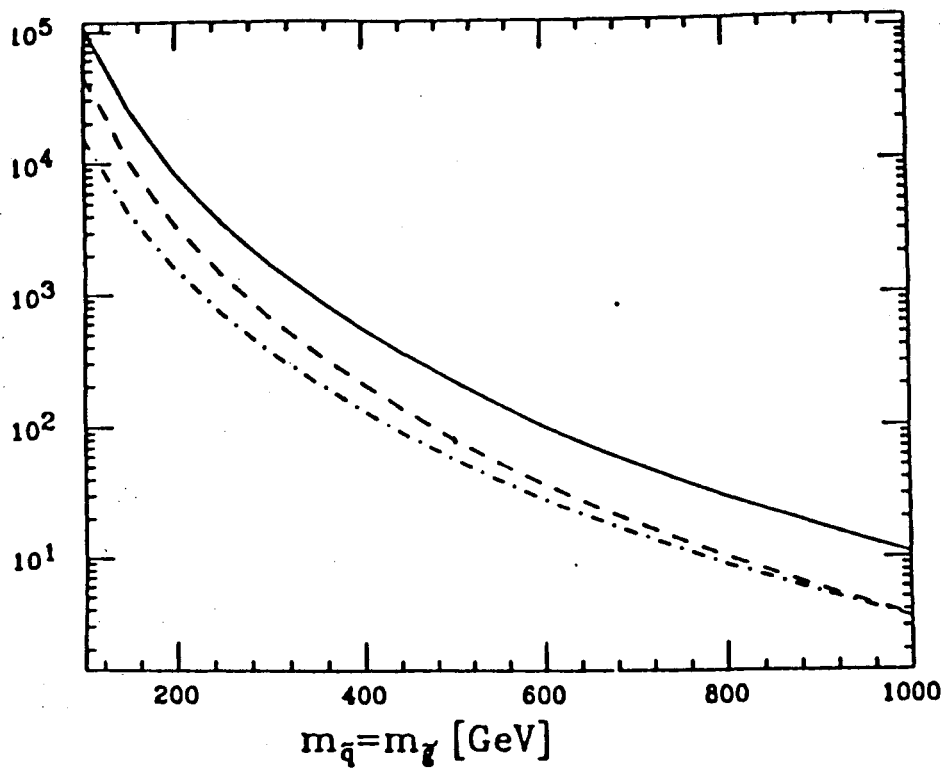


Figure 15: Total squark pair production cross section in picobarns at  $\sqrt{s} = 40$  TeV for  $m_{\tilde{g}} = m_{\tilde{q}}$  (solid curve). Also shown are the  $\tilde{q}_L \tilde{q}_L$  or  $\tilde{q}_R \tilde{q}_R$  cross section (dashed) and the  $\tilde{q}_L \tilde{q}_R$  cross section (dot-dashed) (from ref. 63).

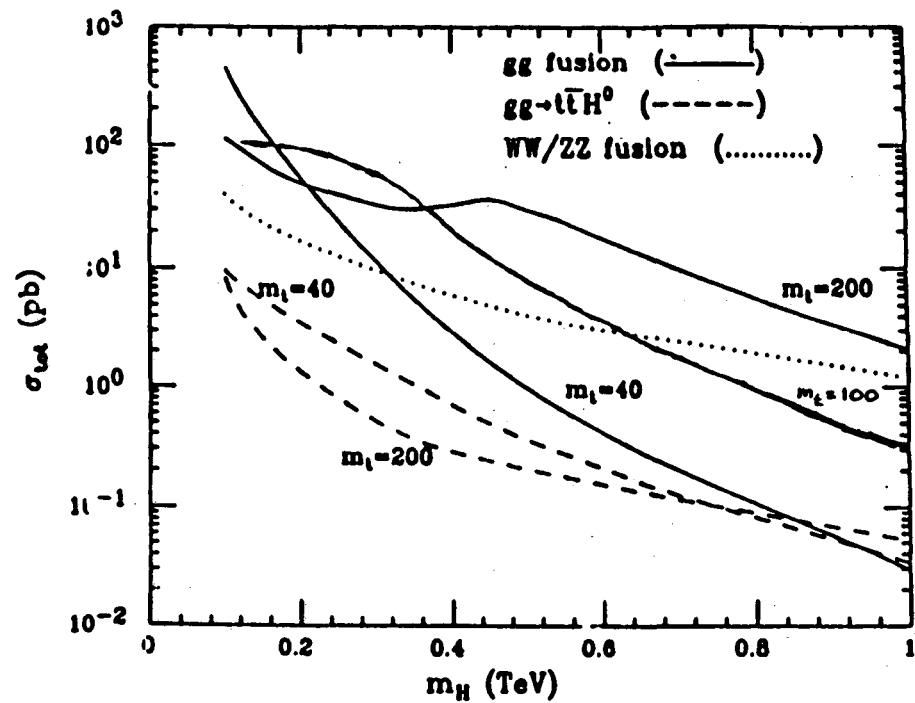


Figure 16: Higgs boson production cross sections from  $WW/ZZ$  fusion and from  $gg$  fusion for various values of  $m_t$  (from ref. 78).

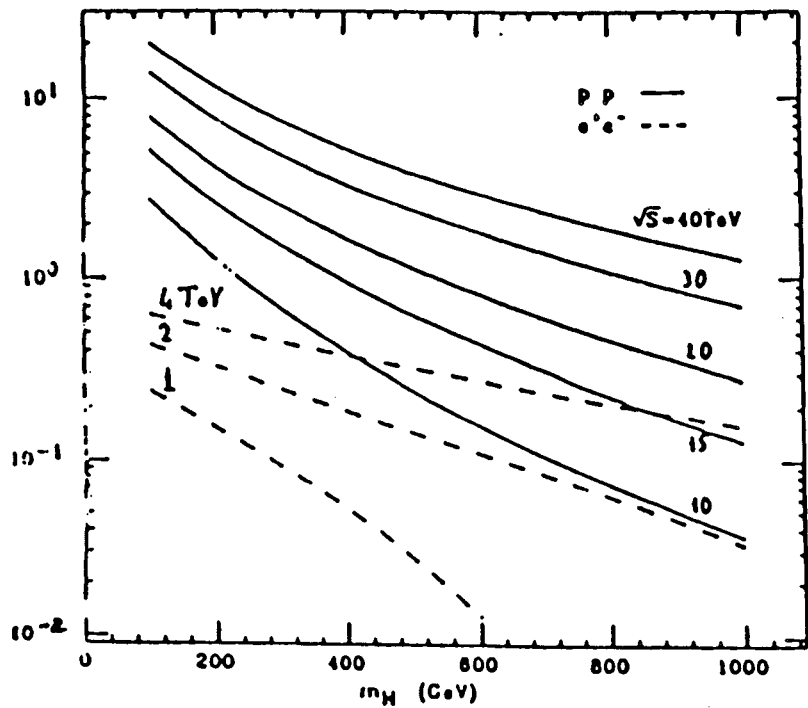


Figure 17: Higgs boson total cross sections as a function of  $m_H$  for various energy  $e^+e^-$  colliders (dashed lines) and pp colliders (solid lines) (from ref. 80).

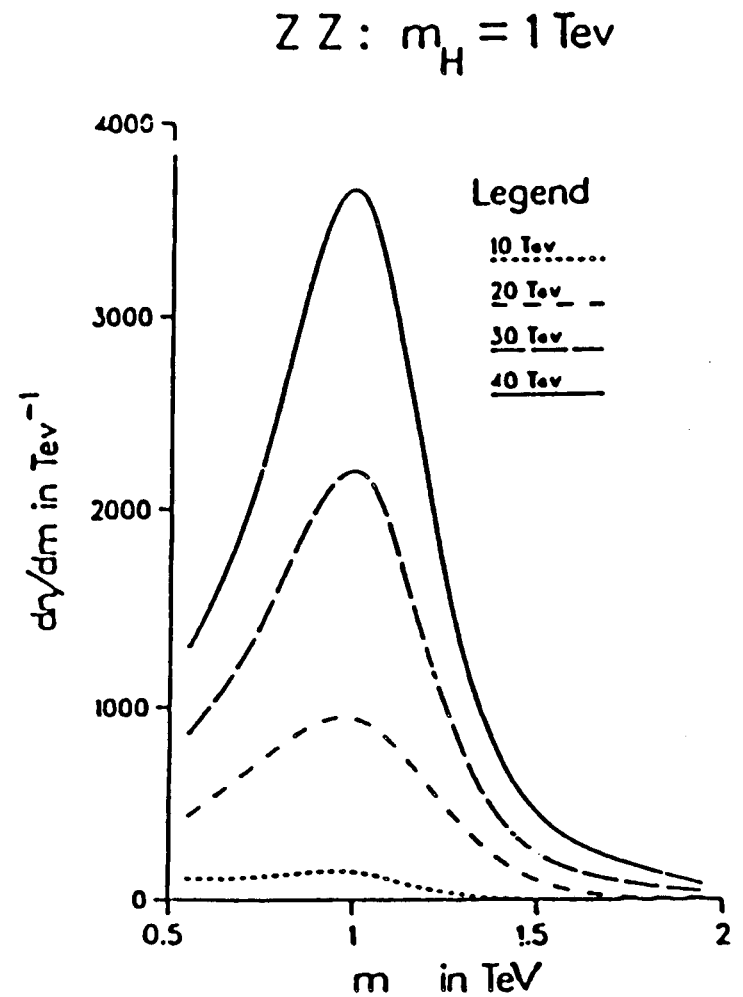


Figure 18: Differential yield per  $10 \text{ fb}^{-1}$  with respect to  $m_{ZZ}$  for production of a 1 TeV Higgs boson at pp colliders of 10, 20, 30, and 40 TeV (from ref. 1).

Z Z : signals + background  
40 Tev

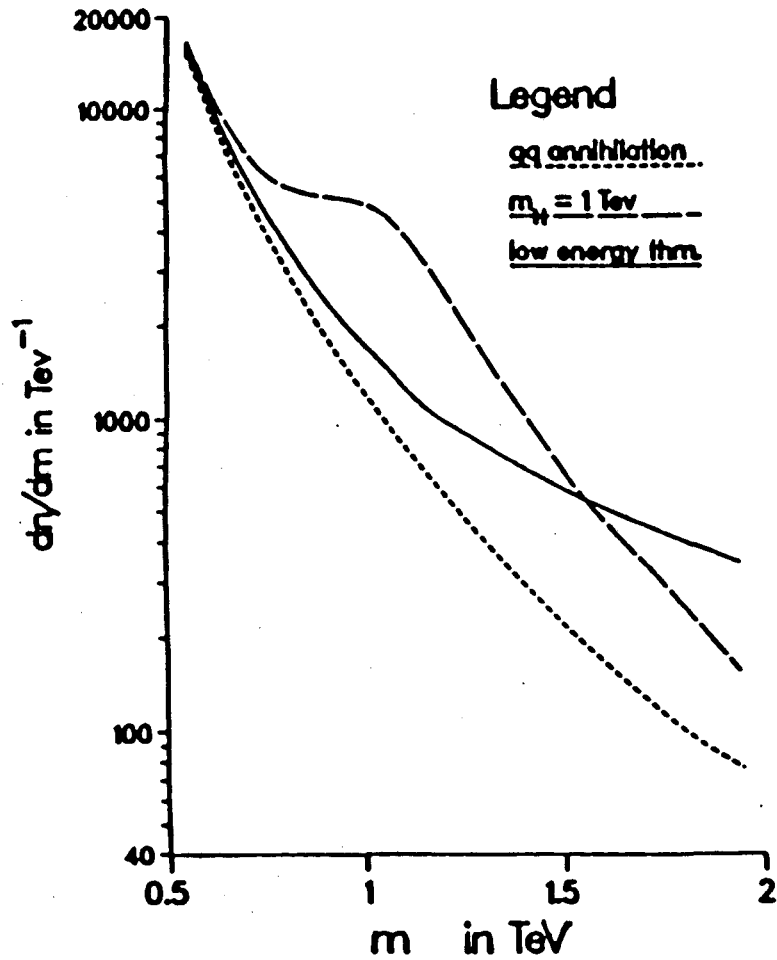


Figure 19: Differential yield per  $10 \text{ fb}^{-1}$  with respect to  $m_{ZZ}$  of the 1 TeV Higgs boson and the model of equation 3.12, both shown as increments on the  $q\bar{q}$  annihilation background with  $\sqrt{s} = 40 \text{ TeV}$  (from ref. 1).

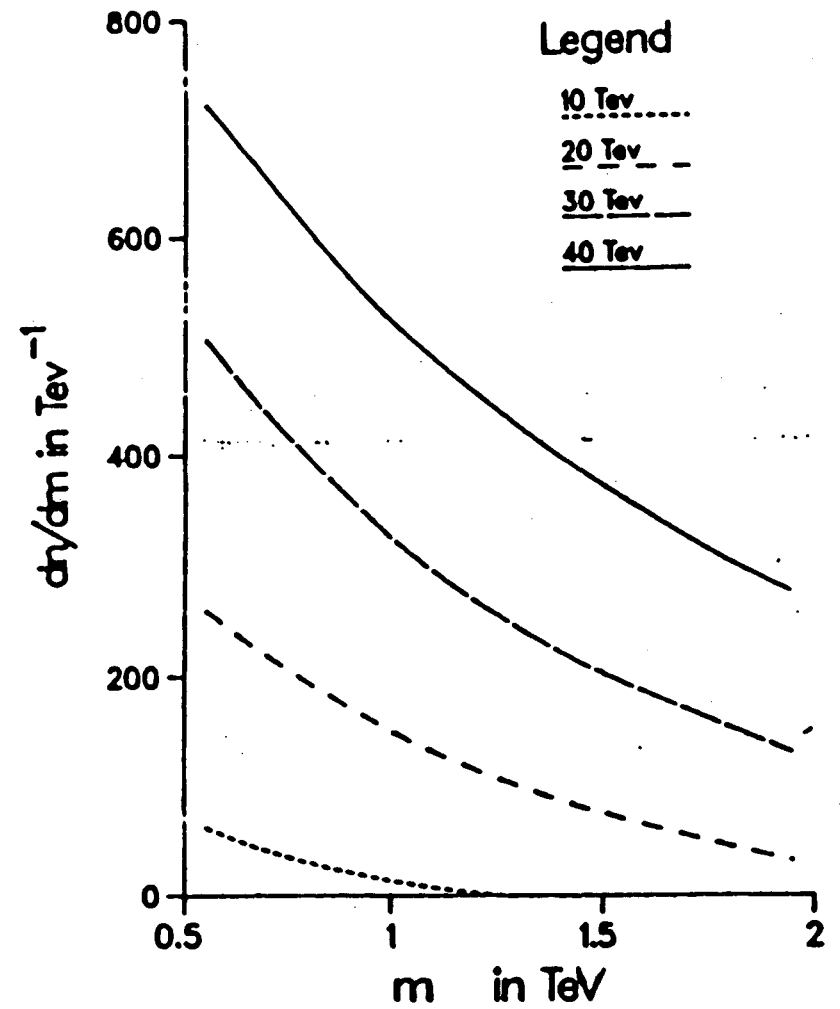


Figure 20: Differential yield per  $10 \text{ fb}^{-1}$  with respect to  $m_{ZZ}$  for the model of equation 3.12, at pp colliders of 10, 20, 30, and 40 TeV (from ref. 1).

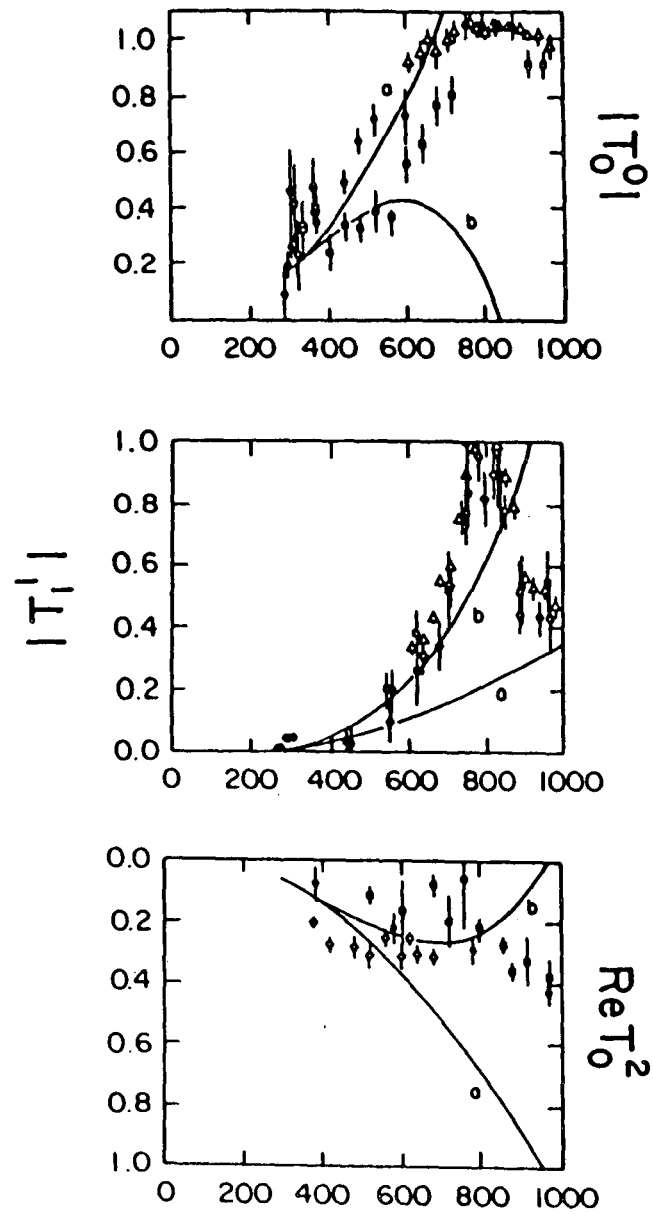


Figure 21: Data for  $\pi\pi$  partial wave amplitudes compared with extrapolated low energy theorems (curves a) as in equation 3.12 (from ref. 91).

LAWRENCE BERKELEY LABORATORY  
TECHNICAL INFORMATION DEPARTMENT  
1 CYCLOTRON ROAD  
BERKELEY, CALIFORNIA 94720